

Mitochondrial Signaling and Bioenergetic Mechanisms that Regulate Neuronal
Cell Death and Survival in Models of Ischemic Brain Injury

by

Matthew J Nichols

Submitted in partial fulfilment of the requirements
For the degree **Doctor of Philosophy**

at

Dalhousie University
Halifax, Nova Scotia
August 2017

© Copyright by Matthew J Nichols, 2017

DEDICATION PAGE

TABLE OF CONTENTS

List of figures	viii
Abstract	xi
List of abbreviations used	xii
Acknowledgements	xv
Chapter 1: Introduction	1
1.1 Stroke subtypes and disease burden	1
1.2 Ischemic preconditioning and neuroprotection	2
1.3 Mitochondrial Ca ²⁺ uptake regulates neuroprotective preconditioning	4
1.4 Neuronal bioenergetics	5
1.5 Regulation of neuronal metabolism by Ca ²⁺	6
1.6 Structural features of the MCU	9
1.7 Mitochondrial Ca ²⁺ influx and efflux pathways	13
1.8 Mitochondrial involvement in cell death	17
1.9 Mitochondrial dysfunction in neurodegenerative disorders.....	19
1.10 Flavonoids as potential neurotherapeutics	21
1.11 Central hypothesis and research aims	22
Chapter 2 – Materials and Methods	23
2.1 Animals.....	23
2.1.1 C57Bl/6 mice.....	23
2.1.2 Global mitochondrial calcium uniporter (G-MCU) nulls	23
2.1.3 Conditional neuron-specific (CNS)-MCU deficient mice.....	24
2.1.4 Primary cortical neuron cultures	24
2.1.5 Oxygen glucose deprivation (OGD).....	25
2.1.6 Drug and siRNA treatments of primary cortical neuron cultures.....	26
2.1.7 Cell viability assays	27
2.1.7.1 MTT- (4,5-dimethylthiazol-2-yl)-2,5-diphenyltetrazolium bromide].....	27

2.1.7.2 Fluorescent Assisted Cell Sorting (FACS)	27
2.1.7.3 Trypan Blue Assay	28
2.1.8 Oxygen Consumptions Rates (OCR) and Extracellular Acidification Rates (ECAR) in primary cortical neuronal cultures	29
2.1.9 Quantitative PCR (qRT-PCR)	30
2.1.10 Multiplexed Enzyme Linked Immunoassays (ELISAs)	31
2.1.11 Confocal imaging of cytosolic calcium concentrations $[Ca^{2+}]_c$ and the mitochondrial membrane potential	33
2.1.12 Hypoxic preconditioning (HPC)	34
2.1.13 Hypoxic-ischemic (HI) brain injury	34
2.1.14 Neuroscore to assess general conditions of sensorimotor behavioural deficits.....	35
2.1.15 Measurement of infarct volume using TTC.....	39
2.1.16 Histological analysis of neuronal damage by Fluorojade staining	39
2.1.17 Transmission electron microscopy	40
2.1.18 NAD ⁺ /NADH and pyruvate measurements	41
2.1.19 Forebrain mitochondrial isolation	41
2.1.20 Mitochondrial Ca ²⁺ uptake	42
2.1.21 Ca ²⁺ -induced mPTP opening.....	42
2.1.22 Western Blotting	43
2.1.23 Statistics and calculations	43
2.1.23.1 Chapter 3 Statistics and calculations	43
2.1.23.2 Chapter 4 Statistics and calculations	44
2.1.23.3 Power calculations for group sizes.....	45
2.1.23.4 Chapter 5 statistics and calculations	45
Chapter 3 - Synergistic Neuroprotection by Quercetin and Epicatechin: Activation of Convergent Mitochondrial Signalling Pathways	46
3.1 Introduction and Rationale	46
3.2 Results	48
3.2.1 Cyanidin and chlorogenic acid fail to enhance neuroprotection by E+Q.....	48
3.2.2 E+Q synergistically protected cortical neurons against OGD-induced cell death.....	50

3.2.3 E+Q enhanced mitochondrial respiration in OGD-exposed cortical neurons.....	53
3.2.4 E+Q increased anti-apoptotic and mitochondrial gene expression in OGD-exposed neurons	55
3.2.5 Activation of Akt and CREB phosphorylation by E and Q	57
3.2.6 Q increases Ca ²⁺ spikes, [Ca ²⁺] _c and the mitochondrial membrane potential	59
3.2.7 The NOS inhibitor L-NAME blocked protection by E or Q against OGD-induced loss of neuronal cell viability.....	61
3.2.8 Oral administration of E+Q reduced HI brain injury.....	63
3.3 Discussion	65
3.3.1 E+Q synergistically protected cortical neurons against OGD-induced cell death.....	66
3.3.2 E+Q prevented spare respiratory capacity loss after OGD	67
3.3.3 E+Q increased anti-apoptotic and mitochondrial gene expression in OGD-exposed neurons	68
3.3.4 Activation of Akt and CREB phosphorylation by E and Q	69
3.3.5 Q increases Ca ²⁺ spikes, [Ca ²⁺] _c and the mitochondrial membrane potential	70
3.3.6 NOS inhibition blocks neuroprotection by E or Q	71
3.3.7 Oral administration of E+Q reduced HI brain injury.....	72
3.3.8 Proposed model for the activation of convergent cell signaling pathways by E and Q.....	73
3.3.9 Q: Cellular uptake and MCU-mediated activation of NOS and CREB activities	75
3.3.10 E activates Akt resulting in elevated NOS and CREB activities	76
Chapter 4: Global Ablation of the Mitochondrial Calcium Uniporter Increases Glycolysis in Cortical Neurons Subjected to Energetic Stressors	78
4.1 Introduction and Rationale	78
4.2. Results	80
4.2.1 Global MCU deficiency impairs Ca ²⁺ uptake and inhibits Ca ²⁺ -induced mPTP opening by forebrain mitochondria	80
4.2.2 MCU deletion blocked HPC but not HI brain injury	82

4.2.3 Ultrastructural features of neuronal mitochondria were similar in WT mice and G-MCU nulls before and after HI brain injury	88
4.2.4 G-MCU deletion did not alter the susceptibility of cortical neurons to ischemic cell death.....	91
4.2.5 G-MCU null neurons exhibited hyper-phosphorylation of the pyruvate dehydrogenase complex	93
4.2.6 G-MCU null neurons displayed reduced spare respiratory capacity offset by increased glycolytic rates	95
4.2.6 Glycolytic induction by OGD was accompanied by Complex I suppression in G-MCU null neurons	96
4.2.7 Forebrain NADH and pyruvate concentrations were reduced in G-MCU nulls subjected to HI.....	97
4.2.7 Global MCU ablation and HPC increased the expression of apoptosis-related and Ca ²⁺ handling genes in the hippocampus	100
4.3 Discussion.....	102
4.3.1 Unaltered HI brain injury in global MCU nulls despite the inhibition of mitochondrial Ca ²⁺ uptake and Ca ²⁺ -induced mPTP opening	102
4.3.2 Metabolic regulation by mitochondrial Ca ²⁺ uptake was impaired in global MCU nulls.....	103
4.3.3 The induction of glycolysis by metabolic stress depleted NADH levels and suppressed Complex I activity in G-MCU null cortical neurons	104
4.3.4 Global MCU deficiency produced similar effects as HPC on apoptosis-related and Ca ²⁺ handling gene expression in the hippocampus.....	106
4.3.5 Global MCU nulls failed to benefit from HPC	106
Chapter 5: Conditional Cre-mediated Ablation of the Mitochondrial Calcium Uniporter in Forebrain Neurons Protects Mice from Hypoxic/Ischemic Brain Injury.....	108
5.1 Introduction and rationale.....	108
5.2 Results	109
5.3 Conclusions.....	117
Chapter 6: Discussion.....	118
6.1 Ischemia/reperfusion-induced mitochondrial dysfunction and neuronal damage	118

6.2 Metabolic compensations for global MCU ablation compromise resistance to ischemic brain injury	123
6.3 Conditional MCU ablation in forebrain neurons at adulthood protects mice from HI brain injury	124
6.4 Transcriptional repression of the MCU is neuroprotective without disrupting mitochondrial activity	125
6.5 Future studies to validate the MCU as a drug target	126
6.6 Limitations	128
References	131
Appendix	158

LIST OF FIGURES

Figure 1.1 Cartoon depiction of the mitochondrial Ca^{2+} uniporter complex	12
Figure 1.2 Mitochondrial Ca^{2+} - transport mechanisms and metabolic control.....	16
Figure 3.1 Protective effects of epicatechin, quercetin, cyanidin and chlorogenic acid against a lethal period of oxygen glucose deprivation	49
Figure 3.2 Epicatechin plus quercetin synergistically protect cortical neurons from damage by a lethal period of oxygen glucose deprivation	52
Figure 3.3 E+Q enhances mitochondrial respiration in OGD-exposed cortical neurons	54
Figure 3.4 E+Q produces supra-additive increases in pro-survival (Bcl-2, PGC-1 α) and mitochondrial gene expression (MT-ND2 and MT-ATP6) in cortical neurons after OGD	56
Figure 3.5 E and Q increase the phosphorylation of protein kinase B (Akt) and cAMP response element binding protein (CREB) in primary cultures of mouse cortical neurons	58
Figure 3.6 Quercetin stimulates Ca^{2+} signaling and elevates the mitochondrial membrane potential.....	60
Figure 3.7 The NOS inhibitor L-NAME blocks protection by E and Q against OGD-induced loss of neuronal cell viability as by an MTT assay	62
Figure 3.8 Oral administration of E+Q reduces HI brain injury	64
Figure 3.9 Convergent signaling pathways proposed to mediate synergistic neuroprotection by epicatechin and quercetin	74
Figure 4.1 Mitochondrial calcium (Ca^{2+}) uptake and Ca^{2+} -induced mitochondrial permeability transition pore (mPTP) opening.	81

Figure 4.2 Neuroscores for WT and global MCU null mice after HI.	84
Figure 4.3 Fluorojade (FJ)-positive neurons damaged by HI brain injury in the dorsolateral striatum of WT and G-MCU nulls.	85
Figure 4.4 Fluorojade (FJ)-positive neurons damaged by HI brain injury in the hippocampus of WT and G-MCU nulls.	86
Figure 4.5 Fluorojade (FJ)-positive neurons damaged by HI brain injury in the motor cortex of WT and G-MCU nulls.	87
Figure 4.6 Electron microscopic images of mitochondria in the CA1 region of the dorsal hippocampus of control or HI injured WT and G-MCU null mice.	89
Figure 4.7 Relative of percentage of damaged mitochondria detected 2 hrs after HI.	90
Figure 4.8 Global MCU ablation did not confer protection to cortical neurons subjected to OGD.	92
Figure 4.9 PDH phosphorylation levels of WT and global MCU nulls under basal and stimulated conditions.	94
Figure 4.10 Analysis of mitochondrial function under basal conditions and after OGD.	98
Figure 4.11 Relative mRNA levels of the complex I member MT-ND2 in WT and global MCU null cortical neurons.	99
Figure 4.12 Relative mRNA levels of mitochondrial apoptotic mediators and plasma membrane calcium handling genes.	101
Figure 5.1 CNS-MCU deficient mice are protected from HI-induced motor deficits, neuronal and mitochondrial damage.	114

Figure 5.2 MCU knockdown protects primary cortical neuron cultures from the loss of cellular viability and mitochondrial function by OGD..... 116

ABSTRACT

Mitochondrial collapse is considered a pivotal event in ischemic brain damage. Compounds that preserve mitochondrial function following an ischemic insult may thus protect the brain from stroke injury. Flavonoids are a diverse group of polyphenolic compounds reported to be neuroprotective in a wide-variety of ischemic stroke models. These compounds appear to increase resistance to ischemic injury by targeting multiple signal transduction and metabolic networks. In view of evidence that increased consumption of the flavonoids epicatechin (E) and quercetin (Q) may reduce stroke-risk, I have measured the effects of combining E and Q on oxygen-glucose deprivation (OGD)-induced damage, mitochondrial function and pro-survival signaling for cortical neuron cultures. Relative to E or Q alone, E+Q synergistically protected cortical neurons from OGD-induced damage in tandem with a corresponding preservation of mitochondrial bioenergetics. E+Q also produced supra-additive inductions of pro-survival pathways involving calcium, Akt, nitric oxide and CREB that converge on the mitochondrion. The therapeutic relevance of these findings was supported by the ability of oral administration of E+Q to protect mice from hypoxic/ischemic (HI) brain damage. Consistent with evidence that Q improves bioenergetics by stimulating the mitochondrial calcium uniporter (MCU), Q increased neuronal cytosolic calcium spikes and the mitochondrial membrane potential. However, excessive MCU-mediated calcium uptake promotes cell death. I therefore employed global MCU (G-MCU) nulls and central neuron-specific MCU (CNS-MCU) deficient mice to compare the effects of constitutive and inducible MCU ablation, respectively, on neuronal mitochondrial bioenergetics and resistance to ischemic damage. Despite reduced mitochondrial calcium uptake by forebrain mitochondria isolated from G-MCU nulls, cortical neuron cultures derived from these mice were not resistant to OGD. My findings suggest that increased neuronal glycolysis resulting in the suppression of Complex I activity may have compromised the resistance of G-MCU nulls to HI brain injury. By contrast, CNS-MCU deficiency, induced at adulthood, protected mice from HI brain injury. MCU suppression by siRNA-mediated silencing also protected cortical neuron cultures from OGD-induced viability loss. Unlike G-MCU ablation, siRNA-mediated MCU silencing did not enhance glycolysis in cortical neurons exposed to OGD. These findings suggest that acute MCU inhibition may be a viable therapeutic approach for stroke.

LIST OF ABBREVIATIONS USED

AGC - aspartate/glutamate transporter
Akt - protein kinase B
AMPK - AMP-activated protein kinase
ATP - adenosine triphosphate
Bcl-2 - B cell lymphoma 2
Ca²⁺ - calcium
CaM/K - calcium/calmodulin-dependent kinases
CNS-MCU - central neuron specific mitochondrial calcium uniporter
cre/ERT2 - cre recombinase that is under the control of a mutated estrogen receptor activate by 4-hydroxy tamoxifen
CREB - cyclic AMP response element binding protein
DNA - deoxyribonucleic acid
E - epicatechin
ECAR - extracellular acidification rate
EMRE- essential MCU regulator
eNOS - endothelial nitric oxide synthase
EPO - erythropoietin
ERK - extracellular signal-related kinases
EVT - endovascular thrombectomy
FACS - fluorescence assisted cell sorting
FBS - fetal bovine serum
FCCP - carbonyl cyanide - 4 - (trifluoromethoxy) – phenylhydrazone
GBD - global burden of disease
G-MCU - global ablation of the mitochondrial calcium uniporter
HI - hypoxic/ischemic
HIF - hypoxia inducible factor

HPC - hypoxic preconditioning
IMM - inner mitochondrial membrane
IPC - ischemic preconditioning
LETM1 - leucine zipper and EF-hand containing transmembrane protein 1
L-NAME - N-nitro - L - arginine methyl ester
MCU - mitochondrial calcium uniporter
MICU1 - mitochondrial calcium uptake 1
MICU2 - mitochondrial calcium uptake 2
mRNA - messenger ribonucleic acid
Na⁺ - sodium
NCLX - mitochondrial sodium and lithium/calcium exchanger
nNOS - neuronal nitric oxide synthase
NOS - nitric oxide synthase
Nrf2 - nuclear respiratory factor 2
OCR - Oxygen consumption rate
OMM - outer mitochondrial membrane
PGC1- α - peroxisome proliferator activated receptor co-activator 1 - alpha
PTP - permeability transition pore
Q - quercetin
RaM - rapid mode of mitochondrial calcium uptake
RT-PCR - reverse transcriptase polymerase chain reaction
SCaMC3/APC - mitochondrial ATP-Mg/Pi carrier
SEM - standard error of the mean
siRNA - short interfering ribonucleic acid
SRC - spare respiratory capacity
TCA - tricarboxylic acid
TG - thapsigargin
Thy1 - thymocyte differentiation 1

t-PA - tissue plasminogen activator

TTC - triphenyl tetrazolium chloride

UCP - uncoupling protein

VDAC - voltage dependent anion channel

VEGF - vascular endothelial growth factor

WT - wild type

YFP - yellow fluorescent protein

ACKNOWLEDGEMENTS

First and foremost, I would like to acknowledge the continuous support of my supervisor Dr. George S. Robertson. Your ambition and curiosity in science has truly inspired me. You have taught me countless lessons in the pursuit of scientific discovery, experimentation and writing for which I will be forever grateful. I could not have accomplished this without your mentorship and friendship. I would also like to acknowledge the support from all members of the Robertson Lab, especially Elizabeth Belland, for of all your support throughout my PhD. You guys have all helped make the hard days easier. I would also like to thank the Department of Pharmacology at Dalhousie University for their continued support.

I would like to thank my family for their continuous support over the course of my education and for encouraging me to follow my interests. You have instilled a sense of dedication and hard-work which I will always carry forward. I can only hope to one day be the same example you have been for me.

Chapter 1: Introduction

1.1 Stroke subtypes and disease burden

Strokes are categorized as either ischemic (~85%) or hemorrhagic (~15%). Ischemic strokes are caused by the physical blockage of cerebral blood flow, usually by plaques and/or thromboembolisms.¹ In the case of hemorrhagic stroke, blood flow is compromised by rupture of the cerebral vasculature, commonly originating from aneurysms or arterio-venous malformations.² The brain is highly sensitive to damage by impaired oxygen and glucose delivery resulting from the interruption of cerebral blood flow by either an ischemic or hemorrhagic stroke. If blood flow is not quickly re-established, irreversible injury will rapidly ensue resulting in permanent neurological deficits and eventually death. Brain regions at risk of injury, by reduced blood flow from a stroke, but are not yet dead, are referred to as the penumbra which represent a major target of neuroprotection. In 2013, the global burden of disease (GBD) study listed stroke as the second leading cause of death and third leading cause of permanent disability world-wide.^{2, 3} Although age-standardized stroke induced fatality rates have decreased, the annual number of strokes, stroke-related deaths and stroke patients with permanent disabilities continues to climb – statistics that are expected to increase with our aging population. The GBD study found that from 1990 to 2013 there were 6.5 million deaths caused by stroke (51% ischemic), 10.3 million new strokes (67% ischemic) and 25.7 million stroke survivors (71%

ischemic) with a total of 113 million disability adjusted life years. From 1990 to 2013 the GBD study found that stroke incidence increased 60.5% and 78.9% for ischemic and hemorrhagic strokes, respectively. This increasing global burden imposed by stroke indicates that additional clinical interventions are urgently required to both decrease stroke incidence and reduce stroke-induced brain damage.

The 2015 Canadian Stroke Best Practice Recommendations for the management of acute stroke provides guidelines for the diagnosis and treatment of hemorrhagic and ischemic stroke. Neurovascular imaging is first recommended to determine the type stroke. In the case of ischemic stroke, current treatment options include the thrombolytic agent tissue plasminogen activator (t-PA) and/or endovascular thrombectomy (EVT).⁴ Treatment with t-PA and/or with EVT attempts to restore cerebral blood flow; however, these treatments must begin within 4.5 and 6 hours, respectively, from the onset of stroke symptoms to be effective. Unfortunately, only a minority of patients (<10%) that have suffered an ischemic stroke are eligible for t-PA and/or EVT.⁵ Hence, there is a considerable need for a neuroprotective therapy that can be safely administered immediately to either hemorrhagic or ischemic stroke patients.

1.2 Ischemic preconditioning and neuroprotection

The adaptive response from non-injurious periods of hypoxia or ischemia to powerfully precondition the brain against injury by a future insult were first

described in 1986.^{6,7} Hypoxic preconditioning (HPC) is produced by a transient (non-injurious) reduction in cerebral oxygen levels, whereas ischemic preconditioning (IPC) is produced by a transient interruption of blood flow to the brain. Neuroprotection by HPC or IPC can occur within minutes and last for several days.⁸ This time course is supported by evidence that protective mechanisms engaged by HPC and IPC involve both rapid (post-translational modifications) and slower processes (transcription and translation).⁸ The profoundly protective effects of HPC and IPC have stimulated intense effort to identify the relevant signaling pathways that may be targeted to treat stroke.

Neurons rely heavily on oxidative phosphorylation for ATP production. Multiple cellular and signaling mechanisms enable neurons to undergo beneficial metabolic adaptations following transient reductions in oxygen and glucose delivery. The transcriptional regulating factor HIF-1 plays a key role in activating a complex adaptive response responsible for HPC and IPC. HIF-1 is stabilized by low oxygen levels resulting in the activation of genes encoding glycolytic enzymes, glucose transporters and neuroprotective growth factors such as erythropoietin (EPO) and vascular endothelial growth factor (VEGF).^{8,9} The suppression of ATP production by hypoxia or ischemia also activates the AMP-activated protein kinase (AMPK) pathway which supports energy production by stimulating catabolic, and reducing anabolic, pathways.¹⁰ HPC and IPC further protect the brain from ischemic damage by activating extracellular signal-related kinases (ERK), protein kinase B (Akt), and calcium/calmodulin-dependent

kinases II/V (CaMKII/IV) that stimulate the transcriptional regulating factors nuclear respiratory factor 2 (Nrf2) and cyclic AMP response element-binding protein (CREB). Activation of this signaling network induces robust resistance to ischemic brain damage by stimulating the expression of genes encoding growth factors, anti-apoptotic factors, proteins that regulate folding machinery, anti-oxidants, enzymes necessary for energy production and Ca^{2+} handling proteins.^{8, 11-14} These findings suggest that HPC and IPC profoundly protect the brain against ischemic injury by activating a complex neuroprotective signal transduction network. Understanding how activation of this network is orchestrated is therefore a major goal in stroke research.

1.3 Mitochondrial Ca^{2+} uptake regulates neuroprotective preconditioning

Mitochondria play a pivotal role in HPC and IPC by shaping the calcium (Ca^{2+}) signaling events that orchestrate neuroprotective signal transduction. However, excessive mitochondrial Ca^{2+} uptake also triggers collapse of this organelle implicated in excitotoxic and ischemic neuronal cell death. High-capacity mitochondrial Ca^{2+} uptake is mediated by the mitochondrial Ca^{2+} uniporter (MCU).¹⁵ Recently, activity-induced preconditioning has been shown to protect primary cultures of mouse hippocampal neurons from excitotoxicity by repressing expression of the MCU.¹⁶ The resultant decrease in MCU-mediated Ca^{2+} uptake reduced excitotoxic neuronal cell death by attenuating mitochondrial Ca^{2+} overloading.¹⁵ Repression of MCU expression was found to be mediated by activation of a Calmodulin Kinase II/Npas 4 pathway. These findings therefore suggest that

MCU repression may also be an important *in vivo* mechanism for HPC and IPC. The primary goal of my thesis was to determine whether MCU inhibition reduced metabolic deficits and neuronal damage in cell-based and mouse models of ischemic injury.

In the following sections, I will describe how Ca^{2+} regulates neuronal bioenergetics and recent findings concerning the identification, molecular characterization and roles of the MCU in energy metabolism and neuronal cell death and survival.

1.4 Neuronal bioenergetics

It has been known for decades that relative to other organs the brain consumes disproportionately high amounts of total oxygen and ATP and relies almost exclusively on glucose as an energy source.¹⁷ Neurotransmission requires vast amounts of energy, primarily to support ionic ATPase activity and vesicle recycling that maintain neuronal activity. It has been estimated that pre- and post-synaptic activity accounts for 55% of total neuronal ATP consumption in active neurons.¹⁸ When imposed with large synaptic activity workloads, neurons rely heavily on oxidative phosphorylation for the efficient generation of ATP.¹⁹ To a lesser extent, glycolytic ATP production supports neurotransmission under aerobic conditions, however, its contribution to ATP synthesis increases during periods of hypoxia.¹⁹ Total ATP production generated by oxidative phosphorylation has been estimated to account for 93% of all ATP generation,

whereas glycolysis has been estimated to contribute 7%.¹⁸ These metabolic activities are supported by both mitochondrial and glycolytic compartments that localize to synapses with an imposed workload.^{20, 21} Relative to astrocytes, neurons shuttle increased amounts of glucose to the pentose phosphate pathway to generate NADPH, which is used to regenerate the glutathione pool to combat oxidative stress imposed by oxidative phosphorylation.¹⁰ This is accomplished by the continual degradation of anaphase promoting complex/cyclosome (APC/C-Cdh-1) that steadily degrades 6-phosphofructo-2-kinase/fructose-2,6-bisphosphate-3 activity, which otherwise potentially induces glycolysis. This further substantiates neuronal reliance upon oxidative phosphorylation because of their limited capacity to increase glycolytic ATP production and elevate glucose consumption via the pentose phosphate pathway.²²

1.5 Regulation of neuronal metabolism by Ca²⁺

Mitochondria are trafficked along dynein and kinesin motors to provide metabolic support for neurotransmission. Elevated local Ca²⁺ concentrations act as a stopping signal that halts mitochondrial movement, resulting in improved local energy delivery.^{23, 24} The redistribution of mitochondria under imposed workloads highlights the importance of proper mitochondrial function and dynamics.²⁵ Elevated local Ca²⁺ concentrations also increase mitochondrial-derived ATP production.²⁶ Regulation of neuronal metabolism by Ca²⁺ can occur in the cytosol, on the surface of mitochondria and within the mitochondria thus enabling the precise spatiotemporal and activity-dependent control of energy production under

different Ca^{2+} induced workloads.²⁶ Since glucose is the primary energy source for neurons, I will now focus on how Ca^{2+} regulates glucose metabolism by glycolysis and oxidative phosphorylation.

Elevated cytosolic Ca^{2+} activates CaMKII which acts upon glycogen phosphorylase to stimulate glycogen breakdown resulting in enhanced glucose supply for oxidation. This is a more prominent mechanism in astrocytes than neurons.²⁶⁻²⁸ The higher glycogen pools in astrocytes are thought to supplement neuronal activity by increasing metabolite transfer. Under aerobic conditions it is thought that lactate is shuttled to neurons under imposed workloads which is used to generate ATP through oxidative phosphorylation. This process is called the lactate shuttle.^{18, 29} Astrocytes also appear to shuttle glucose to neurons to fuel activity under anaerobic conditions by glycolysis. Although the exact mechanisms and direction of metabolite transport are not fully understood, disturbances in metabolite transfer between astrocytes/oligodendrocytes and neurons have been shown to compromise neuronal function. This strongly supports a key role for astrocytes/oligodendrocytes in the metabolic support of neurons.^{30, 31}

A second mechanism for the increased metabolic support of neurons is the up-regulation of Ca^{2+} -dependent metabolite transporters. Metabolite transporters respond to increased Ca^{2+} concentrations through EF- Ca^{2+} domains in the intermembrane space by elevating substrate transfer to mitochondria. There are

two main transporters that are modulated by increased Ca^{2+} concentrations - the aspartate/glutamate transporter (Aralar/AGC) and ATP-Mg/Pi (SCaMC3/APC). AGC is activated by Ca^{2+} (half maximal conductance, $S_{0.5} \sim 324 \text{ nM}$) resulting in the increased transport of reducing equivalents into the mitochondrial matrix that enhances substrate supply for the electron transport chain. Increased AGC transport has also been linked indirectly to improved pyruvate supply to the matrix thus aiding in the maintenance of substrate supply for the TCA cycle.³²⁻³⁴ SCaMC3/APC responds to elevated Ca^{2+} concentrations ($S_{0.5}$ define $\sim 3-4 \mu\text{M}$) by increasing the electroneutral exchange of ATP-Mg²⁺ or ADP for HPO_4 . The direction and magnitude of transport is dependent on the relative concentrations of substrates for the SCaMC3/APCs which function to maintain the adenine pool for the synthesis of ATP.³⁵

Ca^{2+} is also electrogenically taken up into mitochondria through the MCU.³⁶ Once inside the mitochondrial matrix it increases the activity of several dehydrogenases, namely pyruvate, isocitrate and alpha-ketoglutarate dehydrogenase, all rate limiting steps in providing reducing equivalents for complex I.^{37, 38} This increases TCA cycle flux, elevating the production of reducing equivalents, which drive the electron transport chain resulting in elevated ATP production. Lastly, increased Ca^{2+} concentrations in the mitochondrial matrix elevate energy production by stimulating ATP synthase activity.³⁹

1.6 Structural features of the MCU

The MCU functions as a multiprotein complex (~480 kDa) located on the inner mitochondrial membrane where it selectively and electrogenically transports Ca^{2+} into the mitochondrial matrix. The mammalian MCU complex is composed of several core proteins composed of the MCU, MCUB and EMRE. The activity of this complex is regulated by the adaptor proteins MICU1 and MICU2 as well as by an additional MICU3 adaptor protein expressed predominantly in the CNS.⁴⁰⁻⁴²

The pore domain of the MCU complex is composed of MCU, MCUB and EMRE (essential MCU regulator). The pore domain exhibits five-fold symmetry by a predicted pentameric shape composed of MCU and MCUB monomers which form a hydrophilic pore.⁴² Genetic ablation of the MCU results in a near complete loss of Ca^{2+} uptake, implicating its essential role in Ca^{2+} transport. The MCU is a 40 kDa protein with 2 coiled coil domains and 2 transmembrane domains separated by a short hydrophilic acid linker composed of a DXXE motif.^{43, 44} The carboxylate groups of this DXXE motif are strategically located on the proposed pore entrance of the second transmembrane domain, which contributes to the selective gating of Ca^{2+} by the MCU complex.

MCUB shares approximately 50% sequence identity to MCU and contains two predicted transmembrane domains. The MCUB subunit contains several key acidic amino acid substitutions in the pore facing region that restrict Ca^{2+} transduction.⁴² Higher MCUB subunit mRNA expression in heart relative to

skeletal muscle is consistent with the lower MCU complex activity in heart than skeletal muscle.^{45, 46} This suggests that the relative levels of MCU to MCUb represent a mechanism to control absolute Ca^{2+} flux through the MCU complex. EMRE (essential MCU regulator), is a small subunit (~10 kDa) of the MCU complex with a single transmembrane domain which is also required for MCU-mediated complex Ca^{2+} conductance.⁴⁰ Co-expression of the MCU and EMRE is sufficient to transport Ca^{2+} with electrophysiological properties that resemble the human MCU expressed in yeast.⁴⁰⁻⁴² EMRE is proposed to have dual functions where the first is to interact with the MCU to keep it in an open state to conduct Ca^{2+} and the second is to facilitate interactions between the MCU and the adaptor proteins MICU1 and MICU2.⁴²

The basic components of the pore domain in the MCU complex interact with several adaptor proteins, namely; MICU1, MICU2 and the predominantly CNS-expressed MICU3. MICU1 is a 54-kDa protein with two highly conserved EF-hand Ca^{2+} -binding motifs.^{46, 47} MICU1 inhibits mitochondrial Ca^{2+} uptake suggesting that it is a key component for positive regulation of this uniporter. MICU1-silenced cells possess mitochondria constitutively overloaded with Ca^{2+} , suggesting that the MICU1 keeps the MCU pore closed under resting cytosolic Ca^{2+} concentrations $[\text{Ca}^{2+}]_c$, thus serving as a gatekeeper for the uniporter.^{48, 49} MICU1 knockdown increases basal mitochondrial Ca^{2+} concentrations $[\text{Ca}^{2+}]_m$, and MICU1-silenced cells display enhanced mitochondrial Ca^{2+} uptake in response to low $[\text{Ca}^{2+}]_c$ (0.1-2.0 μM). MICU1/2 interact with the basic

components of the MCU pore to coordinately regulate channel activity which gives rise to the observed sigmoidal response of MCU complex activity under differing concentrations of Ca^{2+} . MICU1/2 are localized to the intermembrane space and function as gatekeepers of the MCU complex that set the threshold for Ca^{2+} uptake. Although the exact contributions of MICU1 and MICU2 are not presently clear, together they function to inhibit mitochondrial Ca^{2+} uptake at low Ca^{2+} concentrations, preventing futile cycling, while facilitating MCU mediated Ca^{2+} uptake under stimulated conditions for increased energy production.^{48, 49} The specific expression of MICU3 in the CNS is of interest to neurobiologists. MICU3 is a paralogue of MICU1 and 2, however, the precise role of the MICU3 in the CNS remains unclear.⁵⁰

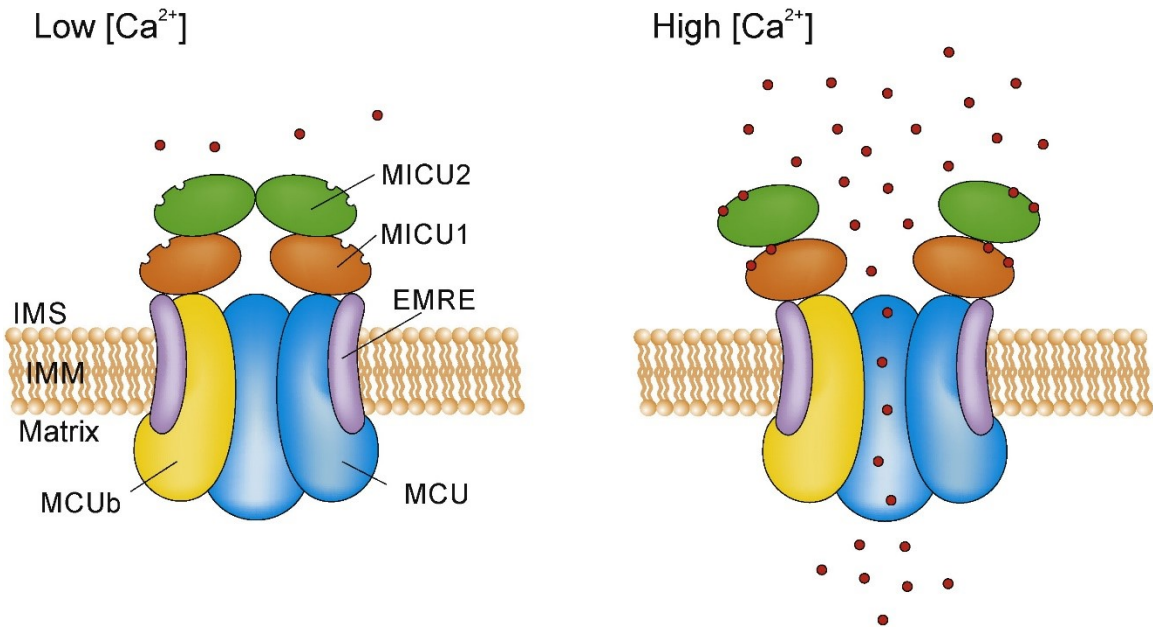


Figure 1.1 Graphical depiction of the mitochondrial Ca²⁺ uniporter complex

The MCU channel exhibits pentameric symmetry and is composed of MCU and MCUb subunits. MCU subunits are conducive to Ca²⁺ transport while relative increases in MCUb subunits reduce Ca²⁺ transport capacity. The essential MCU regulator (EMRE) interacts with the pore forming domain and is necessary for *in vitro* activity. EMRE also interacts with non-pore forming subunits MICU1 and 2. MICU1 and 2 prevent futile Ca²⁺ signaling at low (0.1-2.0 μM) cytosolic Ca²⁺ concentrations and facilitate Ca²⁺ entry at higher (>0.2 μM) cytosolic Ca²⁺ concentrations. Reproduced with permission from Rightslink.⁵¹ Mammucari, C., *et al.* (2013) Molecular structure and pathophysiological roles of the Mitochondrial Ca²⁺ Uniporter. *Biochimica and Biophysica Acta* 10: 2457-2464.

1.7 Mitochondrial Ca²⁺ influx and efflux pathways

Transport of Ca²⁺ into the mitochondrial matrix requires crossing both the outer mitochondrial membrane (OMM) and the inner mitochondrial membrane (IMM). Most studies have focused on Ca²⁺ transport across the IMM because it is impermeable to ions and thus requires transporters for ionic movement. The abundance of voltage dependent anion channels (VDAC) that span the OMM render this membrane relatively permeable to substrates up to 5 kDa.⁵² Over expression of VDAC increases Ca²⁺ entry into the mitochondrial matrix, whereas down-regulation of VDAC decreases Ca²⁺ entry into the mitochondrial matrix. This also implies that VDAC expression levels themselves can modulate mitochondrial Ca²⁺ signalling. VDAC can also exist as 3 isoforms which all contribute to similar Ca²⁺ uptake profiles, however, these isoforms appear to have distinct roles in regulating mitochondrial Ca²⁺ overloading and cell death.⁵²

As previously discussed, transport of Ca²⁺ across the IMM into the matrix is primarily accomplished by the MCU. Although the MCU is the only *bona fide* candidate for the mediation of mitochondrial Ca²⁺ uptake, several other putative mechanisms have been suggested to facilitate Ca²⁺ uptake across the IMM which include: a mitochondrial ryanodine receptor, UCP2/3, LETM1 and the rapid uptake mode called Ram.

The mitochondrial ryanodine receptor has only been reported to transport Ca²⁺ in cardiac tissue, however, evidence for a role of this transporter in mitochondrial

Ca²⁺ uptake is complicated by the possibility of endoplasmic reticulum contamination.⁵³ A direct role for the UCP2/3 in mitochondrial Ca²⁺ transport has also been challenged with the evidence more in keeping with an indirect effect.⁵⁴ Leucine Zipper-EF-hand containing transmembrane protein 1 (LETM1) is a Ca²⁺/H⁺ antiporter located in the mitochondrial IMM. Currently, the role of this antiporter in both mitochondrial Ca²⁺ uptake and efflux is unresolved. However, its significance is supported by impaired mitochondrial calcium dynamics and metabolism resulting from heterozygous mutations in LETM1 associated with Wolf-Hirschhorn Syndrome.^{55, 56} The rapid mode of Ca²⁺ uptake (RaM) was first identified as a mechanism for mitochondrial Ca²⁺ sequestration in liver.⁵⁷ Like the MCU, RaM activity is blocked by ruthenium red and depends upon the mitochondrial membrane potential to drive Ca²⁺ uptake.^{57, 58} However, given the lack of information concerning the genetic and structural bases for RaM, these similarities with the biochemical properties of the MCU may only indicate that RaM is a separate conductance state of the MCU.^{59, 60}

Mitochondrial Ca²⁺ efflux occurs through the mitochondrial Na⁺/Ca²⁺ exchanger. This protein has been termed NCLX because it can transport lithium in place of sodium.⁶¹ NCLX is an isoform of the plasma-membrane NCX family. Lithium transport abilities distinguishes the NCLX from plasma membrane sodium/Ca²⁺ exchangers (NCXs) and, unlike NCXs, has been shown by immunogold electron microscopy to be localized to the IMM.⁶² Most recently, a prominent role for the NCLX in mitochondrial Ca²⁺ extrusion has been demonstrated. Cre-mediated

excision of NCLX resulted in mitochondrial Ca^{2+} overloading and sudden cellular necrosis that was partially rescued by permeability transition pore (PTP) inhibition.⁶³

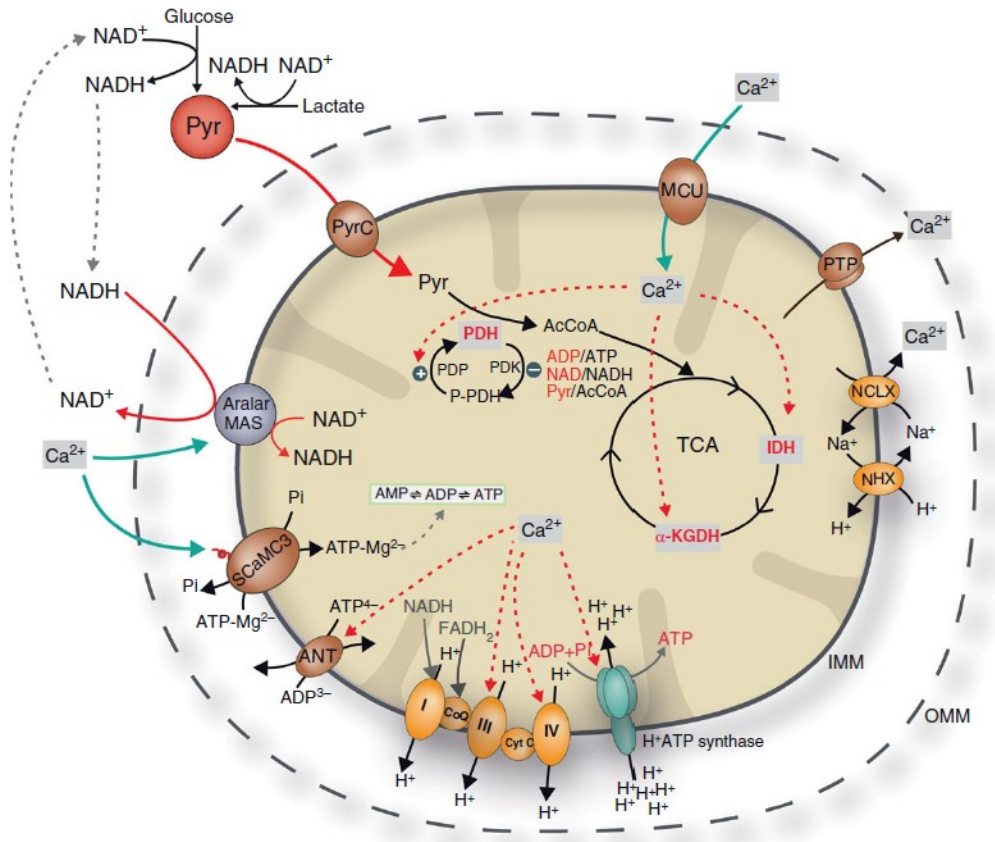


Figure 1.2 Mitochondrial Ca^{2+} - transport mechanisms and metabolic control

Increases in intermembrane space Ca^{2+} are sensed through the EF- Ca^{2+} binding domains of Aralar/AGC and SCaMC3 resulting in elevated NADH delivery to drive oxidative phosphorylation (AGC) and adenine nucleotides and inorganic phosphate (SCaMC3) for ATP production. Ca^{2+} is electrogenically transported into the mitochondrial matrix through the MCU where it activates dehydrogenases within the matrix and members of the electron transport chain increasing the production of reducing equivalents and ATP. Ca^{2+} is extruded from mitochondria through sodium/ Ca^{2+} exchangers (NCXs) and through the mitochondrial permeability transition (mPTP) pore. In the matrix, Ca^{2+} interacts with ATP synthase increasing ATP production. Reproduced with permission from John Wiley and sons through Rightslink. Original publication: Llorente-Folch et al. (2015) The regulation of neuronal mitochondrial metabolism by calcium. *Journal of Physiology*.²⁶

1.8 Mitochondrial involvement in cell death

The first clue that apoptosis might be regulated by mitochondria came when Bcl-2 was reported to be localized in the IMM (in fact, it is on the OMM)⁶⁴ and absence of the C-terminal transmembrane domain blocked the ability of Bcl-2 to inhibit apoptosis.⁶⁴ The subsequent molecular dissections of various cell death pathways have now firmly established a pivotal role for mitochondria in the initiation of apoptosis, necroptosis and necrosis.^{65, 66, 67} In 2009, the Nomenclature committee on cell death proposed twelve distinct forms of cell death.⁶⁵ In this thesis, only those pathways involving the mitochondrion will be discussed, however, for a more detailed description of the roles played by mitochondria in neuronal cell death, the reader is referred to excellent reviews of this topic.^{65, 66, 67}

The critical requirement of energy production to drive the chemical reactions essential for life has strategically positioned mitochondria in the regulation of cell death and survival. Indeed, a common feature of apoptosis and necrosis is cellular bioenergetic collapse. Severe reductions in ATP levels deprive ion pumps of the energy required to maintain ionic homeostasis leading to cellular and mitochondrial swelling. This, in turn, activates Ca^{2+} sensitive proteases, such as calpains and cathepsins that perpetuate cellular demise.^{65, 66} MCU-mediated mitochondrial Ca^{2+} overloading causes mitochondrial swelling that induces the formation of a permeability transition pore (PTP). The PTP is formed in the IMM where its opening triggers mitochondrial collapse and the release of cytochrome-

C and other factors that execute cell death. Opening of the PTP is promoted by mitochondrial Ca^{2+} overloading and the excessive generation of thiol oxidants while PTP activity is opposed by magnesium and adenine nucleotides.⁶⁸ The exact molecular identity of the PTP remains heavily debated despite the knowledge of its existence since the 1970's. Although genetic and pharmacological studies have shown that cyclophilin D promotes PTP activity and that ATP synthase appears to be associated with formation of the PTP, the precise structure of the PTP remains elusive.⁶⁸

Mitochondrial mediated cell death can also be regulated through mitochondrial outer membrane permeabilization (MOMP). MOMP is controlled by the balance of anti-apoptotic (i.e. Bcl-2 and Bcl-xL) and pro-apoptotic (i.e. Bax and Bak) members of the Bcl-2 family, a family now including over 30 members.⁶⁹ Under apoptotic stimuli, pro-apoptotic Bcl-2 family members, such as Bax, oligomerize and insert themselves into the mitochondrial outer membrane, inducing its permeabilization. MOMP is inhibited by anti-apoptotic factors that physically associate pro-apoptotic factors to prevent their insertion, oligomerization and permeabilization of the mitochondrial outer membrane.^{69, 70} Once the outer mitochondrial membrane is permeabilized, additional pro-apoptotic factors, such as cytochrome C, are released.⁶⁹ Within the cytosol, cytochrome c interacts with apoptosis activating factor (Apaf) and caspase-9 to proteolytically activate caspase-3 that is the final executioner of apoptosis.⁷¹ MOMP can also induce caspase-independent apoptosis by releasing additional pro-apoptotic proteins

such as apoptosis inducing factor (AIF) and endonuclease G.^{72, 72} AIF is tethered to the IMM and faces the intermembrane space. Following MOMP, AIF is proteolytically cleaved, released and transported to the nucleus where it causes chromatin condensation and DNA fragmentation.⁷²

1.9 Mitochondrial dysfunction in neurodegenerative disorders

Neurons face tremendous challenges in maintaining bioenergetic homeostasis, especially at distal sites such as synapses that have large ATP demands.²⁵ Since mitochondria supply the majority of ATP in neurons, dysfunction of these organelles has disastrous consequences for neuronal bioenergetics and viability. Neurotransmission depends heavily on the rapid positioning of healthy mitochondria to synaptic regions in urgent need of energy. Although the precise mechanisms that regulate mitochondrial movement are poorly understood, impaired mitochondrial trafficking has been implicated in numerous neurodegenerative and neurological disorders.²⁵ Conversely, improvements in the transport of healthy mitochondria to sites at risk of injury improves neuronal survival.^{73, 74} These findings support the importance of mitochondrial motility in meeting the dynamic energy demands required for optimal neuronal function.

Neuronal survival also depends on the transport of healthy mitochondria to maintain rapid and efficient ATP production. A pivotal role for mitochondrial fidelity in neuronal survival is strongly supported by neurological impairments associated with many mitochondrial diseases.⁷⁵ Mitochondrial dysfunction has

also been implicated in numerous non-familial acute and chronic neurodegeneration such as traumatic brain injury, stroke, Alzheimer's disease, multiple sclerosis and Parkinson's disease.⁶⁵ Furthermore, Complex I (methyl-phenyl-tetrahydropyridine (MPTP); rotenone) and Complex III (3-nitropropionic) inhibitors produce neuropathological and behavioural deficits in animals that are characteristic of Parkinson's disease and Huntington's disease, respectively.⁷⁶⁻⁷⁸

In addition to inefficient ATP production, mitochondrial dysfunction is often associated with increased reactive oxygen species (ROS) production.⁷⁹ Excessive ROS production causes the local damage of mitochondrial DNA, lipids and proteins creating a vicious feedforward cycle of increased mitochondrial damage and dysfunction. Adding to the activation of these intrinsic cell death pathways, mitochondria can also act as damage associated molecular patterns (DAMPs) that induce inflammatory injury.⁸⁰ These findings provide an important link between mitochondrial dysfunction and pathological inflammation observed in numerous neurodegenerative conditions.⁸⁰

Given the complex impact of mitochondrial dysfunction on various aspects of neuropathology, mitochondrial-based therapeutics should have broad benefits for the prevention and treatment of neurodegenerative disorders by improving energy production, decreasing oxidative stress and reducing inflammation.

1.10 Flavonoids as potential neurotherapeutics

Flavonoids are biologically active phenolic compounds abundant in teas, fruits and vegetables that have attracted considerable attention for the prevention and treatment of Alzheimer's disease, Parkinson's disease and stroke.⁸¹⁻⁸³ Habitual consumption of dietary flavonoids has been inversely associated with neurodegenerative disorders, cardiovascular disease and stroke. One of the largest meta-analysis to date covering 11 independent studies including a total of 356,627 patients found that increased flavonoid consumption was associated with reduced stroke-risk.⁸⁴ This study found a dose-response relationship in which there was an associated 9% risk-reduction per 100 mg incremental increase of total flavonoid ingestion per day.⁸⁴ Evidence that a flavonoid-enriched diet may reduce stroke-risk is further supported by the neuroprotective effects of these compounds against ischemic brain injury in numerous animal studies.⁸⁵

Over 11,000 flavonoids have been identified to date that exert beneficial effects through the modulation of multiple cell signalling pathways.^{91,86,84, 87} In brain, supra-physiologically concentrations ($\geq 10 \mu\text{M}$) for several flavonoid subtypes activate pro-survival signalling pathways (CREB and Akt), inhibit inflammatory signalling (NF- κB), reduce oxidative stress through the activation of Nrf-2, increase mitochondrial biogenesis by induction of PGC1- α and suppress platelet aggregation and vasodilation by elevating nitric oxide production.⁸⁸⁻⁹⁰ Flavonoids therefore exhibit pleiotropic effects that improve cellular bioenergetics, reduce oxidative stress and alleviate inflammation - all desirable features for the

treatment of a wide-range of neuropathological states. Since mitochondrial dysfunction is a central feature of many neurodegenerative disorders that appears to be alleviated by dietary flavonoid supplementation, understanding how flavonoids improve mitochondrial function may lead to the development of treatments for a broad-array of neurodegenerative disorders.⁹¹

1.11 Central hypothesis and research aims

My central hypothesis is that treatments which preserve mitochondrial function will be neuroprotective in cell-based and animal models of ischemic brain injury. This central hypothesis was tested by completing the following three research aims:

1. Assessment of the effects of combining the dietary flavonoids epicatechin and quercetin on mitochondrial function, cell signaling and neuronal survival in models of ischemic brain injury.
2. Examination of the effects of global MCU deletion on hypoxic/ischemic brain injury, neuronal Ca^{2+} handling, bioenergetics and hypoxic preconditioning.
3. Determination of the neuroprotective potential of conditional neuron-specific MCU deficiency at adulthood against hypoxic/ischemic brain injury, mitochondrial bioenergetic deficits and damage.

Chapter 2 – Materials and Methods

2.1 Animals

All animal experiments were conducted in accordance with the Canadian Council of Animal Care and were approved by Dalhousie University committee of Laboratory Animals.

2.1.1 C57Bl/6 mice

Male C57Bl/6 mice aged 8-12 weeks of age were purchased from Charles Rivers and allowed to acclimate in the new animal care facility for 1 week prior to use. Animals were maintained on a 12/12 hour (h) light dark cycle and had *ad libitum* access to standard chow and water. Animals were gavaged with 37.5 mg/kg epicatechin (Sigma-Aldrich) and 37.5 mg/kg quercetin (Sigma-Aldrich) once daily for 5 consecutive days and were used for experimentation several hours following the final flavonoid dose.

2.1.2 Global mitochondrial calcium uniporter (G-MCU) nulls

A breeding pair of heterozygous MCU null (MCU^{+/-}) mice was generously provided by Dr. Toren Finkel (NIH, Bethesda, MD) and genotyped according to methods described by his laboratory.²³⁸ Mice were bred as Trios in wild-type x wild-type (WT), MCU^{+/-} x MCU^{+/-} and MCU^{-/-} x MCU^{-/-} to generate sufficient animals for experimentation. Age matched male animals were used for experimentation between 8 and 12 weeks of age. Animals were maintained on a 12/12 h light dark cycle and given *ad libitum* access to standard chow and water.

2.1.3 Conditional neuron-specific (CNS)-MCU deficient mice

Thy1-cre/ERT2-eYFP mice (The Jackson Laboratory; Stock No: 012708) were crossed with C57Bl/6 MCU-floxed (MCU^{fl/fl}) mice (generously provided by Dr. Jeffrey Molkenin, Philadelphia, Ohio, USA) to generate Thy1-cre/ERT2-eYFP^{+/-}/MCU^{fl/fl} mice. Tamoxifen (80 mg/kg) (Sigma-Aldrich) was administered once daily for 5 days by oral gavage to male Thy1-cre/ERT2-eYFP^{+/-}/MCU^{fl/fl} mice followed by a 3-week washout period to produce CNS-MCU deficiency. Thy1-cre/ERT2-eYFP^{+/-} mice which received the same tamoxifen dosing and washout period were used as controls. Age-matched male mice were used for experimentation between 8-12 weeks of age. Animals were maintained on a 12/12 h light dark cycle and given *ad libitum* access to standard chow and water.

2.1.4 Primary cortical neuron cultures

For the studies described in chapter 3 that investigated the neuroprotective properties of epicatechin and quercetin, and chapter 5 that examined the neuroprotective effects siRNA-mediated MCU knockdown, embryos were harvested from pregnant C57Bl/6 mice (Charles Rivers at E15-16). For the studies described in chapter 4 that examined the effects of global MCU (G-MCU) loss on ischemic neuronal damage, CD1 breeding pairs were established in house. Breeding pairs were (WT x WT) and (G-MCU null x G-MCU null). Breeding pairs were placed together for 3 days and then separated. Pregnant female mice were harvested 14 days later producing embryos with an age range

of E14-16. Embryonic brains were aseptically removed and placed in Neurobasal medium containing 10% fetal bovine serum (FBS) on ice. The meninges were then peeled back and the cortices transferred to 35 mm petri dishes containing Hanks Balanced salt solution (HBSS; Invitrogen) at 4°C. Cortices were pooled and treated with 2 ml of Stem-Pro® Accutase® cell dissociation reagent. The cortices were then triturated with a fire polished pipette 3-4 times and allowed to incubate for 15 minutes (min) at 37°C. This procedure was repeated a second time. Protease activity was inhibited by the addition of 1 ml FBS and the cortical tissue was transferred to a 15 ml falcon tube containing 3 ml of neurobasal mix (Neurobasal 500 ml + B27 + 500 µM glutamine + 20 µg/ml gentamicin; Life Technologies) at 4°C. The solution was then triturated 3-4 more times and allowed to settle. The supernatant was then collected and passed through a 40 micron filter. The neurons were then centrifuged at 300x G for 7 min and resuspended in neurobasal mix, counted and plated for experiments. Media changes were 60% of the total volume and occurred on the fourth day and every third day thereafter.

2.1.5 Oxygen glucose deprivation (OGD)

Primary cortical neuron cultures were used after 8-10 days *in vitro* for all OGD testing in chapters 3 and 4. Primary cortical neuron cultures were used after 7-8 days *in vitro* for all cultures used in chapter 5. Glucose-free balanced salt solution (GBSS) was prepared by bubbling nitrogen through the solution to remove oxygen. The cultures were then washed twice with oxygen free HBSS and placed

in air-tight containers that were purged with a gas mixture of 90% nitrogen, 5% carbon dioxide and 5% hydrogen for 5 min. Next, the air-tight containers holding the cultures were placed in a 37°C incubator for 1.5 h. OGD was terminated by aspirating the HBSS and replacing it with the original media. Cells were then harvested for future experiments at the indicated time points.

2.1.6 Drug and siRNA treatments of primary cortical neuron cultures

Cultures from chapter 3 were pretreated with epicatechin (E), quercetin (Q) or E+Q for 24 h before OGD, but not during OGD. Immediately after OGD, flavonoids were re-added to the cell cultures with the return of neurobasal media. Flavonoids stock solutions were prepared in DMSO (10 mg/ml) and diluted into 100 µl of neurobasal and then applied to neuronal cultures at final working concentrations (0.1-10 µM). DMSO (0.02%) containing neurobasal media was used as the control.

Neuronal cultures from chapter 5 were subjected to siRNA mediated knockdown. Four days after preparing the primary neuronal cultures, either a non-targeting siRNA or siRNA against the MCU [Accell non-targeting and Accell mouse MCU (215999), GE Healthcare Bio-sciences Co] was administered at a final concentration of 1 µM for 72 h in neurobasal media.

2.1.7 Cell viability assays

2.1.7.1 MTT [3-(4,5-dimethylthiazol-2-yl)-2,5-diphenyltetrazolium bromide]

Cell viability was assessed using an MTT (Sigma-Aldrich) assay performed in 48-well plates that each contained about 150,000 neurons. Briefly, 60 μ l of 10 mg/ml MTT (dissolved in no phenol red neurobasal) was added to each well. After incubation at 37°C for 1.0 h, 5% CO₂, the supernatant was removed and the formazan crystal was then dissolved in 200 μ l/well of dimethyl sulfoxide (DMSO, Sigma). The absorbance of each well was then measured at 592 nm with a plate reader (ELx 800, BioTek). The absorbance of blank wells (200 μ l DMSO) were subtracted from the absorbance of all of the other wells. The net absorbance of untreated no-OGD control wells were defined as 100% cell viability.

2.1.7.2 Fluorescent Assisted Cell Sorting (FACS)

Primary cortical neurons were used day 10-14 *in vitro* for FACS analysis using a FACSAria III (BD Biosciences, San Jose, CA, USA). OGD was performed as previously described.⁸⁸ Briefly, cells were washed in chilled HBSS containing 25 μ g/ml DNase followed by trypsin (2.5%) treatment for 5 min. The plates were then agitated by hand to completely lift the cells from the plates. Trypsin activity was terminated by the addition of neurobasal media containing 10% FBS. The neurons were then collected and centrifuged at 400x g for 5 min. The supernatant was then decanted and the neurons were resuspended in chilled HBSS containing 25 μ g/ml DNase and centrifuged at 400x g for 5 min. The neurons were then suspended in the binding buffer provided by the manufacturer

with the addition of 1% FBS and 25 µg/ml DNase, to a concentration of 10^6 cells/ml. A 100 µl aliquot of this cell suspension was treated with both Annexin V conjugated to phycoerythrin (PE) and 7-AAD provided in the PE Annexin V Apoptosis Detection Kit (BD Biosciences, Mississauga, Canada). Annexin V binds to extracellularly exposed phosphatidylserine. Annexin V-positive cells were considered early apoptotic. 7-AAD is a cell impermeant dye that only enters cells which have suffered membrane damage. 7-AAD-positive cells were considered late apoptotic and/or necrotic. Neurons negative for both PE Annexin V and 7-AAD were defined as viable. Percent cell viability in OGD-exposed cortical cultures was expressed relative to the number of double negative cells in untreated (control) cortical cultures.

2.1.7.3 Trypan Blue Assay

Neurons were washed with phosphate buffered saline (0.01 M, pH 7.4; PBS) and trypsinized with 50 µl of 2.5% trypsin (Sigma) for 3 min. Enzymatic activity was stopped by the addition of neurobasal culture medium containing 10% FBS (100 µl). Neurons were then treated with 150 µl of 0.4 % trypan blue (Sigma) and incubated for 10 min at 37°C. Neurons were then counted using a Bio-Rad TC20™ automated cell counter.

2.1.8 Oxygen Consumptions Rates (OCR) and Extracellular Acidification Rates (ECAR) in primary cortical neuronal cultures

OCR and ECAR measurements were performed for cortical neurons cultured in 24 well Seahorse plates and read with an XF24 extracellular flux analyzer (Seahorse Bioscience). Calibration of sensor cartridges and the XF24 analyzer were done according to the manufacturer's recommendations. Neurons were cultured and subjected to OGD according to sections 2.1 and 2.2.

Experimentation was performed on neurons at 7-9 days *in vitro*. Culture media was replaced 30 min before experimentation with Seahorse assay media (cat# 102352-000) supplemented with 10 mM Glucose, 2 mM sodium pyruvate and 1 mg/ml fatty acid free bovine serum albumin (BSA) (chapter 3) or artificial cerebral spinal fluid containing: NaCl (120 mM), KCl (3.5 mM), CaCl₂ (1.3 mM), KH₂PO₄ (0.4 mM), MgCl₂ (1 mM) HEPES (20 mM), glucose (15 mM), sodium pyruvate (2 mM) and fatty acid free BSA (4 mg/ml) (chapters 4 and 5). Mitochondrial function was probed by measuring OCR following the sequential addition of oligomycin (2 μM), FCCP [carbonyl cyanide 4-(trifluoromethoxy) phenylhydrazone] (2 μM), rotenone (300 nM) and antimycin (5 μM) (all compounds purchased from Sigma-Aldrich). Mitochondrial function measurements were performed 1-2 h after OGD. A minimum of three measurements were performed for each condition. OCR was normalized against the total number of live cells (chapter 3 and 4) or protein concentration (chapter 5) at the end of the experiment determined by a trypan blue assay or the Bio-rad protein assay, respectively.

2.1.9 Quantitative PCR (qRT-PCR)

RNA was extracted with an Aurum total RNA minikit (Bio-Rad, cat# 732-6820) from primary neurons. Brain RNA was extracted using an Aurum total RNA Fatty and Fibrous Tissue pack (cat#732-6670). The spin protocols were performed according to the manufacturer's instructions. After elution, the quality and integrity of the RNA was assessed using a Bio-Rad experion bioanalyzer with an RNA StdSns analysis kit. Only RNA with values above 7.5 were used for further analysis. RNA was quantified using an Epoch microplate spectrophotometer (BioTek Instruments, Vermont, USA). Reverse transcription was carried out with the iScript cDNA synthesis kit (Bio-Rad) using 750 ng of template RNA for each sample. Negative controls (without the reverse transcriptase present) were run in every reaction. qRT-PCR was performed with a SsoFast EvaGreen Supermix kit (Bio-Rad) with β -actin, GAPDH, B2M and HPRT1 evaluated as reference genes (Table 1). Individual genes were optimized for both annealing temperature and concentration. Thus, the qRT-PCR program was: 95°C \times 30 seconds (s) + (95°C \times 5 s + 58°C \times 5 s + plate reading) \times 40 cycles + melting curve. The melting curve programme was a 2 second stop with plate reading for every 0.5°C increase from 65°C to 95°C. Each qRT-PCR experiment was performed with a Bio-Rad CFX 96 real time system C1000 Touch thermal cycler. All qRT-PCR protocols were done in accordance with the MIQE guidelines⁹². Analysis was performed using the Bio-Rad CFX Manager 3.1 software using the $\Delta\Delta Cq$ method. The primer sets are listed below:

Gene	Forward Primer	Reverse Primer
Bcl-xL	AGCAGGTAGTGAATGAACTCTTTCCG	CCATCCAACCTTGCAATCCGACTC
BAX	TGCTGATGGCAACTTCAACTG	GATCAGCTCGGGCACTTTAGTG
MT-ND2	GGGCATGAGGAGGACTTAACCAAAC	TGAGGTTGAGTAGAGTGAGGGATGG
NCX-1	AAAGAGTGCAGTTTCTCCCTTG	TGAAGCCACCTTTCAATCCTC
NCX-2	ATGGCTCCCTTGGCTTTGATG	CAGCGGTAGGAACCTTGGC
NCX-3	GTGAACCGAAATGGATGGAACG	TCACCCAATACTGGCTTTCCC
PMCA2	AAAGAGAAGTCGGTGCTTCAG	GTGTGCATTCCGTCAGCCA
β -actin	GTGACGTTGACATCCGTAAAGA	GCCGGACTCATCGTACTCC
GAPDH	AGGTCGGTGTGAACGGATTTG	GGGGTCGTTGATGGCAACA
B2M	TTCTGGTGCTTGTCTCACTGA	CAGTATGTTCCGGCTTCCCATTC
HRPT	TCAGTCAACGGGGGACATAAA	GGGGCTGACTGCTTAACCAG
PGC-1 α	CAATGAATGCAGCGGTCTTA	GTGTGAGGAGGGTCATCGTT
Bcl-2	ATGCCTTTGTGGAACATATATGGC	GGTATGCACCCAGAGTGATGC
MT-ATP6	AATTACAGGCTTCCGACACAAAC	TGGAATTAGTGAAATTGGAGTTCCT

2.1.10 Multiplexed Enzyme Linked Immunoassays (ELISAs)

Multiplex ELISAs were performed using Bio-Plex® reagents purchased from Bio-Rad (Mississauga, Ontario) to measure levels of phospho-Akt (Ser-473; cat# 171V60001M), Phospho-CREB (Ser-133; cat# 171V50028M), Total-Akt (cat# 171V60001M) and Total-CREB (cat# 171V60013M). Primary cortical neuron cultures were treated with vehicle (0.02% DMSO), E, Q or E+Q (0.1 or 0.3 μ M) for 30 min, washed and lysed using reagents purchased from Bio-Rad (cat#171304006M). In the case of the lysis buffer, phenylmethanesulfonyl fluoride was included to reach a final concentration of 2 mM immediately prior to

use. Protein samples (100 µg/ml) were then added to Bio-Plex® plates loaded with the capture antibody and allowed to incubate for approximately 15 h on a shaker set at 400 rotations per min (rpm). Next the wells were washed and treated with the detection antibody for 30 min in the dark with shaking at 400 rpm. The wells were then washed, treated with streptavidin-phycoerythrin, washed and analyzed using a Bio-Plex® 200 system that employs Luminex® xMAP® technology.

The phosphorylation of pyruvate dehydrogenase was examined using a multi-species pyruvate dehydrogenase complex magnetic bead panel (cat# PDHMAG-13K, EMD Millipore). This kit is a multiplex ELISA for total pyruvate dehydrogenase as well as three serine (Ser) phosphorylated isoforms: PDH (Ser 232), PDH (Ser 293) and PDH (Ser 300). Analyses were performed using primary neurons derived from WT or G-MCU null embryos cultured for 8-10 days treated with 1 of the 3 conditions: control, glutamate (Sigma-Aldrich) or ionomycin (Cayman Chemicals). Controls were naïve to any treatment and harvested directly from the neurobasal media. Glutamate samples were treated with glutamate (25 µM) for 30 minutes and immediately harvested. Ionomycin samples were treated with ionomycin (2 µM) for 30 minutes and immediately harvested. Samples were split into 2 aliquots – one for protein concentration determination and one for PDH analyses. Protein concentration was determined using the Bio-Rad protein assay (Cat# 500-0006). All procedures were done in accordance with the manufactures instructions and analyzed on a Bio-Plex® 200

system. Protease and phosphatase inhibitor cocktails (EMD chemicals cat # 535140 and 524629) were also added to the lysis buffer following the manufacture's suggestions.

2.1.11 Confocal imaging of cytosolic calcium concentrations $[Ca^{2+}]_c$ and the mitochondrial membrane potential

Neurons were seeded onto 35 mm imaging dishes at a density of 10^6 /dish and maintained as described in section 2.1. Imaging was performed on days 8-10 *in vitro*. Neurons were pretreated with Fluo-4 AM (5 μ M; Sigma-Aldrich) for 30 minutes in a 37°C incubator prior to imaging. This was followed by replacement of the culture media with artificial cerebral spinal fluid (aCSF: 120 mM NaCl, 3.5 mM KCl, 1.3 mM $CaCl_2$, 0.4 mM KH_2PO_4 , 1mM $MgCl_2$, 20 mM HEPES, 15 mM glucose, 2mM pyruvate and 4 mg/ml fatty acid free BSA, pH 7.2).

Tetramethylrhodamine methylester (TMRM, 50 nM; Sigma-Aldrich) was then loaded for 10 min followed by imaging with a Zeiss LSM meta 510 confocal microscope using a 40X magnification oil immersion lens to measure the mitochondrial membrane potential. TMRM was excited using a 543 nm laser and the emission detected at 560 nm. A 488 nm Argon laser was used to excite Fluo-4 with the emission detected at 505-550 nm to measure $[Ca^{2+}]_c$. Laser intensity was kept to a minimum to avoid bleaching for both lasers (held between 1.8-2.0% of maximum laser output). Pinhole size varied among experiments and ranged between 60-90 μ m. Images were captured with scanning area resolution of 1024 x1024. Thapsigargin (TG, 5 μ M; Sigma-Aldrich) was added to estimate

Ca²⁺ stored in the endoplasmic reticulum. FCCP (2 μM) was added next to measure the effects of complete mitochondrial depolarization on the Fluo-4 and TMRM signals.

2.1.12 Hypoxic preconditioning (HPC)

Wild-type (WT) or G-MCU null mice were placed in a chamber maintained at 36.5°C and vented with 8% oxygen balanced with nitrogen flowing at a rate of 4 l/min for 50 min to induce HPC. Mice that served as sham controls for HPC were placed in the same apparatus maintained at 36.5°C except the chamber was vented at 4 l/min with normal atmospheric air (20% oxygen) for 50 min.

2.1.13 Hypoxic-ischemic (HI) brain injury

Common carotid artery occlusion followed by placement in a low oxygen chamber to produce HI brain injury in mice was adapted from the method developed by Levine for rats⁹³. All procedures were ethically approved by the University Committee on Laboratory Animals at Dalhousie University. Male mice (8-12 weeks of age) were anesthetized using isoflurane (3% with medical oxygen at a flow rate of 3 l/min). The ventral portion of the neck was shaved and cleaned with soluprep and betadiene (SoluMed Inc; Laval, QC Canada and Purdue Frederick Inc; Pickering, ON, Canada, respectively). Anesthesia was maintained with 3% isoflurane with an oxygen flow rate of 1.0 l/min. To alleviate pain following recovery, mice were injected intraperitoneally (i.p.) with ketoprofen (5 mg/kg; Cayman Chemicals). An incision (1 cm) was made with a scalpel to

expose the sternohyoid and sternomastoid muscles. The left carotid artery was isolated and removed from the vagus nerve by blunt dissection. The common carotid was then permanently occluded using a high temperature electrocautery pen (Bovie Instruments; St. Perersberg, FL, USA). Incomplete occlusions and/or animals displaying blood loss were immediately euthanized and excluded from the study. Following a 2-3 h recovery period, animals were placed in a low oxygen chamber (8% oxygen balanced with nitrogen, flow rate 4 l/min). Following the low oxygen chamber, mice were removed and individually housed to recover for 24 h. Animals in chapters 3 and 4 were placed in the hypoxia chamber for 40 minutes. Animals in chapter 5 were placed in the hypoxia chamber for 50 minutes.

2.1.14 Neuroscore to assess general conditions of sensorimotor behavioural deficits

A comprehensive behavioural assessment of sensorimotor deficits produced by HI brain injury was performed using a neuroscore scale developed by Dr. Ulrich Dirnagl (Charité - Universitätsmedizin Berlin, Germany). Scores ranged from 0 (healthy) to 56 (the worst performance in all categories) and represented the sum of scores for 6 general deficit categories (hair, ears, eyes, posture, spontaneous activity and epileptic behaviour categories) and 7 focal deficits categories (body symmetry, gait, climbing on angled surface, circling behaviour, front limb symmetry, compulsory circling, whisper response to light touch).

The 6 general deficit categories were scored as follows: 1. *Hair*. Mouse observed on an open bench top (OBT) without interference: 0 - Hair neat and clean, 1 - Localized piloerection and dirty hair in 2 body parts (typically nose and eyes); 2 - Piloerection and dirty hair in more than 2 body parts. 2. *Ears*. Mouse on observed on an OBT without interference. Mouse then stimulated by snapping fingers. 0 - Normal reaction, ears are stretched laterally and behind; 1 - Partial reaction, ears stretched laterally but not behind (one or both); 2 - No reaction to noise. 3. *Eyes*. Mouse on OBT. Observed with no interference. 0 - Open, clear, quickly follow the surrounding environment/movement. 1 - Open and characterized by aqueous mucus. Slowly follow the surrounding environment; 2 - Open and characterized by dark mucus; 3 - Ellipsoidal shaped and characterized by dark mucus; 4 - Closed. 4. *Posture*. Mouse placed on the palm and swung gently. 0 - The mouse stands up in the upright position with the back parallel to the palm. During the swing, it stands rapidly; 1 - The mouse stands humpbacked. During the swing, it flattens the body to gain stability; 2 - The head or part of the trunk lies on the palm; 3 - The mouse lies on one side, barely able to recover into the upright position; 4 - The mouse lies in a prone position, not able to recover/stand. 5. *Spontaneous Activity*. Mouse on OBT. No interference. 0 - The mouse is alert and explores actively; 1 - The mouse seems alert but it is calm and sluggish; 2 - The mouse explores intermittently and sluggishly, 3 - The mouse is somnolent and numb, few movements on the spot; 4 - No spontaneous movements. 6. *Epileptic behaviour*. Mouse on OBT. The worst behaviour is recorded during the whole observation period. 0 - None; 3 - The mouse is reluctant to handling,

shows hyperactivity; 6 - The mouse is aggressive, stressed and stares at environment; 9 - The mouse shows hyper-excitability, chaotic movements and presence of convulsion during handling or after handling; 12 - Generalized seizures associated with wheezing and unconsciousness.

The 7 focal deficits categories were scored as follows: 1. *Body Symmetry*. Mouse on OBT, observation of resting behaviour, the nose-tail line observed. 0 - Normal (normal posture, tail is straight); 1 - Slight asymmetry (body leans on one side with fore- and hind-limbs beneath the body, tail is slightly bent); 2 - Moderate asymmetry (body leans on one side with fore and hind-limbs stretched out, tail is slightly bent); 3 - Prominent asymmetry (body bent, one side is on the OBT, tail is bent); 4 - Extreme asymmetry (highly bent, on one side constantly lies on the OBT). 2. *Gait*. Mouse on OBT, undisturbed movements. 0 - Normal. Flexible, symmetric and quick; 1- Stiff, inflexible. Walks humpbacked, slower than normal; 2 - Limping with asymmetric movements; 3 - Trembling, drifting, falling; 4 - Does not walk spontaneously (gently pushed with pen to stimulate walking. If mouse takes no more than 3 steps, then receives a score of 4). 3. *Climbing*. Place mouse on a gripping surface 45 degrees to OBT. Placed in the centre of the surface and observed. 0 - Normal, climbs quickly to the top; 1 - Climbs with strain, limb weakness apparent; 2 - Holds onto slope, does not slip or climb; 3 - Slides down slope, unsuccessful effort to prevent fall; 4 - Slides immediately, no effort to prevent fall. 4. *Circling behaviour*. Mouse observed on OBT. 0 - Absent. Turns equally to both sides; 1 - Predominately one sided turns; 2 - Circles to one sides, not constantly; 3 - Circles constantly to one side; 4 - Pivoting, swaying or

no movement. 5. *Forelimb symmetry*. Mouse suspended by the tail. Movements and position of forelimbs are observed. 0 - Normal. Both forelimbs are extended towards the bench and move actively; 1 - Light asymmetry. Contralateral limb does not extend entirely; 2 - Marked asymmetry. Contralateral forelimb bends towards the trunk. The body slightly bends on ipsilateral side; 3 - Prominent asymmetry. Contralateral forelimb adheres to the trunk; 4 - Slight asymmetry. Body/limb movement. 6. *Compulsory circling*. Forelimbs on bench. Hind-limbs are suspended by the tail. This position reveals the presence of contralateral limb palsy. 0 - Absent. Normal extension of both forelimbs; 1 - Tendency to turn to one side. The mouse extended both forelimbs, but starts to turn preferably to one side; 2 - Circles to one side. The mouse turns towards one side with a slower movement compared to healthy mice; 3 - Pivots to one side sluggishly. The mouse turns towards one side failing to perform a complete circle; 4 - Does not advance. The front part of the trunk lies on the bench. Slow and brief movements. 7. *Whisker Response*. Mouse on the bench. Using a pen, whiskers touch gently at the tip of the ears from behind, first one on the side with a lesion, then on the contralateral side. 0 - Normal symmetrical response. The mouse turns the head towards the stimulated area and withdraws from the stimulus; 1 - Light asymmetry, the mouse withdraws slowly when stimulated on the ischemic side. Normal response on the contralateral side; 2 - Prominent asymmetry. No response when stimulated on the side contralateral to ischemic injury. Normal response on the contralateral side; 3 - Absent response on the contralateral side, slow response when stimulated on the ipsilateral side; 4 - Absent response, no response when stimulated on the ipsilateral or contralateral sides. Single blinding was used for behavioural analysis.

2.1.15 Measurement of infarct volume using TTC

Infarct volume was evaluated using TTC (2,3,5-Triphenyltetrazolium chloride; Sigma-Aldrich) staining. Mice were humanely euthanized by injection of sodium pentobarbital (150 mg/kg; i.p.) and perfused with PBS. The brain was rapidly removed and cut into 1 mm coronal sections that were stained with PBS containing 2% TTC for 15 min at 37 °C. Sections were then fixed in PBS containing 4% formaldehyde for 20 min and stored in PBS containing 1% formaldehyde until image analysis. Images were captured with a Canon PowerShot SD1400IS Digital ELPH 14.1 megapixel camera. The area encompassing the infarct for 5 serial sections (1 mm thick) that spanned bregma 3.0 mm to -2.0 mm was calculated and converted into a volume using image J (version 1.48v).

2.1.16 Histological analysis of neuronal damage by Fluor Jade staining

Mice were injected intra-peritoneally (i.p.) with an overdose of pentobarbital (150 mg/kg) and perfused transcardially with saline (10 ml) followed by 0.1 M phosphate buffer containing 4% paraformaldehyde (pH=6.5; 10 ml) to fix the brain. The brain was then removed and post-fixed in 0.1 M phosphate buffer containing 2% paraformaldehyde for 24 h followed by cryoprotection for 48 hr in 0.1 M phosphate buffer containing 30% sucrose. The brain was then frozen and coronal sections 30 µm thick were cut at the level of dorsal hippocampus (-1.7 to -1.9 mm from bregma) and striatum (1.18 to 0.98 from bregma) with a cryostat.

Sections were stained with Fluoro-Jade (FJ; AG325-30MG; EMD Millipore Canada) according to the manufacturer's recommendations. Slides were then cover-slipped with Fluorescence-preserving VECTASHIELD Mounting medium (Vector, H-1,000) and observed under a Zeiss fluorescence microscope equipped with a computer-assisted image analysis system. FJ staining was quantified by determining the area occupied by FJ-positive neurons in CA1 region of the dorsal hippocampus (150 x 300 μm), motor cortex (300 x 300 μm) and dorsolateral striatum (300 x 300 μm).

2.1.17 Transmission electron microscopy

Mice were injected with an overdose of pentobarbital (150 mg/kg, i.p.) and perfused transcardially with saline (10 ml) followed by 0.1 M phosphate buffer containing 2.5% glutaraldehyde (10 ml) to fix the brain. Whole brains were fixed in 2.5% glutaraldehyde in PBS (pH 7.4) over night and processed in the EM Core Facility (Dalhousie University). Briefly, the samples were rinsed 3 times in 0.1 M sodium cacodylate buffer and fixed in 1% osmium tetroxide for 2 hr and, after dehydration, embedded in epon araldite resin. Sections 100 nm thick were cut with an ultramicrotome and placed on 300 mesh copper grids which were stained with 2% aqueous uranyl acetate, rinsed and treated with lead citrate, then rinsed and air dried. Images were captured with a Jeol Jem 1230 transmission electron microscope at 80 kV attached to a Hamatsu ORCA-HR digital camera. The effects of HI brain injury on mitochondrial damage were assessed in the ipsilateral CA1 region of the dorsal hippocampus. Mitochondria were considered

damaged if the integrity of the cristae were compromised. Ten photomicrographs from each animal were captured from the ipsilateral dorsal hippocampus and mitochondria (categorized as either healthy or damaged) were manually counted.

2.1.18 NAD⁺/NADH and pyruvate measurements

WT or G-MCU null mice were subjected to sham conditions or HI-induced brain injury as previously described. Thirty min later, all animals were humanely euthanized with an overdose of sodium pentobarbital (150 mg/kg, i.p.) and then perfused transcardially with saline (10 ml). The brains were then rapidly removed and the ipsilateral striatum and hippocampus dissected on ice and snap frozen in liquid nitrogen. Striatal NAD⁺ and NADH levels (abcam ab65348, Toronto, ON, Canada) and hippocampal pyruvate concentrations (ab65342) were determined according to the manufacturer's instructions.

2.1.19 Forebrain mitochondrial isolation

Mice were euthanized by overdose injection of sodium pentobarbital (150 mg/kg, i.p.) followed by decapitation. Brains were immediately removed and the forebrain (cortex, hippocampus, thalamus, striatum and hypothalamus) placed in chilled isolation buffer [300 mM sucrose, 5 mM Tris-HCl, 2 mM EDTA, 0.5 mg/ml bovine serum albumin (BSA)]. The forebrains were then cut into small pieces and immediately homogenized with a dounce homogenizer. The forebrain homogenate was spun at 1000 xG for 10 min. The supernatant was then transferred to a new tube of isolation buffer and spun at 6500 xG for 10 min. The

supernatant was then discarded and the pellet was homogenized in 300 mM sucrose and 5 mM Tris-HCl, and spun at 6500 xG for 10 min. The supernatant was then discarded and the pellet containing mitochondria was homogenized in 300 mM sucrose and 5 mM Tris-HCl, creating a concentrated stock mitochondrial preparation which was used for subsequent experiments.

2.1.20 Mitochondrial Ca²⁺ uptake

Mitochondria were diluted in 2 ml of measuring buffer composed of mannitol (210 mM), sucrose (70 mM), MgCl₂ (5 mM), KH₂PO₄ (0.1 mM), calcium green 5-N (2 μM), rotenone (1 μM), succinate (10 μM), Tris-HCl (5 mM), pH 7.4, with or without ruthenium red (RR; 5 μM, data not shown). Uptake was monitored by calcium green 5-N fluorescence with excitation at 506 nm and emission at 532 nm.

Fluorescence was monitored over sequential additions of calcium to raise free Ca²⁺ concentrations by 5 μM increments. Each experiment was terminated with the addition of carbonyl cyanide p-trifluoromethoxyphenylhydrazone (FCCP, 10 μM).

2.1.21 Ca²⁺-induced mPTP opening

Forebrain mitochondria were reconstituted in the measuring buffer that contained CGP-37157 (10 μM; Tocris Bioscience) to inhibit the mitochondrial Na⁺/Ca²⁺ exchanger. Tetramethylrhodamine methyl ester (TMRM, Sigma-Aldrich) was loaded at a concentration of 0.125 μM. Opening of the mPTP in WT mitochondria was induced by sequential additions of Ca²⁺ to raise the free Ca²⁺ concentrations

by 10, 25, 100 and 100 μM . Since G-MCU null mitochondria did not show Ca^{2+} -induced mPTP opening, FCCP (10 μM) was added to confirm depolarization of the mitochondrial membrane potential.

2.1.22 Western Blotting

Western blotting using antibodies against the MCU (1:1000) (D2Z3B, Cell Signalling) and β -actin (1:2500) (A2066, Sigma-Aldrich) was performed on protein extracts from the hippocampus to confirm MCU deficiency. Proteins were separated on a 5% stacking and 10% acrylamide gel run for 30 minutes at 50 V and at 150V until approximately 0.5-1.0 cm from the bottom of the gel. Transfer to PVDF membrane was run at 350 mA for 20 minutes. PVDF membranes were blocked using 5% dehydrated milk solution for 1 hour and washed three times with TBS-T. Primary antibodies were incubated overnight at 4°C and then washed three times with TBS-T. Appropriate secondary antibodies were run at a concentration twice that of the primary antibody. Bands were visualized using a GE healthcare Amersham ECL Prime western blotting detection kit (RPN2232) and imaged with a Bio-Rad ChemiDoc™ Touch (732BR0710). Semi-quantitative analysis was performed using Image J analysis.

2.1.23 Statistics and calculations

2.1.23.1 Chapter 3 Statistics and calculations

A one-way ANOVA followed by group comparisons with the Tukey's post hoc test was used to assess the effects of E, Q or E+Q on cell viability, OCR, mRNA

levels for Bcl-2, PGC-1 α , MT-ND2 or MT-ATP6 and the phosphorylation of Akt and CREB as well as the effects of L-N^G-Nitroarginine methyl ester on neuroprotection by E or Q was used to assess potential differences in infarct volume between mice pretreated with water or E+Q before HI.

A combinatorial index was used to measure the drug interactions between the flavonoids. The combinatorial index is calculated as written below:

$$CI = \frac{C_{a,x}}{IC_{x,a}} + \frac{C_{b,x}}{IC_{x,b}}$$

Here, C_{a,x} and C_{b,x} are the concentrations of each drug, when used in combination, to achieve X% drug effect. IC_{a,x} and IC_{b,x} are the concentrations of drug, when used individually, to achieve the same X% drug effect. When used in chapter 3, the effect used for calculations was the viability changes as measured by FACS analysis.

2.1.23.2 Chapter 4 Statistics and calculations

A two-way ANOVA followed by group comparisons with the Bonferroni's post-hoc test was used to assess potential differences between WT and G-MCU nulls for neuroscores, central neuron loss, cortical neuron viability loss after OGD, cortical neuron phosphorylation levels of PDH, cortical neuron OCRs and ECARs, NAD⁺/NADH ratios and pyruvate concentrations and mRNA levels in the hippocampus. An unpaired t-test was used to assess potential differences for mitochondrial damage and complex I (MT-ND2) mRNA levels between WT and G-MCU null mice.

2.1.23.3 Power calculations for group sizes

Power calculations were performed to determine the group sizes required to detect statistical differences for the animal experimentation. A group size of 12 mice with a standard deviation of 75% was needed to detect an 80% difference between the means for measurements of neuroscores, neuronal cell counts, NAD⁺/NADH and pyruvate concentrations with 100% accuracy for an alpha (α) level of 0.05.

2.1.23.4 Chapter 5 statistics and calculations

Power calculations were performed to determine the group sizes required to detect statistical differences for the animal experimentation. A group size of 8 mice with a standard deviation of 45% was needed to detect a 50% difference between the means for measurements of neuroscores and neuronal cell counts an alpha level of 0.05. Mann-Whitney tests were performed to assess potential differences between control and CNS-MCU deficient mice for neuroscores and mitochondrial damage. A two-tailed unpaired t-test was used to assess potential differences in MCU mRNA levels and cortical neuron viability loss after OGD. A two-way ANOVA followed by group comparisons with the Bonferroni's post-hoc test was used to assess potential differences between control and MCU-knockdown cortical neuron OCRs and ECARs and cortical neuron PDH phosphorylation levels.

Chapter 3 - Synergistic Neuroprotection by Quercetin and Epicatechin: Activation of Convergent Mitochondrial Signalling Pathways

3.1 Introduction and Rationale

Flavonoids are a diverse group of polyphenolic compounds comprised of approximately 9000 members that have received considerable attention for the prevention and treatment of stroke.^{85,86} These compounds have excellent safety,⁹⁴⁻⁹⁶ efficacy in a wide variety of models for ischemic stroke^{97, 98} and when consumed in the form of a flavonoid-enriched diet may reduce the risk of stroke.^{99, 100} Flavonols (quercetin) and flavan-3-ols (epicatechin), abundant in apple peel, are implicated in the protective effects of a flavonoid-enriched diet against stroke.^{81, 101-103}

I have proposed that these flavonoid sub-types activate distinct signal transduction pathways that converge on the mitochondrion, resulting in synergistic improvements in respiratory performance that confer profound resistance to ischemic brain injury.⁸⁷ In keeping with this hypothesis, oral administration of the flavonoid-enriched fraction AF4 (isolated from the peel of Northern Spy apples) improved mitochondrial function and reduced motor deficits, pro-inflammatory cytokine expression and damage in the central nervous system (CNS) of mice subjected to an experimental stroke or experimental autoimmune encephalomyelitis.^{88, 89} Epicatechin (E) and quercetin (Q) account for over 80% of the total phenolic content of AF4.⁸⁸ Cyanidin is a minor flavonoid

component that, together with chlorogenic acid, comprises most of the remaining phenolic content of AF4. Each of these four compounds exhibit anti-oxidant, anti-inflammatory and neuroprotective properties in a broad array of models for ischemic brain injury.^{97, 98, 104, 105} However, the effects of combining these compounds on neuronal mitochondrial function and resistance to ischemic brain damage have not been systematically studied.

I first compared the effects of E, Q, cyanidin and chlorogenic acid, either alone, or in combination, on the survival of primary cultures of mouse cortical neurons exposed oxygen glucose deprivation (OGD) that models energy depletion and reduced oxygen levels in ischemic stroke. These studies showed that combining E and Q (E+Q) synergistically reduced the death of cultured neurons exposed to a lethal period of OGD. Addition of cyanidin and chlorogenic acid did not enhance neuroprotection by E+Q suggesting that E and Q are primarily responsible for neuroprotective effects of AF4. Since mitochondrial collapse plays an important role in ischemic brain damage,^{87, 106, 107} I next compared the effects of E, Q and E+Q on key aspects of mitochondrial function and examined the signaling mechanisms that mediate neuroprotection by these flavonoids. Findings from these studies suggest that the activation of protein kinase B (Akt) and the elevation of cytosolic Ca^{2+} concentrations $[Ca^{2+}]_c$ by E and Q, respectively, synergistically improve key aspects of neuronal mitochondrial function, conferring marked resistance to ischemic damage. Oral administration of E+Q reduced brain damage in a mouse model hypoxic/ischemic (HI) brain

injury suggesting that combined treatment with these flavonoids may have therapeutic utility for the treatment of stroke.

3.2 Results

3.2.1 Cyanidin and chlorogenic acid fail to enhance neuroprotection by E+Q

Primary cortical neuron cultures subjected to OGD were used to model neuronal cell death resulting from ischemic/reperfusion injury.¹⁰⁸ I first determined the duration of OGD required to produce about a 50% loss in cell viability, as detected by a MTT assay, for subsequent experimentation (figure 3.1A). Relative to control cultures, cell viability was progressively reduced 24 h after 30, 60, 90, 120, 150 and 180 min of OGD to 91.5 ± 2.5 , 78 ± 3.5 , 49 ± 4.0 , 35 ± 5.0 , 30 ± 2.0 and $23 \pm 2.0\%$ (mean \pm SEM), respectively. A duration of 90 min (1.5 h) of OGD was therefore selected to assess flavonoid-mediated neuroprotection.

Pretreatment for 24 h with E (1 μ M) or Q (1 μ M), modestly elevated cell viability after OGD to $62.5 \pm 3.3\%$ and $65 \pm 4.9\%$, respectively (figure 3.1B). By contrast, E+Q (1 μ M) appeared to synergistically increase cell viability ($92 \pm 6.1\%$).

Neuroprotection by E+Q in combination with the other major AF4 phenolics, cyanidin (C) and chlorogenic acid (D), was no better than that observed with E+Q alone (E+Q+C, $79 \pm 9.2\%$; E+Q+C+D, $72 \pm 7.8\%$). Note that for each combination the individual flavonoids concentrations were proportionately reduced to maintain a total concentration of 1 μ M. Neuroprotection by E+Q (1 μ M) was reduced to $66.1 \pm 4.4\%$ by delaying addition to 0.5 h before OGD, indicating that pretreatment is required for full protection (data not shown).

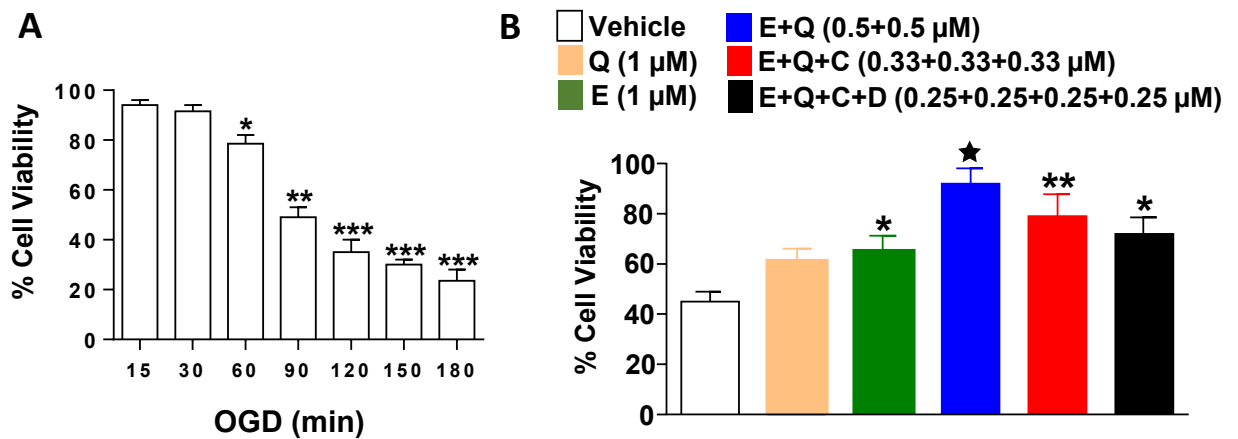


Figure 3.1 Protective effects of epicatechin, quercetin, cyanidin and chlorogenic acid against a lethal period of oxygen glucose deprivation

A) OGD duration-cell viability response relationship for primary cultures of mouse cortical neurons. Exposure to 90 min of OGD produced about a 50% loss of viability 24 h later as assessed by an MTT assay. * $p < 0.05$, ** $p < 0.01$ and *** $p < 0.001$ relative to no OGD. B) Percent cell viability 24 h after OGD (1.5 h) for cortical neuron cultures pretreated with vehicle (DMSO 0.02%), Q, E, E+Q, E+Q+C or E+Q+C+D (1 μ M) for 24 h before OGD. Each bar represents the mean \pm SEM of data from 6 experiments performed in duplicate (N=72 wells). * $p < 0.05$, ** $p < 0.01$ relative to vehicle. $\star p < 0.05$ relative to E or Q.

3.2.2 E+Q synergistically protected cortical neurons against OGD-induced cell death

Detailed concentration-response relationships for neuroprotection by E, Q and E+Q against OGD were performed next using the more sensitive method of Fluorescence Activated Cell Sorting (FACS) to count viable neurons. Cortical neuron cultures were pretreated with vehicle (DMSO 0.02%; 0 μ M), Q, E or E+Q (0.1-10 μ M) for 24 h and then subjected to OGD (1.5 h). Neurons were incubated 24 h later with Annexin V-PE and 7AAD. Viable (no staining), early apoptotic [Annexin V-PE (+)], late apoptotic [Annexin V-PE (+)/7AAD (+)] and necrotic [7AAD (+)] cells were detected using a FACS Aria III instrument. A-E:

Representative scatter plots showing viable (blue), apoptotic (magenta) and necrotic (red) neurons in control (no OGD) or OGD-exposed cultures pretreated with vehicle, Q, E or E+Q (figure 3.2A-E). Relative to OGD-exposed cultures pretreated with vehicle, Q or E (0.3 μ M), E+Q (0.3 μ M; E 0.15 μ M + Q 0.15 μ M) increased cell viability and reduced apoptosis. Concentration-response relationships for neuronal viability in OGD-exposed cultures were performed in cortical cultures pretreated with Q, E or E+Q (0.1-10 μ M) (figure 3.2F). Relative to control cultures (no OGD), neuronal viability was reduced from 42-49% by 90 min of OGD. Pretreatment with E, Q or E+Q produced concentration-dependent increases in neuronal survival after OGD. Moreover, sub- μ M concentrations of either E or Q were sufficient to increase neuronal survival [E (0.1 μ M = $57.7 \pm 2.0\%$; 0.3 μ M = $65.2 \pm 4.6\%$), Q (0.3 μ M = $61.8 \pm 6.9\%$)]. By comparison, equivalent concentrations of E+Q (0.1 μ M = E 0.05 μ M + Q 0.05 μ M; E+Q 0.3 μ M

= E 0.15 μ M + Q 0.15 μ M) produced larger increases in viable neurons [E+Q (0.1 μ M = 67.2 \pm 2.1%; 0.3 μ M = 80.6 \pm 3.1%)]. However, increasing concentrations of E, Q or E+Q beyond 0.3 μ M did not produce further increases in neuroprotection. Isobologram analyses of the resultant concentration-response data for Q, E and E+Q generated a combination index (CI) = 0.7 for E+Q, indicating synergism (CI < 1.0 = synergism) ¹⁰⁹ and thus confirming that pretreatment with E+Q synergistically protected cortical neuron cultures against OGD-induced cell death.

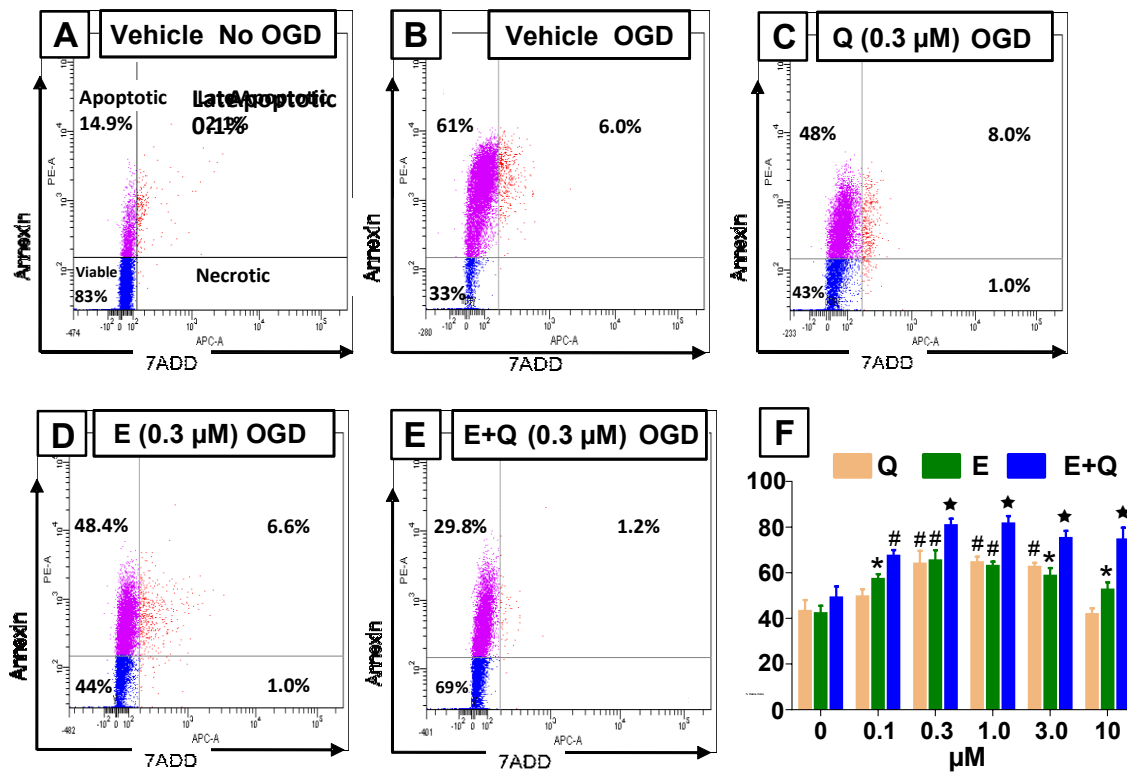


Figure 3.2 Epicatechin plus quercetin synergistically protect cortical neurons from damage by a lethal period of oxygen glucose deprivation

Cortical neuron cultures were pretreated with vehicle (DMSO 0.02%; 0 μM), Q, E or E+Q (0.1-10 μM) for 24 h and then subjected to OGD (1.5 h). A-E) Representative scatter plots showing viable (blue), apoptotic (magenta) and necrotic (red) neurons in control (no OGD) or OGD-exposed cultures pretreated with vehicle, Q, E or E+Q. F) Bar graph showing the concentration-response relationships for neuronal viability in OGD-exposed cultures pretreated with Q, E or E+Q. Each bar represents mean ± SEM of data from 5 experiments; n=5. *p<0.05 relative to cultures pretreated with vehicle and exposed OGD. #p<0.05 relative to E or Q (0.1 μM). ★p<0.05 relative to E+Q (0.1 μM).

3.2.3 E+Q enhanced mitochondrial respiration in OGD-exposed cortical neurons

To establish the effects of a neuroprotective concentration of E, Q or E+Q (0.3 μ M) on cellular bioenergetics, mitochondrial respiratory parameters including basal respiration, maximal respiration, spare respiratory capacity (SRC), ATP production and proton leak were measured with a Seahorse Extracellular Flux analyzer (figure 3.3A). Oxygen consumption rates (OCR) are expressed as percent change relative to basal respiration (100%). The SRC in cortical neurons treated with vehicle (V; 0.02% DMSO) for 24 h was 70% (figure 3.3B). E, Q or E+Q (0.3 μ M) elevated SRC to 110% (figure 3.3B). OGD reduced the SRC from 70 to 30% in vehicle-treated cultures (figure 3.3C). E or Q (0.3 μ M) failed to prevent this OGD-induced loss of the SRC. By contrast, pretreatment with E+Q (0.3 μ M) maintained the SRC in OGD neurons at 110%, consistent with the possibility that preserved mitochondrial function contributed to neuroprotection by this flavonoid combination.

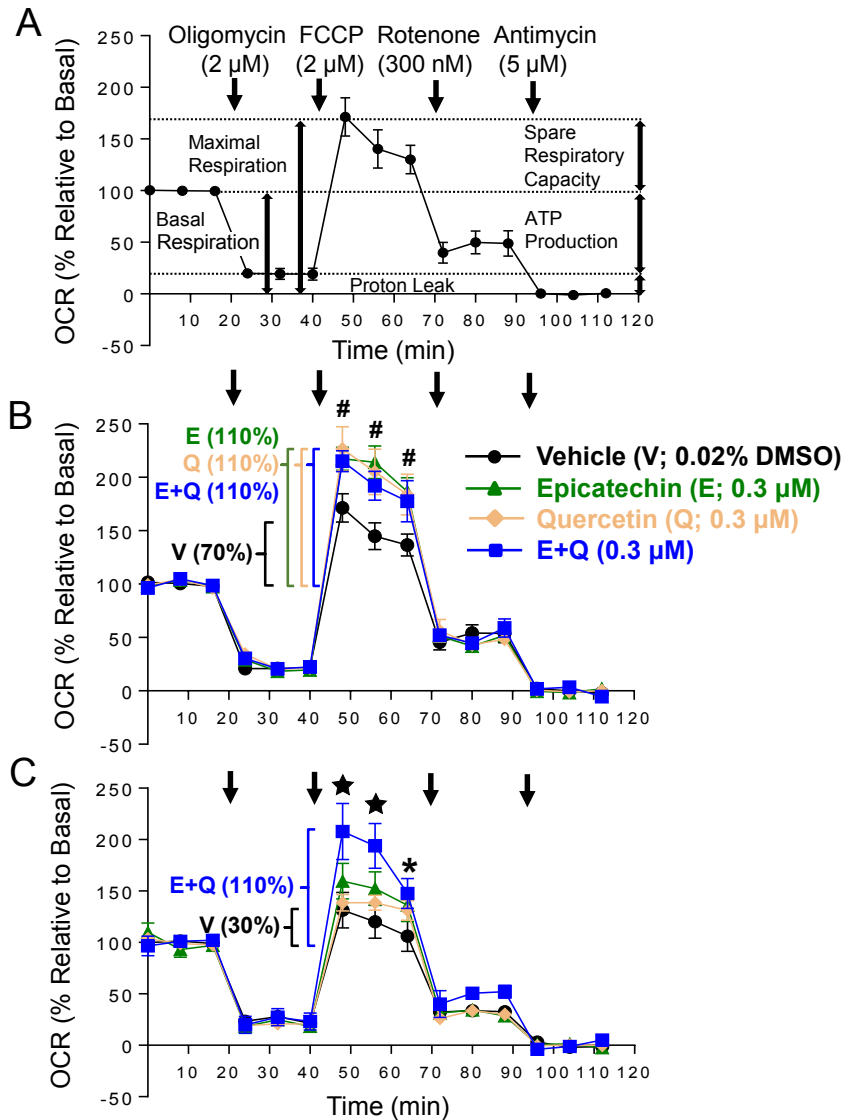


Figure 3.3 E+Q enhances mitochondrial respiration in OGD-exposed cortical neurons

A) Mitochondrial respiratory parameters including basal respiration, maximal respiration, spare respiratory capacity, ATP production and proton leak measured with a Seahorse efflux analyzer. Oxygen consumption rates (OCR) are expressed as percent change relative to basal respiration (100%). B) OCR in cortical neurons treated for 24 h with vehicle (V; 0.02% DMSO), E, Q or E+Q (0.3 μM). C) Mitochondrial respiration in cortical neurons 2 h after OGD (1.5 h). Each point represents the mean \pm SEM of data from 3 experiments performed in quintuplicate. * $p < 0.05$ relative to vehicle, $\star p < 0.05$ relative to all other groups.

3.2.4 E+Q increased anti-apoptotic and mitochondrial gene expression in OGD-exposed neurons

Quantitative RT-PCR was used to measure the effects of neuroprotective concentrations of E, Q or E+Q (0.1 or 1 μ M) on mRNA levels for proteins that inhibit apoptosis (Bcl-2), promote mitochondrial biogenesis (PGC-1 α) or comprise the electron transport chain [MT-ND2 (Complex I subunit) and MT-ATP6 (Complex V subunit)] in control and OGD-exposed neuronal cultures (figure 3.4). Consistent with neuroprotection by E and E+Q (0.1 μ M), Bcl-2 mRNA levels were elevated by these flavonoids in neurons subjected to OGD. Similarly, superior neuroprotection produced by E+Q (1.0 μ M) was accompanied by a larger increase in Bcl-2 mRNA levels relative to E or Q (1.0 μ M). The formation of new mitochondria (biogenesis) is initiated by the transcriptional regulating factor PGC-1 α ^{110, 111}. E+Q (0.1 or 1.0 μ M) elevated the expression of PGC-1 α to a greater extent than E or Q (0.1 or 1.0 μ M). Consistent with the potential induction of mitochondrial biogenesis by E+Q (0.1 and 1.0 μ M), MT-ND2 and ATP6 mRNA levels were also elevated by E+Q (0.1 or 1.0 μ M) and more than by E or Q (0.1 or 1.0 μ M) alone. These findings suggest that an elevation of mitochondrial gene expression may contribute to preservation of the SRC after OGD by E+Q.

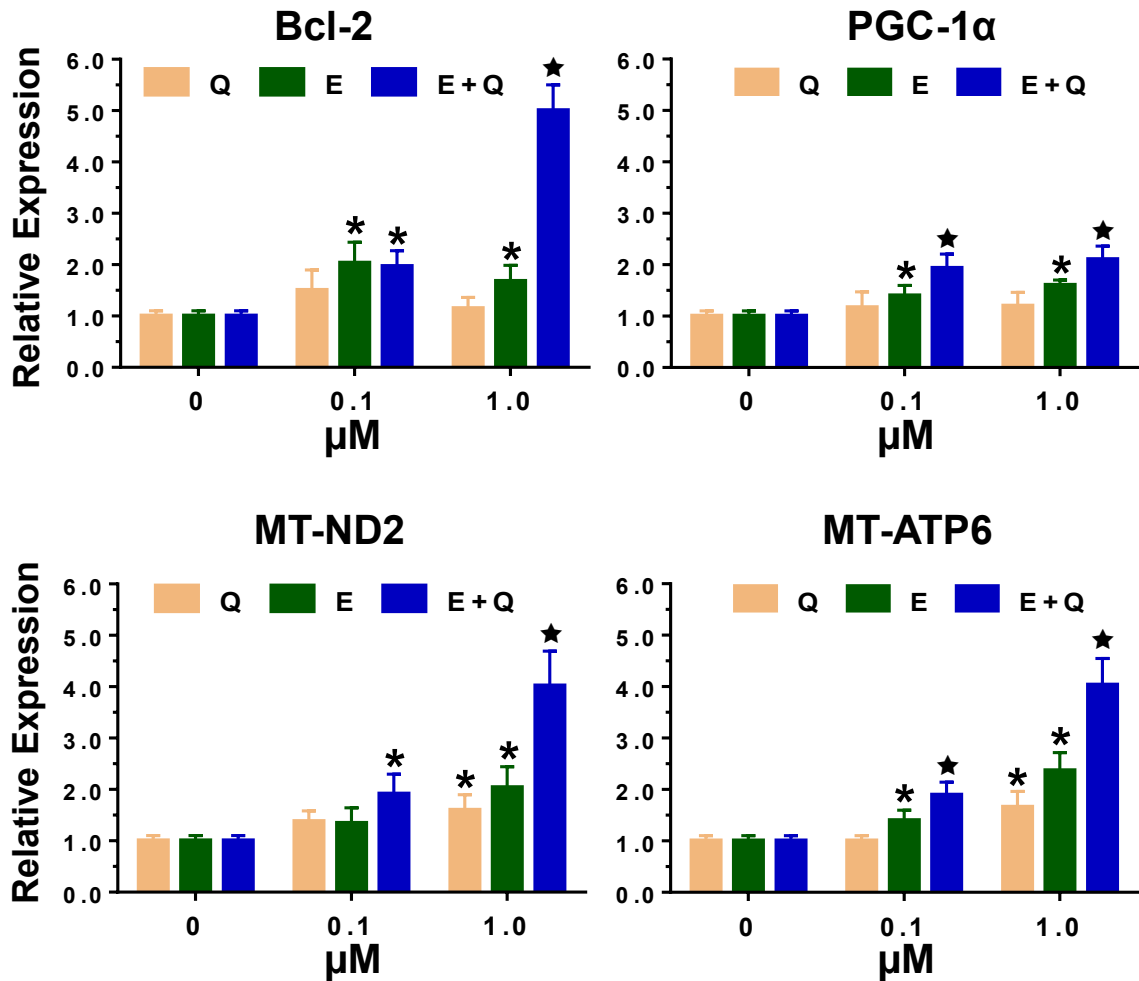


Figure 3.4 E+Q produces supra-additive increases in pro-survival (Bcl-2, PGC-1α) and mitochondrial gene expression (MT-ND2 and MT-ATP6) in cortical neurons after OGD

Levels of mRNAs are expressed relative to values for control cultures that were not subjected to oxygen glucose deprivation (OGD). Primary cultures of mouse cortical neurons were pretreated with vehicle (DMSO, 0.02%; 0 μM flavonoid) or E or Q or E+Q (0.1 or 1 μM) for 24 h before OGD (1.5 h) and mRNA levels measured 12 h later by qRT-PCR. *p < 0.05 relative to vehicle (0 μM), ★p < 0.05 relative to all other groups. Each bar shows the mean ± SEM of data from 3 experiments performed in quadruplicate, n=3.

3.2.5 Activation of Akt and CREB phosphorylation by E and Q

Neuroprotective concentrations of E and E+Q (0.1 and 0.3 μM) increased the phosphorylation of Akt at Ser-473. Activation of Akt stimulates pro-survival signaling, synaptic plasticity and mitochondrial biogenesis in neurons by phosphorylating Ser-133 of CREB that induces PGC-1 α gene expression.¹¹²⁻¹¹⁵ Consistent with the activation of this pathway, E and E+Q (0.1 and 0.3 μM) elevated the phosphorylation of CREB (Ser-133) (figure 3.5) and increased mRNA levels for PGC-1 α (figure 3.4). E and E+Q (0.1 μM) increased both CREB phosphorylation and mRNA levels for Bcl-2. Lastly, at a concentration of 1.0 μM , Q also enhanced CREB phosphorylation.

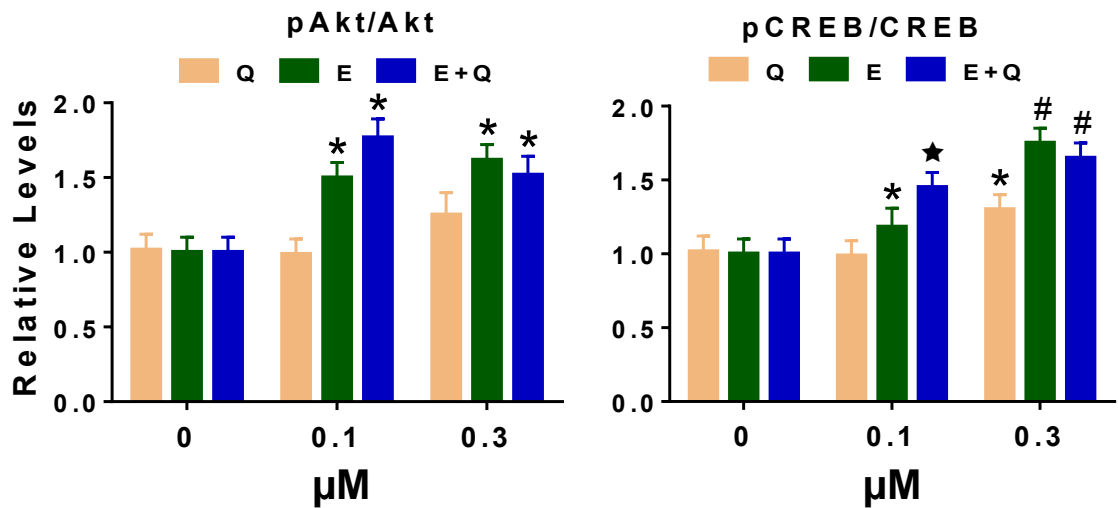


Figure 3.5 E and Q increase the phosphorylation of protein kinase B (Akt) and cAMP response element binding protein (CREB) in primary cultures of mouse cortical neurons

Primary cultures of mouse cortical neuron were treated with vehicle (DMSO, 0.02%; 0 μM flavonoid) or E or Q or E+Q (0.1 or 0.3 μM) for 30 minutes followed by total protein extraction. Levels of Akt, phosphorylated Akt (Ser-473; pAkt), CREB and phosphorylated CREB (Ser-133; pCREB) were determined by ELISA in the protein extracts. Phosphorylation of Akt and CREB are shown as the relative levels of pAkt to Akt and pCREB to CREB. *p<0.05 relative to vehicle (0 μM), ★p <0.05 relative to all other groups. #p<0.05 relative to Q. Each bar shows the mean ± SEM of data from 3 experiments performed in duplicate, n=3.

3.2.6 Q increases Ca²⁺ spikes, [Ca²⁺]_c and the mitochondrial membrane potential

Q increased the frequency of cytosolic Ca²⁺ oscillations which coincided with increased mitochondrial membrane potential. These measures were elevated in a concentration dependent manner by Q.

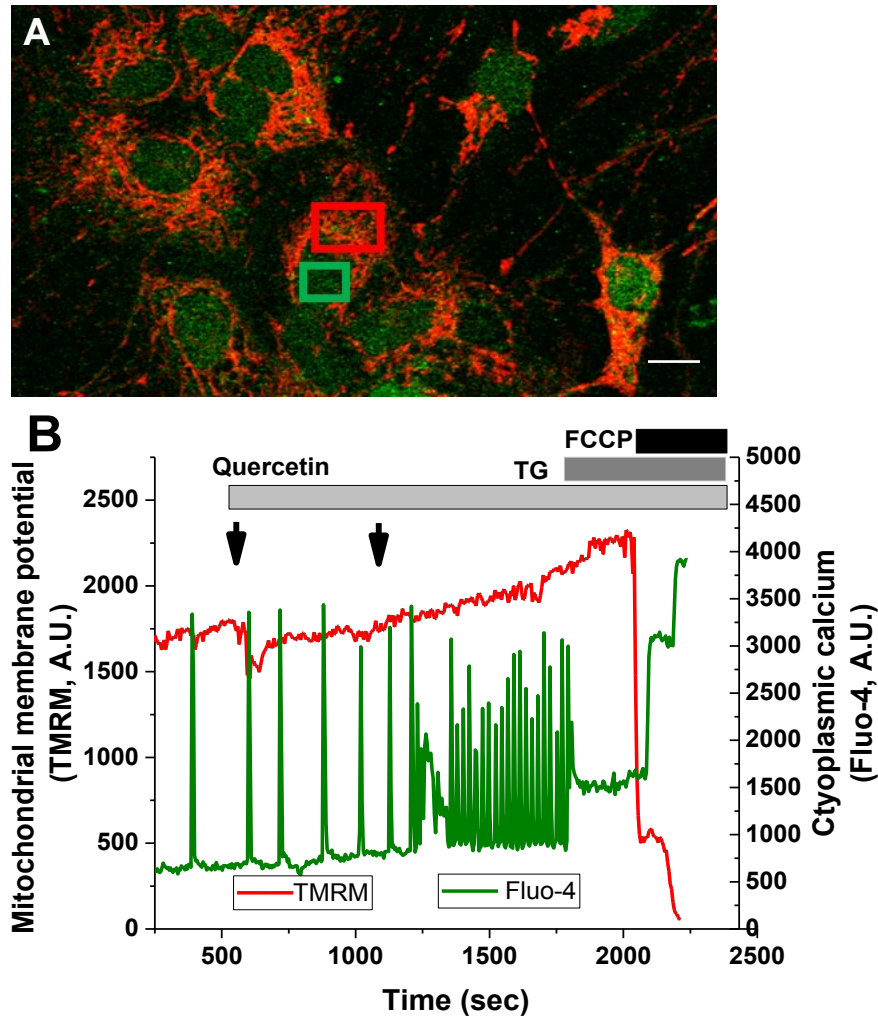


Figure 3.6 Quercetin stimulates Ca^{2+} signaling and elevates the mitochondrial membrane potential

A) Confocal image of cortical neurons co-loaded with probes for the mitochondrial membrane potential (TMRM, red signal) and cytoplasmic Ca^{2+} (Fluo-4, green signal). B: Time dependent measurements of fluorescent signals from representative individual Regions Of Interest (ROI: Boxes in A). Increasing concentrations of quercetin (0.3 and 3.0 μM ; arrows) stimulated Ca^{2+} oscillations (green spikes) and increased the mitochondrial membrane potential (red trace). Thapsigargin (TG; 5 μM) was added to estimate Ca^{2+} stored in the endoplasmic reticulum. FCCP (2 μM) induced complete mitochondrial depolarization and released Ca^{2+} from the mitochondrial matrix into the cytoplasm as evidenced by the increase in the Fluo-4 signal. Results are representative of 3 experiments performed in duplicate, $n=3$. Scale bar 5 μm .

3.2.7 The NOS inhibitor L-NAME blocked protection by E or Q against OGD-induced loss of neuronal cell viability

The induction of hypoxic preconditioning against OGD-induced neuronal cell death is blocked with the NOS inhibitor N-nitro-L-arginine and mimicked by NO donors.¹³⁶ Since E has been shown to increase NOS activity in endothelial cells,¹³⁷ I examined the effects of NOS inhibition with L-N^G-Nitroarginine methyl ester (L-NAME) on neuroprotection by E against the loss of cell viability produced by OGD (1.5 h). Relative to control cultures, OGD (1.5 h) reduced cell viability to $44 \pm 4.2\%$ (figure 3.7A). Pretreatment (24 h) with L-NAME (1 μM) did not alter viability after OGD ($47.3 \pm 4.1\%$) while E (0.3 μM) increased cell viability to $65.1 \pm 7.0\%$. However, inclusion of L-NAME (1 μM) with E (0.3 μM) blocked neuroprotection by E ($50.3 \pm 3.1\%$). Q activates endothelial NOS (eNOS) in a Ca^{2+} -dependent manner.^{138, 139} This suggests that Q-induced increases in $[\text{Ca}^{2+}]_c$ may precondition cortical neurons against OGD by activating NOS. I therefore examined the effects of NOS inhibition on neuroprotection by Q. Pretreatment with Q (1 μM ; 24 h) increased cell viability after OGD from $52.0 \pm 3.5\%$ to $69.0 \pm 6.0\%$ (figure 3.7B). Inclusion of L-NAME (1 μM) with Q (1 μM) reduced cell viability to $47 \pm 5.9\%$ indicating that NOS activity is also required for neuroprotection by this flavonoid.

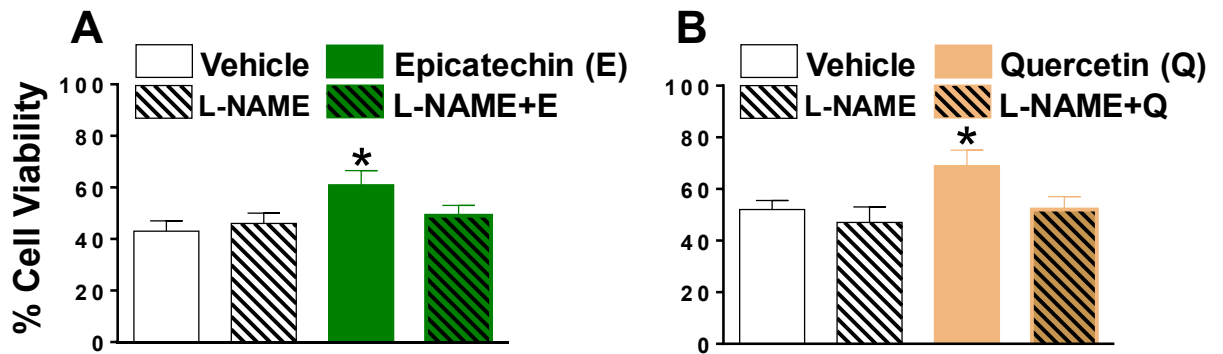


Figure 3.7 The NOS inhibitor L-NAME blocks protection by E and Q against OGD-induced loss of neuronal cell viability as by an MTT assay

A) Viability of cortical neurons pretreated (24 h) with vehicle (0.02% DMSO), L-NAME (1 μ M), E (0.3 μ M) or L-NAME (1 μ M) + E (0.3 μ M) 24 h after OGD (1.5 h). B) Viability of cortical neurons pretreated (24 h) with vehicle (0.02% DMSO), L-NAME (1 μ M), Q (1.0 μ M) or L-NAME (1 μ M) + Q (1.0 μ M) 24 h after OGD (1.5 h). * $p < 0.05$ relative to all other groups. Each bar shows the mean \pm SEM of data from 3 experiments performed in quadruplicate, $n = 3$.

3.2.8 Oral administration of E+Q reduced HI brain injury

In a final experiment, I determined whether oral administration of E+Q reduced brain damage in mice subjected to HI. Two groups of adult C57Bl/6 mice were dosed orally with either E+Q [75 mg/kg: E (37.5 mg) + Q (37.5 mg)] or water (8 ml/kg) once daily. Following five consecutive days of drug administration, all mice were subjected to HI (40 min). Infarct volume was measured 24 h later by staining of serial brain sections with the vital dye triphenyl tetrazolium chloride (TTC) (figure 3.8A). Relative to vehicle-treated mice, E+Q reduced the average infarct volume from $70 \pm 6 \text{ mm}^3$ to $38 \pm 7 \text{ mm}^3$ that represents a 46% reduction in infarct volume (figure 8B).

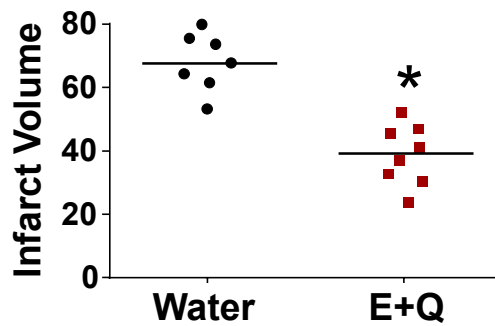
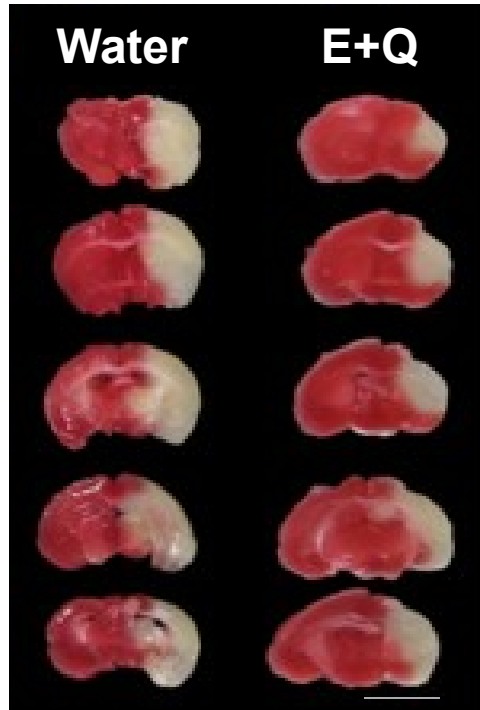


Figure 3.8 Oral administration of E+Q reduces HI brain injury

Mice were dosed orally with vehicle (water; 8 ml/kg) or E+Q (75 mg/kg) once daily. Five days later, all mice were subjected to HI and infarct volume measured 24 hrs later by TTC staining of brain sections (Top panel). E+Q significantly reduced infarct volume (mm³) (Bottom panel). *p<0.05 relative to water. Scale bar 0.5cm.

3.3 Discussion

The majority of cell-based studies have used concentrations of 5-10 μM of either E or Q to reduce the death of cultured neurons exposed to excitotoxins,¹⁴⁰⁻¹⁴³ free radical generators,¹⁴³⁻¹⁴⁷ mitochondrial toxins¹⁴⁸⁻¹⁵⁰ or OGD.^{140, 143, 151-156} Oral administration of these compounds to rodents at doses equivalent to amounts that appear to reduce the risk of neurodegenerative disorders^{95, 157, 158} are neuroprotective in models for stroke, Alzheimer's disease and multiple sclerosis, but only produce brain concentrations in the sub- μM range (0.1-0.4 μM).^{89, 117, 119, 159, 160} The relevance of findings from neuronal cell culture studies that have utilised flavonoid concentrations above 1 μM to assess their neuroprotective effects *in vivo* is therefore questionable.^{87, 157, 161-163} Hence, I have compared the neuroprotective effects of E, Q and E+Q on cultured neurons subjected to OGD at therapeutically relevant concentrations (0.1-1.0 μM). These compounds were selected for assessment based on their high content in the flavonoid-enriched fraction AF4 that we have shown to reduce motor deficits and CNS damage in mice subjected to HI brain injury and experimental autoimmune encephalomyelitis.^{88, 89} The protective effects of AF4 against OGD were not examined because it is composed mainly of Q glycosides⁸⁸ that must be metabolised to generate the more biologically active Q aglycone.^{164, 165}

3.3.1 E+Q synergistically protected cortical neurons against OGD-induced cell death

Primary cortical neuron cultures subjected to OGD were used to model neuronal cell death resulting from cerebral ischemia¹⁰⁸. OGD (90 min; 1.5 h) reduced cell viability to $49.0 \pm 4.0\%$ of control cultures (figure 1A). Pretreatment with E (1 μM) or Q (1 μM) modestly elevated cell viability after OGD to $62.5 \pm 3.3\%$ and $65 \pm 4.9\%$, respectively (figure 3.1B). By contrast, E+Q (1 μM) appeared to synergistically increase cell viability ($80.6 \pm 6.1\%$). Neuroprotection produced by E+Q in combination with the other major AF4 phenolics, cyanidin (C) and chlorogenic acid (D), was no better than that observed with E+Q alone. These findings indicate that E and Q are primarily responsible for the neuroprotective effects of AF4. Neuroprotection by E+Q was reduced when they were added only 0.5 hr before OGD (data not shown). This result is supported by numerous reports showing that flavonoid pretreatment for 24 h produces maximal neuroprotection by allowing sufficient time for adaptive changes in gene expression to occur that help resist oxidative damage.^{88, 140, 151, 153, 155, 156, 166}

Detailed concentration-response relationships for neuroprotection by E, Q and E+Q against OGD were performed using the more sensitive method of Fluorescence Activated Cell Sorting (FACS) to count viable neurons (figure 3.2). Relative to control cultures (no OGD), neuronal viability was reduced to approximately 45% by only 90 min of OGD. Pretreatment (24 h) with E, Q or E+Q produced a concentration-dependent increase in the resistance of cortical neurons to OGD-induced death (figure 3.2F). Moreover, sub- μM concentrations

of either E (0.1 μ M) or Q (0.3 μ M) were sufficient to increase neuronal survival. By comparison, equivalent concentrations of E+Q were more effective at protecting cortical neurons against OGD-induced death. Isobologram analyses of the resultant concentration-cell viability response data for E, Q and E+Q generated a combination index (CI) = 0.7 for E+Q (synergism: CI<1.0),¹⁰⁹ confirming that pretreatment with E+Q synergistically protected cortical neuron cultures against OGD. These findings suggest that E+Q are neuroprotective at the sub- μ M concentrations achieved in the brain following oral administration of these compounds.

3.3.2 E+Q prevented spare respiratory capacity loss after OGD

The effects of E, Q and E+Q on key aspects of mitochondrial function were assessed in cortical neuron cultures using a Seahorse Bioscience XF24 Extracellular Flux Analyzer (XF24). The XF24 creates a transient, 7 μ l chamber in specialized microplates enabling oxygen concentrations associated with respiring neurons to be determined in real time. Oxygen consumption rate (OCR) is a measure of electron transport chain activity.¹⁶⁷ Oligomycin (ATP synthase inhibitor; 2 μ M) blocks oxidative phosphorylation yielding a measure of cellular ATP production (figure 3.3A).^{168, 169} The remaining OCR after oligomycin treatment represents proton leak across the mitochondrial membrane.¹⁷⁰ To determine the maximal OCR that cells can sustain, the proton ionophore (uncoupler) FCCP (2 μ M) was injected. Use of FCCP at a concentration of 2 μ M was established by titration studies. The difference between basal and maximal

OCR is termed spare respiratory capacity (SRC).¹⁷¹ The SRC enables neurons to cope with the added energetic demands imposed by neurotransmission.¹⁶⁹

Treatment with E, Q or E+Q (0.3 μ M) for 24 h increased the SRC from 70% to 110%. Relative to control neurons (figure 3.3B), the SRC was reduced to from 70 to 30% by OGD (figure 3.3C). This loss was not reversed by E or Q (0.3 μ M), although there was a non-significant trend for preservation of the SRC by E ($p=0.1$ relative to vehicle treated cultures). By contrast, E+Q (0.3 μ M) completely prevented loss of the SRC in OGD neurons. Since SRC also confers resistance against oxidative injury,^{168, 172} these findings suggest that preservation of the SRC in OGD neurons contributed to neuroprotection by E+Q.

3.3.3 E+Q increased anti-apoptotic and mitochondrial gene expression in OGD-exposed neurons

Expression of mRNA was measured for proteins that inhibit apoptosis (Bcl-2), promote mitochondrial biogenesis (PGC-1 α) and members of the electron transport chain [MT-ND2 (Complex I subunit) and MT-ATP6 (Complex V subunit)] under both control and OGD-exposed neuronal cultures (figure 3.4). E+Q (0.1 μ M and 1.0 μ M) consistently induced similar or greater expression levels, relative to E or Q individually at the same concentration, for Bcl-2, PGC-1 α , MT-ND2 and MT-ATP6. These findings suggest an induction of mitochondrial biogenesis and mitochondrial-associated anti-apoptotic gene

expression that may contribute to the superior preservation of the SRC after OGD by E+Q.

3.3.4 Activation of Akt and CREB phosphorylation by E and Q

The flavonoids E and E+Q (0.1 and 0.3 μM) increased the phosphorylation of Akt at Ser-473, which activates a variety of pro-survival signaling pathways involved in synaptic plasticity and mitochondrial biogenesis in neurons. Akt stimulates these pathways by activating CREB via phosphorylation of Ser-133 of this transcriptional factor. Activated CREB then induces PGC-1 α gene expression resulting in elevated mitochondrial biogenesis.¹¹²⁻¹¹⁵ Consistent with CREB activation, E and E+Q (0.1 and 0.3 μM) induced the downstream phosphorylation of CREB (Ser-133) (figure 3.5) and increased mRNA expression for PGC-1 α (figure 3.4). E has previously been shown to increase CREB phosphorylation (Ser-133) in cortical neuron cultures in an Akt-dependent manner (0.1 and 0.3 μM).¹¹⁶ E reduced neuronal viability loss by OGD occurred at low concentrations (0.1-0.4 μM ; figure 3.2) achieved in brain following ingestion of neuroprotective doses of this flavonoid.¹¹⁷⁻¹¹⁹ Hence, this pathway may be relevant for the neuroprotective effects of this flavonoid in animals. E and E+Q (0.1 μM) increased both CREB phosphorylation and mRNA levels for Bcl-2. These findings are in keeping with the ability of CREB to promote neuronal survival by directly activating cAMP response elements (CRE) that drive Bcl-2 expression.¹²⁰⁻¹²² Lastly, at a concentration of 1.0 μM , Q also enhanced CREB phosphorylation. This suggests that a convergence of signaling pathways

activated by E and Q enabled E+Q (0.1 μ M) to produce a larger increase in CREB phosphorylation than E (0.1 μ M).

3.3.5 Q increases Ca^{2+} spikes, $[\text{Ca}^{2+}]_c$ and the mitochondrial membrane potential

The increased frequency of spikes in cytosolic Ca^{2+} induced by Q resulted in elevated $[\text{Ca}^{2+}]_c$ and mitochondrial membrane potential indicative of enhanced cellular bioenergetics.¹²³ Within 1-10 minutes of the addition of Q (10 μ M) to Jurkat cells, this flavonoid is selectively detected in mitochondria.¹²⁴ It has been estimated that this preferential mitochondrial accumulation enables Q to reach concentrations over 100 times greater in mitochondria than in the extracellular space.¹²⁴ This exquisite mitochondrial targeting is complimented functionally by evidence that flavonols (kaempferol and Q) increase mitochondrial Ca^{2+} uptake^{125, 126} and neuronal activity^{127, 128} by directly activating the mitochondrial Ca^{2+} uniporter (MCU) located in the inner mitochondrial membrane.¹²⁵ The primary role of mitochondrial Ca^{2+} is to stimulate energy production^{129, 130} which is achieved by the allosteric activation of mitochondrial enzymes necessary for generating reducing equivalents,¹²⁹ metabolic substrates¹³¹ and electron transfer.¹³² The increase in mitochondrial membrane potential produced by Q that drives ATP production is therefore suggestive of improved mitochondrial efficiency. Q also elevates $[\text{Ca}^{2+}]_c$ by activating L-type Ca^{2+} channels,¹³³ $\alpha 7$ nicotinic acetylcholine receptors¹³⁴ and ryanodine channels¹³⁵ indicating that a

variety of mechanisms may account for the ability of this flavonoid to increase Ca^{2+} spikes, $[\text{Ca}^{2+}]_c$ and the mitochondrial membrane potential.

3.3.6 NOS inhibition blocks neuroprotection by E or Q

The NOS inhibitor L-NAME blocked protection by E or Q against OGD (figure 3.7). These findings suggest that both E and Q precondition neurons against ischemic injury by activating NOS and stimulating NO production. Strong evidence indicates that NO participates in the signaling events responsible for hypoxic and ischemic preconditioning.¹⁷³⁻¹⁷⁵ In neuronal cultures, protection by hypoxic preconditioning against OGD-induced cell death is blocked with the NOS inhibitor N-nitro-L-arginine and mimicked by NO donors.¹³⁶ In mice lacking either eNOS or neuronal (nNOS), the neuroprotective effects of ischemic preconditioning are lost.¹⁷⁶ Relative to WT littermates, central neurons of eNOS knockout mice have reduced mitochondrial gene expression and DNA content indicative of depressed mitochondrial function.^{177, 178} The loss of neuronal energetic capacity following either genetic ablation or pharmacological inhibition of eNOS results in increased susceptibility to oxidative damage.^{177, 179, 180} Furthermore, eNOS or nNOS deficiency prevents NO-dependent signaling events that orchestrate the adaptive changes in neuronal mitochondria responsible for hypoxic¹⁷⁷ or ischemic preconditioning.^{176, 181} NO is produced in cortical neurons by both eNOS and nNOS¹⁸²⁻¹⁸⁴ and these enzymes are activated by elevated $[\text{Ca}^{2+}]_c$,¹⁸⁵⁻¹⁸⁸ another key signaling event in hypoxic preconditioning.^{189, 190} In endothelial cells, E activates eNOS in a Ca^{2+} -

independent manner by stimulating protein kinase B (Akt)-induced phosphorylation of this enzyme.¹³⁷ By contrast, Q stimulates NO production in a Ca²⁺-dependent manner.^{191, 192} Consequently, I speculate that E+Q may synergistically increase NOS activity (eNOS and/or nNOS) in neurons by activating both Ca²⁺-independent and Ca²⁺-dependent signaling pathways that converge on these enzymes.

3.3.7 Oral administration of E+Q reduced HI brain injury

Although administration of either E¹⁵³ or Q¹⁹³⁻¹⁹⁶ has been shown to reduce ischemic brain injury, the benefits of combining these compounds have not been reported. Two groups of adult (male) C57Bl/6 mice were dosed orally with either E+Q [75 mg/kg: E (37.5 mg) + Q (37.5 mg)] or water (8 ml/kg) once daily. Five days later, all mice were subjected to HI (40 min). Infarct volume was measured 24 hr later by staining of serial brain sections with the vital dye triphenyl tetrazolium chloride (TTC) (figure 3.8A). Relative to vehicle-treated mice, E+Q reduced the average infarct volume from $70 \pm 6 \text{ mm}^3$ to $38 \pm 7 \text{ mm}^3$ (figure 3.8B). This 46% reduction in infarct volume produced by E+Q is comparable in magnitude to that observed previously with AF4 (figure 3.2)⁸⁸ suggesting that E and Q are primarily responsible for the neuroprotective effects of this flavonoid-enriched fraction.

3.3.8 Proposed model for the activation of convergent cell signaling pathways by E and Q

To provide a framework for future experimentation, I have developed a model that describes the cell signaling pathways implicated by my findings in the mediation of neuroprotection by E and Q (figure 3.9). This model proposes that E and Q synergistically increase the resistance of neurons to ischemic damage by activating distinct signal transduction pathways that converge on NOS and CREB. Concordant activation of NOS and CREB is proposed to synergistically elevate mitochondrial Ca^{2+} handling, gene expression and respiratory performance resulting in profound resistance against ischemic neuronal cell death.

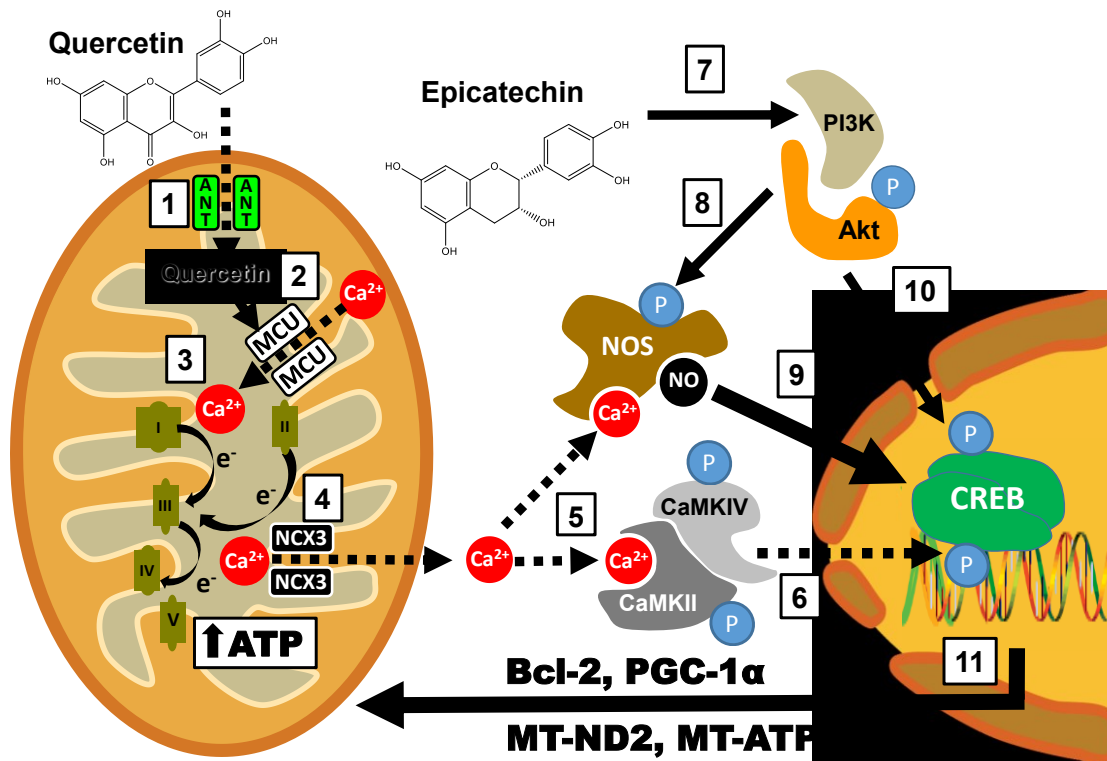


Figure 3. 9 Convergent signaling pathways proposed to mediate synergistic neuroprotection by epicatechin and quercetin

Thin solid and dashed lines show pathways activated by E and Q, respectively. The thick line shows a hypothesized convergent activation of nitric oxide synthase (NOS). 1) Q enters the mitochondrial matrix via the adenine nucleotide translocator (ANT). 2) Q activates the mitochondrial Ca²⁺ uniporter (MCU), stimulating Ca²⁺ entry into the mitochondrial matrix. 3) Elevated Ca²⁺ concentrations increase electron transport chain activity. 4) Extrusion of Ca²⁺ by the mitochondrial Na⁺/Ca²⁺ exchanger (NCX3). 5) Elevated cytosolic Ca²⁺ concentrations stimulate nitric oxide (NO) production by NOS and activate Ca²⁺/calmodulin-dependent kinases II and IV (CaMKII/IV). 6) CaMKII undergoes autophosphorylation then activated CaMKII phosphorylates and shuttles CaMKIV to the nucleus triggering further CREB phosphorylation. 7) E stimulates phosphoinositide 3-kinase (PI3K)-induced phosphorylation of protein kinase B (Akt). 8) Activated Akt phosphorylates NOS, further stimulating NO production. 9) NO stimulates cAMP response element-binding protein (CREB) binding to DNA. 10) Akt activates CREB by phosphorylation. 11) Activated CREB promotes the expression of genes that protect mitochondria (Bcl-2) and enhance mitochondrial biogenesis (PGC-1α) indicated by increased expression of the mitochondrial encoded genes MT-ND2 and MT-ATP6.

3.3.9 Q: Cellular uptake and MCU-mediated activation of NOS and CREB activities

Flavonoids are substrates for a variety of transporters that include the sodium (Na^+)-dependent glucose transporter (SGLT1),¹⁹⁷ bilitranslocases,¹⁹⁸ ATP-binding cassette transporters¹⁹⁹ and organic cation transporters (OCTs).²⁰⁰ SGLT1 mediates absorption of Q from the gut²⁰¹ while movement of this flavonoid across the blood brain barrier appears to involve ATP-binding cassette transporters.²⁰² Q is then rapidly transported into neurons²⁰³ that express functional OCT3.²⁰⁴ However, the transport mechanism responsible for the massive accumulation of Q in mitochondria is unclear.¹²⁴ The most abundant protein in the mitochondrial inner membrane is the adenine nucleotide translocator (ANT) with which Q is known to interact.²⁰⁵ This suggests that ANT may concentrate Q in the mitochondrial matrix (figure. 3.9, Box 1). Within this compartment, Q is able to increase mitochondrial Ca^{2+} concentrations $[\text{Ca}^{2+}]_m$ and neuronal activity by activating the MCU^{125, 127, 128} (figure. 3.9, Box 2). The resultant increase in $[\text{Ca}^{2+}]_m$ enhances ATP synthesis^{129, 130} by increasing the production of reducing equivalents,¹²⁹ metabolic substrates¹³¹ and electron transfer¹³² (figure. 3.9, Box 3). Elevation of $[\text{Ca}^{2+}]_m$ by hypoxic preconditioning has recently been shown to protect neurons from damage by a subsequent ischemic insult by stimulating activity of the mitochondrial $\text{Na}^+/\text{Ca}^{2+}$ exchanger (NCX3).²⁰⁶ This suggests that Q-induced increases in $[\text{Ca}^{2+}]_m$ may also engage this protective mechanism that prevents an injurious rise in $[\text{Ca}^{2+}]_m$ responsible for ischemic neuronal cell death²⁰⁷ (figure. 3.9, Box 4). The elevation in $[\text{Ca}^{2+}]_c$

produced by Q is proposed to activate NOS and Ca²⁺/calmodulin-dependent protein kinase II (CaMKII) (figure. 9, Box 5). A central role for NOS activation is supported by the complete inhibition of Q-mediated neuroprotection with L-NAME (figure. 3.7B). With respect to CaMKII, activation of this kinase has been linked to the extension of lifespan in *C. elegans*²⁰⁸ and prevention of lead-induced neurotoxicity by Q.²⁰⁹ Activated CaMKII phosphorylates CaMKIV at Thr-196 and shuttles this kinase to the nucleus where it directly phosphorylates CREB²¹⁰ triggering Bcl-2 and mitochondrial expression^{177, 211, 212} (figure. 3.9, Box 6). Q is therefore hypothesized to precondition neurons against ischemic injury by activating an MCU/CaMKII/IV/CREB pathway.

3.3.10 E activates Akt resulting in elevated NOS and CREB activities

E is thought to activate a cell surface receptor positively coupled to phosphatidylinositol-3-kinase (PI3K)-mediated activation of Akt, however, the identity of this receptor is unknown²¹³ (figure. 3.9, Box 7). In endothelial cells, E initiates PI3K-Akt signalling that activates NOS^{137, 213, 214} by phosphorylating this enzyme at Ser-1177.²¹⁵ My own findings (figure. 5A) as well as those of Schroeter et al. (2007) indicate that E also stimulates Akt phosphorylation in cortical neurons. Since Akt activates NOS^{137, 214} and E-induced neuroprotection was completely inhibited by L-NAME (figure. 7A), it seems likely that E may also activate NOS in neurons in an Akt-dependent manner. As a consequence, Akt-mediated phosphorylation of NOS may act to further enhance the Ca²⁺-dependent activation of this enzyme by Q (figure. 3.9, Box 8). NO stimulates

CREB-mediated mitochondrial biogenesis by nitrosylating CREB and CREB-accessory proteins that enhance CREB binding to the CRE in the PGC-1 α promoter.^{216, 217} The increase in CREB-driven gene expression (Bcl-2 and PGC-1 α)^{122, 212} that accompanies neuroprotection by E+Q is consistent with this mechanism (figures. 3.4 and 3.9, Box 9). Akt also promotes mitochondrial gene expression, neuronal survival and synaptic plasticity by phosphorylating Ser-133 of CREB that triggers PGC-1 α expression¹¹²⁻¹¹⁵ (figure. 3.9, Box 10). CREB is therefore proposed to be a second major point of convergence between signaling pathways activated by E+Q. This hypothesis is supported by the ability of E+Q (0.1 μ M) to produce a larger elevation of CREB phosphorylation than E or Q (0.1 μ M) (figure. 3.5). Lastly, the convergent activation of NOS and CREB is proposed to mediate the profound increases in mitochondrial gene expression produced by E+Q (figures. 3.4 and 3.9, Box 11) that results in a complete preservation of the SRC and profound neuroprotection following an ischemic insult. I acknowledge that this model is limited by evidence that E and Q interact with a wide variety of cellular targets which may contribute to the neuroprotective effects of these compounds.^{169,163,224} Nevertheless, I feel that this model will serve as a useful framework to guide future studies on the pharmacological bases for flavonoid-mediated neuroprotection.

Chapter 4: Global Ablation of the Mitochondrial Calcium Uniporter Increases Glycolysis in Cortical Neurons Subjected to Energetic Stressors

4.1 Introduction and Rationale

Stroke is the second leading cause of death in the world population.²¹⁸

Approximately 16 million first-ever strokes occur globally each year, causing a total of 5.7 million deaths.²¹⁸ Nearly half of stroke survivors suffer disabilities that force them to seek the assistance of others for daily living which places a considerable burden on their family, friends and the health care system.²¹⁹ The staggering human and economic costs inflicted by stroke have driven an intensive effort to understand how the brain can be rendered more resistant to damage by a stroke.^{220, 221} HPC activates powerful adaptations that dramatically protect the brain from subsequent damage by cerebral ischemia.²²²⁻²²⁴ Clinical studies suggest that these protective mechanisms render patients which have experienced a transient ischemic attack more resistant to brain damage by a subsequent stroke.²²⁵ Identification of the signaling events that mediate HPC are therefore of considerable therapeutic interest.^{220, 221}

Mitochondria are strategically positioned to sense and respond to elevations in cytosolic Ca^{2+} concentrations $[\text{Ca}^{2+}]_c$ that range from the physiological to toxic.^{35, 226} Each neuron contains about 1000-2000 of these dynamic organelles that are rapidly transported by kinesin motors to synaptic sites in urgent need of metabolic support for neurotransmission.^{227, 228} Mitochondria also play a pivotal

role in orchestrating the Ca^{2+} signaling events that activate complex genetic networks, which protect neurons by enhancing mitochondrial Ca^{2+} handling, antioxidant defense, energy production and biogenesis.^{177, 224} These key features enable mitochondria to exert exquisite positive control over the neuroprotective events implicated in HPC.^{222, 229, 230} However, mitochondria can also promote neuronal cell death. Excessive mitochondrial Ca^{2+} uptake triggers the formation of a mPTP that executes both apoptotic^{231, 232} and necrotic²³³⁻²³⁵ cell death. Identification of the transport mechanisms for increased mitochondrial Ca^{2+} uptake that promote neuronal cell death and survival may thus open new therapeutic avenues for the prevention of ischemic brain injury.^{223, 236, 237}

The MCU is responsible for rapid and high capacity mitochondrial Ca^{2+} uptake in the heart.²³⁸ Genetic identification of the MCU in 2011^{239, 240} has enabled the generation of various genetic mouse lines in which MCU activity is blocked by either global MCU deletion,²³⁸ cardiac-specific expression of a dominant-negative MCU (DN-MCU)^{241, 242} or inducible cardiac MCU ablation at maturity.^{243, 244} Experimentation with these genetic lines has clearly demonstrated that the MCU is required for both adaptive and destructive increases of mitochondrial Ca^{2+} uptake in the heart.^{238, 241-244}

In view of the considerable implications of these findings for ischemic brain damage, I have examined the effects of global MCU (G-MCU) deficiency on Ca^{2+} uptake and Ca^{2+} -induced mPTP opening by forebrain mitochondria, resistance of

primary cortical neuron cultures to oxygen-glucose deprivation-induced viability loss, various aspects of neuronal energy production and the ability of HPC to prevent central neuron loss and sensorimotor deficits in a model of hypoxic-ischemic (HI) brain injury.

4.2. Results

4.2.1 Global MCU deficiency impairs Ca^{2+} uptake and inhibits Ca^{2+} -induced mPTP opening by forebrain mitochondria

I first examined Ca^{2+} uptake and Ca^{2+} -induced opening of the mPTP in forebrain mitochondria isolated from WT or G-MCU null mice. As expected, Ca^{2+} uptake into MCU deficient forebrain mitochondria was inhibited (figure 4.1.A) in the same manner to that observed for heart mitochondria isolated from these global MCU knockouts.²³⁸ Ca^{2+} -induced mPTP opening in brain mitochondria that lacked the MCU was also inhibited (figure 4.1.B). Global MCU deficiency therefore suppressed both mitochondrial Ca^{2+} uptake and Ca^{2+} -induced mPTP opening, considered to be pivotal events in ischemic neuronal cell death.^{107, 234}

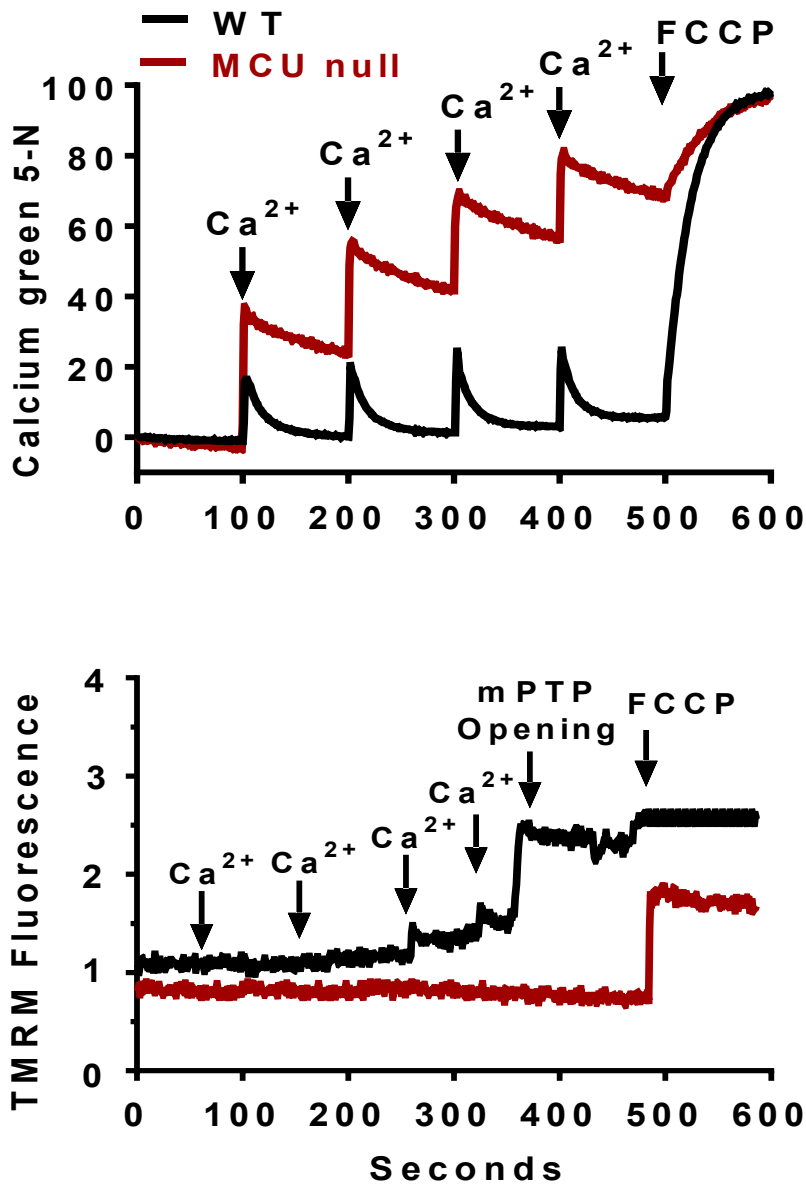


Figure 4.1 Mitochondrial Ca^{2+} uptake and Ca^{2+} -induced mitochondrial permeability transition pore (mPTP) opening

A) Mitochondrial Ca^{2+} uptake and B) Ca^{2+} -induced mitochondrial permeability transition pore (mPTP) opening in brain mitochondria isolated from WT and G-MCU null mice. These data are representative of the results from three separate experiments.

4.2.2 MCU deletion blocked HPC but not HI brain injury

In a second series of experiments, I assessed the effects of global MCU deficiency on HPC using a model of HI brain injury that impairs sensory-motor function by damaging the motor cortex, dorsolateral striatum and dorsal hippocampus. HPC was induced 24 hr before HI by exposure to a low oxygen atmosphere (8% O₂) for 50 min. Control mice for HPC were simply placed in the experimental apparatus under normal atmospheric conditions (20% O₂) for the same amount of time. HI brain injury was induced 24 hr later. HI-induced behavioural deficits were measured 24 hr later using a comprehensive scoring system of neurological function. Immediately afterwards, neuronal damage in the dorsolateral striatum, motor cortex and CA1 region of the dorsal hippocampus was measured by quantifying Fluoro-Jade-positive neurons in these brain regions using Image J. Despite the inhibition of mitochondrial Ca²⁺ uptake and Ca²⁺-induced mPTP opening in G-MCU deficient brain mitochondria, global MCU null mice displayed comparable HI-induced sensorimotor deficits (figure 4.2) and central neuronal damage [dorsolateral striatum (figure 4.3), motor cortex (figure 4.4) and CA1 region of the dorsal hippocampus (figure 4.5)] as WT mice. These findings demonstrate that MCU-mediated mitochondrial Ca²⁺ uptake is dispensable in the progression of HI brain injury. HPC profoundly attenuated HI-induced sensorimotor deficits (figure 4.2) and central neuronal damage [dorsolateral striatum (figure 4.3), motor cortex and CA1 region of the dorsal hippocampus (figures 4.4 & 4.5)]. However, HPC failed to decrease HI-induced

sensorimotor deficits and central neuronal damage for MCU nulls (figure 4.3F)
indicating that global MCU loss interfered with HPC.

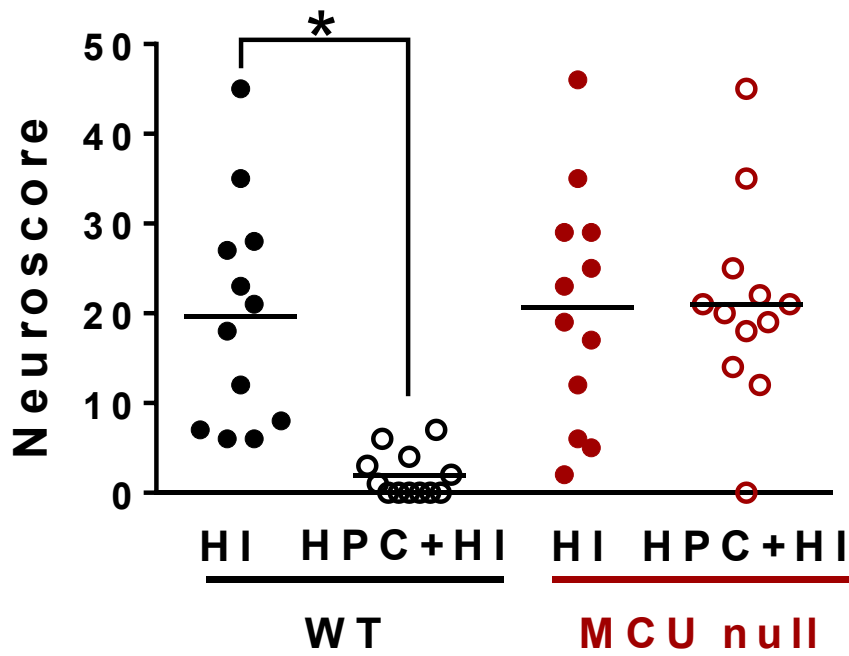


Figure 4.2 Neuroscores for WT and global MCU null mice after HI

Neuroscores for wild-type (WT) and global MCU null mice after HI brain injury that were subjected to sham conditions or HPC. Mice were graded on a 56-point scale that rated increased levels of neurobehavioural impairment. * $p < 0.05$, Two-way ANOVA followed by Bonferroni's post-hoc test.

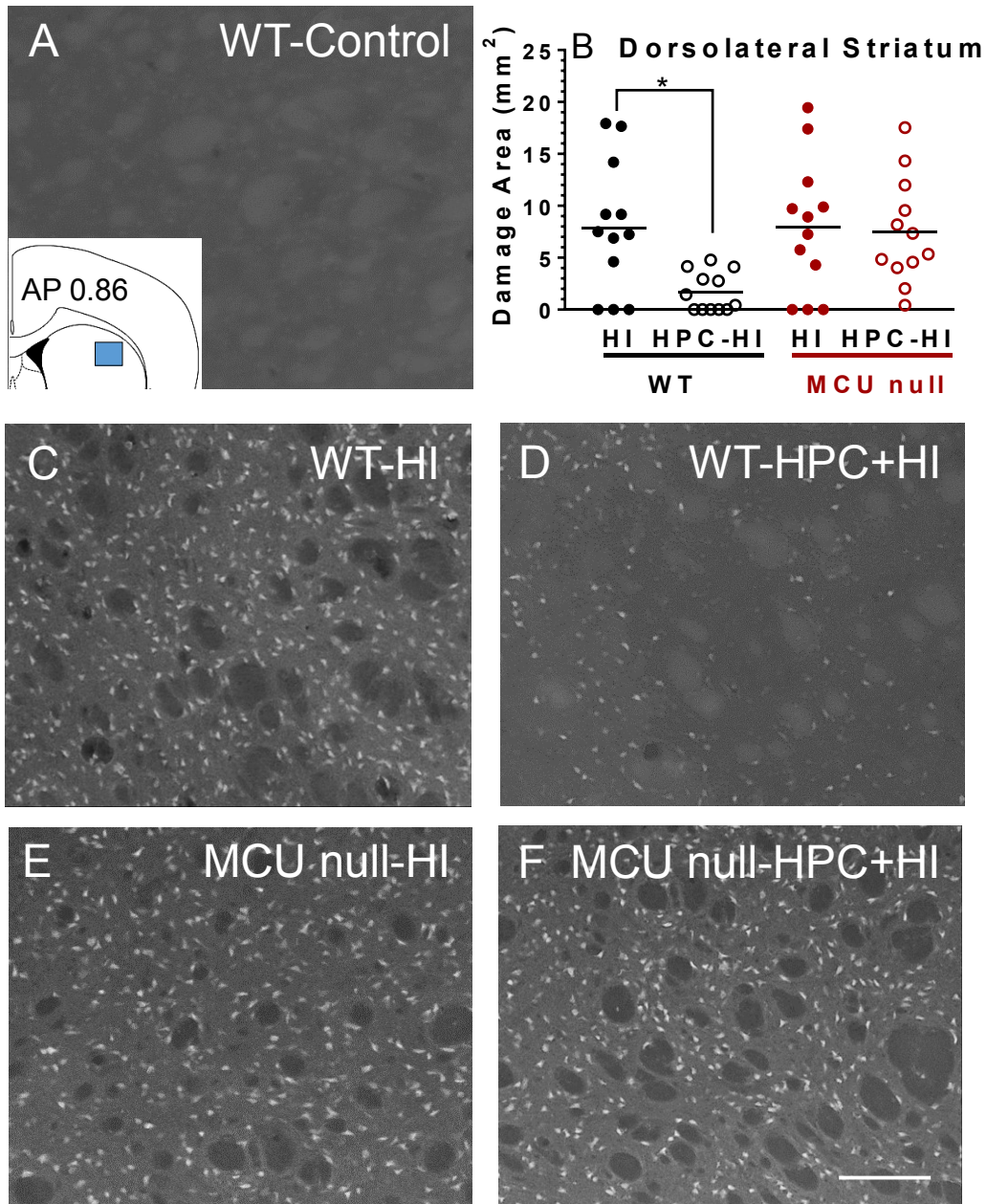


Figure 4.3 Fluorojade (FJ)-positive neurons damaged by HI brain injury in the dorsolateral striatum of WT and G-MCU nulls

Fluorojade (FJ)-positive neurons damaged by HI brain injury in the dorsolateral striatum of WT (C) and G-MCU nulls (E) subjected to sham conditions (A) or HPC (D, F). Top right panel (B) - HI damage quantified by determining the area occupied by FJ-positive cells within the indicated sector of dorsolateral striatum (insert, top left panel). * $p < 0.05$, Two-way ANOVA followed by Bonferroni's post-hoc test. Scale bar = 150 μ m.

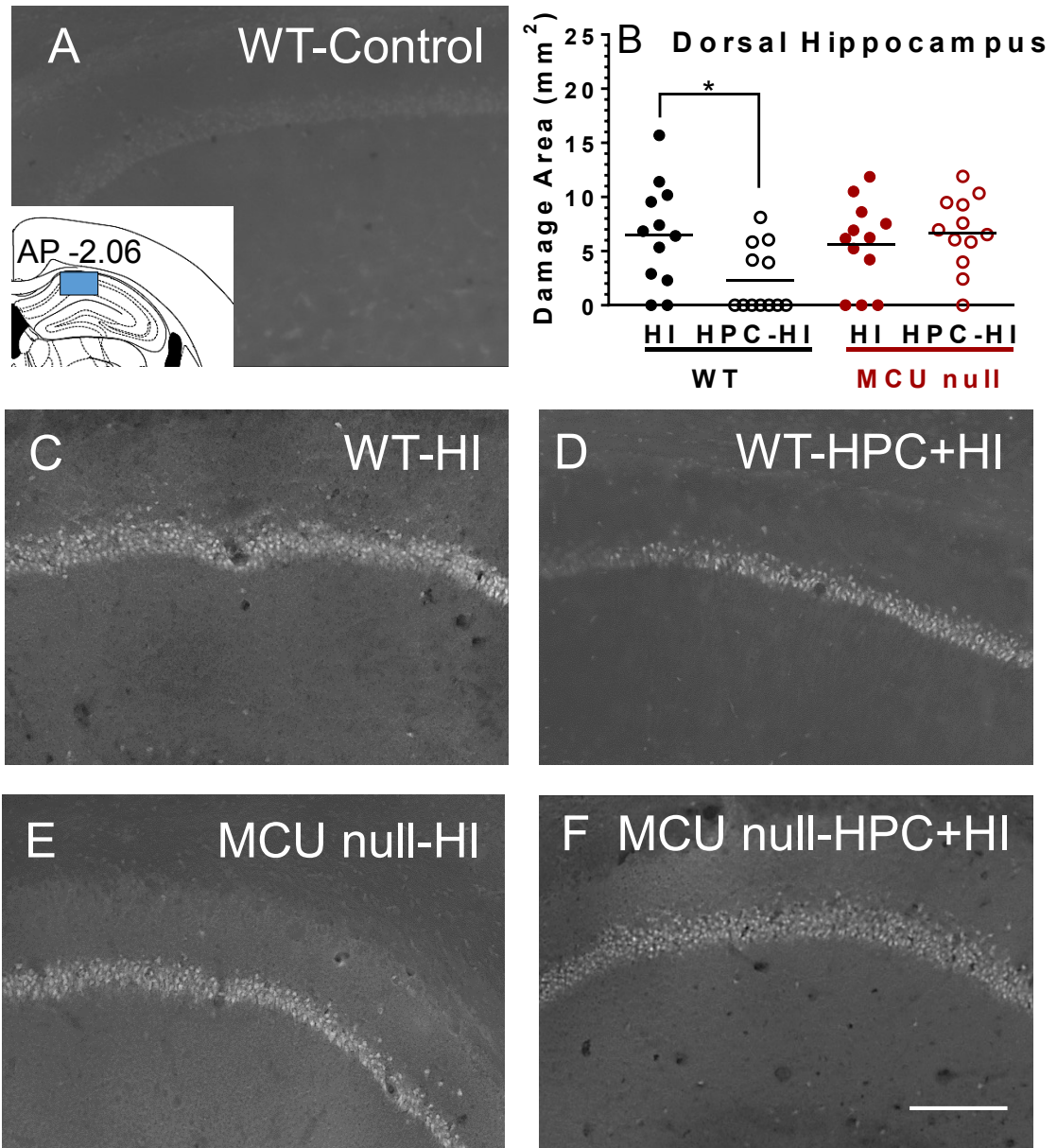


Figure 4.4 Fluorojade (FJ)-positive neurons damaged by HI brain injury in the hippocampus of WT and G-MCU nulls

Fluorojade (FJ)-positive neurons damaged by HI brain injury in the CA1 region of the hippocampus of WT (A, C, D) and G-MCU nulls (E, F) subjected to sham conditions or HPC. (B) HI damage quantified by determining the area occupied by FJ-positive cells within the indicated sector of CA1 (insert, top left panel). * $p < 0.05$, Two-way ANOVA followed by Bonferroni's post-hoc test. Scale bar = 150 μm .

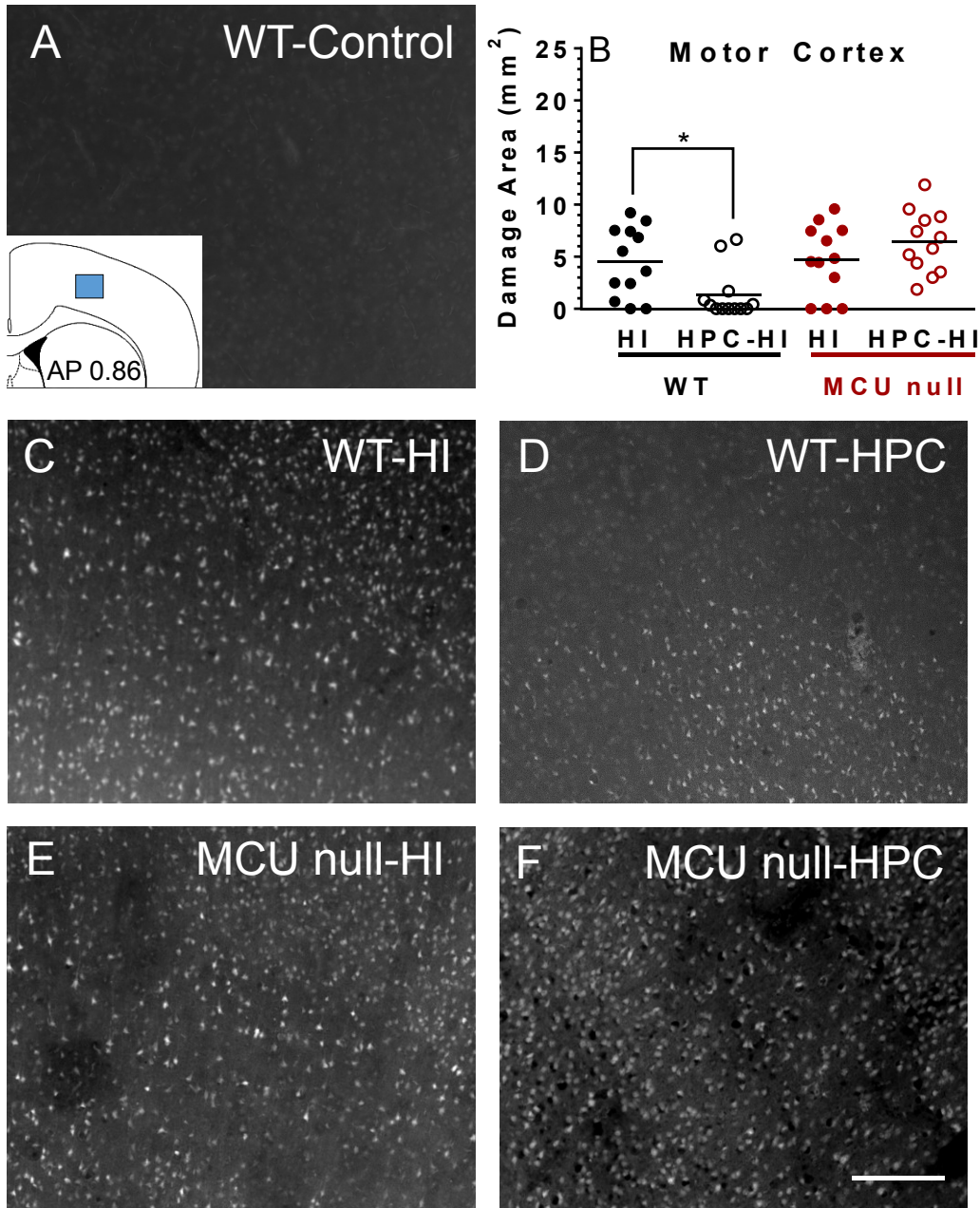


Figure 4.5 Fluorojade (FJ)-positive neurons damaged by HI brain injury in the motor cortex of WT and G-MCU nulls

Fluorojade (FJ)-positive neurons damaged by HI brain injury in the motor cortex of WT (A, C, D) and G-MCU nulls (E, F) subjected to sham conditions or HPC. (B) HI damage quantified by determining the area occupied by FJ-positive cells within the indicated sector of CA1 (insert, top left panel). * $p < 0.05$, Two-way ANOVA followed by Bonferroni's post-hoc test. Scale bar = 150 μm .

4.2.3 Ultrastructural features of neuronal mitochondria were similar in WT mice and G-MCU nulls before and after HI brain injury

Electron microscopic analyses showed that the morphology of mitochondria in the CA1 region of global MCU nulls appeared normal and comparable to that of WT mice (figure 4.6). The disrupted morphology (loss of cristae integrity) and degree of mitochondrial damage in the dorsal hippocampus of WT and G-MCU null mice after HI brain injury were also the same (figure 4.7).

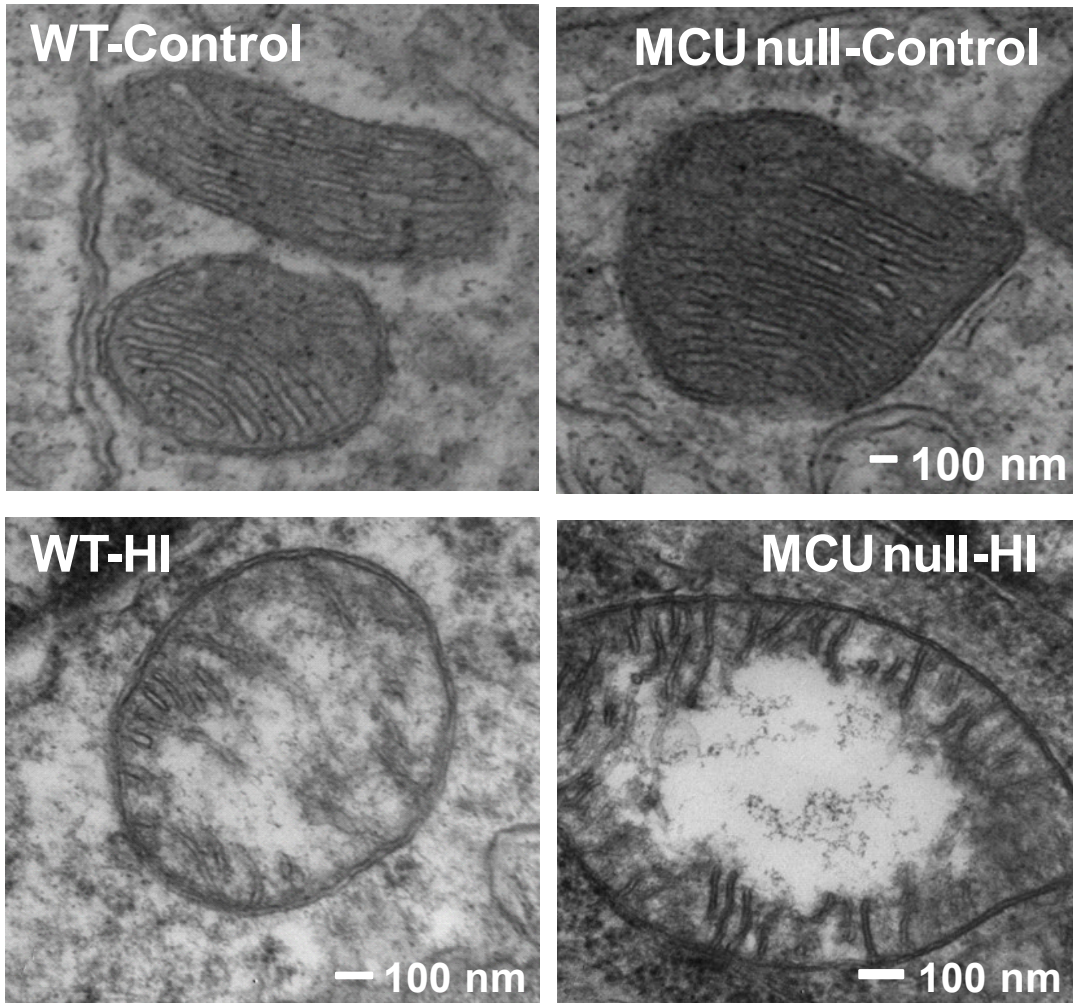


Figure 4.6 Electron microscopic images of mitochondria in the CA1 region of the dorsal hippocampus of control or HI injured WT and G-MCU null mice

Control mitochondria from both WT and G-MCU nulls display clear double membrane structure with well-formed cristae. Following HI brain injury both WT and G-MCU nulls display damaged cristae and reduced electron density.

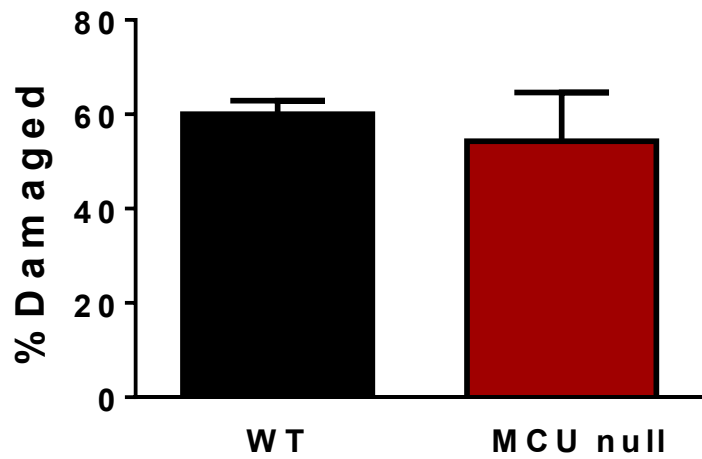


Figure 4.7 Relative of percentage of damaged mitochondria detected 2 hrs after HI

Images of 1024 mitochondria from the ipsilateral CA1 region in WT or G-MCU mice were visually assessed for damage (loss of double membrane or cristae integrity). * $p < 0.05$, Mann-Whitney U test. Each bar represents the mean \pm SEM (n=3/group).

4.2.4 G-MCU deletion did not alter the susceptibility of cortical neurons to ischemic cell death

To determine whether global MCU deficiency alters the resistance of central neurons to ischemic injury, cell viability loss produced by oxygen glucose deprivation (OGD) was compared in primary cultures of cortical neurons derived from WT and global MCU null mice. Neurons exposed to OGD undergo rapid energetic decline, failure of ATP-dependent ion pumps, excessive reactive oxygen species generation, N-methyl-D-aspartate receptor hyper-stimulation and mitochondrial dysfunction resulting in both apoptotic and necrotic cell death.²⁴⁵ Consistent with my *in vivo* findings, OGD produced the same degree of cell viability loss for WT and G-MCU deficient cortical neurons (figure 4.8). Global MCU deletion therefore does not alter the susceptibility of central neurons to OGD-induced damage.

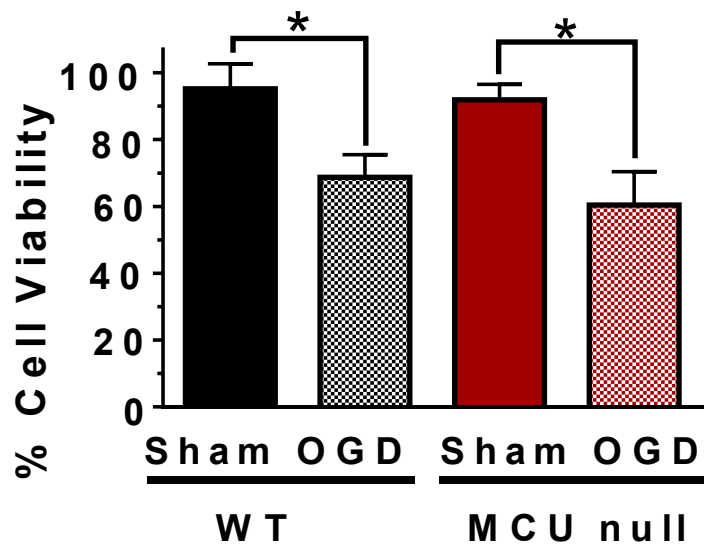


Figure 4.8 Global MCU ablation of the MCU did not confer protection to cortical neurons subjected to OGD

Primary neurons obtained from either WT or global MCU null were subject to either sham or 1.5h OGD. Cell viability was measured 24 h following OGD using the MTT assay. Global MCU ablation in neurons did not confer protection to OGD. * $p < 0.05$, Two-way ANOVA followed by Bonferroni's post-hoc test.

4.2.5 G-MCU null neurons exhibited hyper-phosphorylation of the pyruvate dehydrogenase complex

Consistent with findings using cardiac or skeletal myocytes, phosphorylation of the PDH complex at all 3 serine sites (pS233, pS292, pS300; figure 4.5A-C) were dramatically increased in MCU null relative to WT cortical neurons.^{238, 242-244} In total, PDH phosphorylation was elevated by 3-fold in MCU null relative to WT neurons (figure 4.9). Exposure to glutamate (25 μ M; 30 min) and ionomycin (2 μ M; 30 min) decreased the relative levels of PDH phosphorylation by comparable amounts in WT and G-MCU null cortical neurons (figure 4.9). However, by comparison to WT neurons, PDH in G-MCU null neurons was significantly hyper-phosphorylated across basal, glutamate and ionomycin stimulated conditions (figure 4.9). These findings indicate that mitochondria in G-MCU null neurons may utilize alternative Ca^{2+} transport and/or metabolic substrates to regulate energy metabolism.^{35, 246}

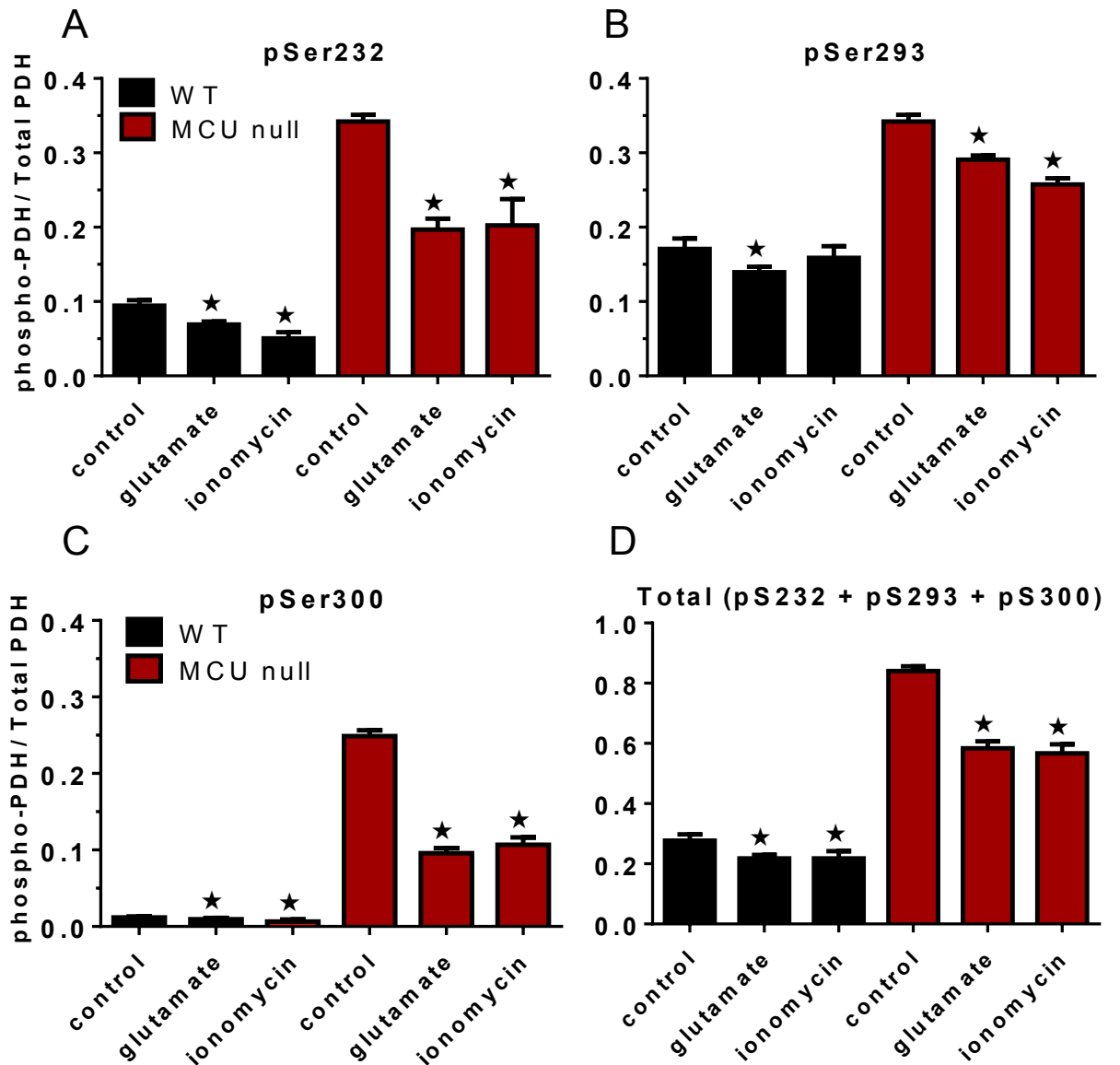


Figure 4.9 PDH phosphorylation levels of WT and global MCU under basal and stimulated conditions

PDH phosphorylation levels for pSer232 (A), pSer293 (B), pSer300 (C) and total pSer (D) in WT and global MCU null cortical neurons under control conditions or 30 min after stimulation with glutamate (25 μ M) or ionomycin (2 μ M). * $p < 0.001$, Two-way ANOVA followed by Bonferroni's post-hoc test ($n = 7/\text{group}$).

4.2.6 G-MCU null neurons displayed reduced spare respiratory capacity offset by increased glycolytic rates

Oxygen consumption rates (OCR) under control and oligomycin-inhibited conditions were comparable for both WT and G-MCU null neurons, indicating a similar reliance on mitochondrial oxidative phosphorylation for basal ATP production (figure 4.10). PDH hyper-phosphorylation is known to suppress tricarboxylic acid flux.²⁴⁷ Despite PDH hyper-phosphorylation in G-MCU null neurons, basal OCRs were comparable to WT neurons. Two possibilities may account for unaltered basal OCRs in G-MCU null neurons: 1) residual unphosphorylated PDH provides sufficient substrate supply²⁴⁷ and 2) alternative substrates and metabolic pathways generate the necessary reducing equivalents to maintain oxidative phosphorylation.^{35, 246} When stimulated with FCCP, which induces maximal respiratory capacity by dissipating the mitochondrial membrane potential and uncoupling Complex I-IV activity from ATP synthase, G-MCU null cortical neurons showed a reduced spare respiratory capacity compared to WT neurons. This was accompanied by an increase in ECARs for G-MCU null relative to WT neurons indicating an enhanced reliance on glycolysis for ATP production during energetic stress (figure 4.10). Treatment with both rotenone and antimycin A resulted in matching OCR reductions for both WT and G-MCU nulls (figure 4.10). However, ECARs for G-MCU null neurons remained elevated above those for WT neurons after Complex I (rotenone) and Complex I/III (rotenone + antimycin A) inhibition (figure 4.10). These findings suggested that G-MCU null neurons employ glycolysis to meet increased metabolic demands.

4.2.6 Glycolytic induction by OGD was accompanied by Complex I suppression in G-MCU null neurons

OCRs were also measured 1 hr post OGD (figure 4.10). This delay provided a measure of the early impact of *in vitro* ischemic/reperfusion injury on mitochondrial respiration and glycolysis. Relative to WT neurons after OGD, G-MCU null neurons displayed reduced OCRs under basal, oligomycin-inhibited and FCCP-stimulated conditions indicating a diminished capacity to produce energy by oxidative phosphorylation (figure 4.10). By contrast, G-MCU neurons showed a marked increase in ECARs compared to WT neurons after OGD (figure 4.10). This result further supports an increased dependence of MCU null neurons on glycolysis for energy production during metabolic stress. The formation of glycolytic compartments was recently discovered in neurons at sites of local synaptic activity, where I propose these sites are enhanced in G-MCU nulls relative to WT.²⁴⁸ Following all measurement conditions after OGD, ECARs for G-MCU null neurons remained higher than those for WT neurons. Treatment with rotenone reduced OCRs in WT neurons to those seen in G-MCU neurons thus demonstrating that reduced Complex I activity was responsible for deficient mitochondrial respiration in G-MCU null neurons.

4.2.7 Forebrain NADH and pyruvate concentrations were reduced in G-MCU nulls subjected to HI

Forebrain NAD⁺/NADH ratios (striatum) and pyruvate (hippocampus) concentrations were measured in WT and G-MCU null 30 min after exposure to HI (figure 4.10). Relative to WT mice, striatal NAD⁺/NADH ratios were increased in G-MCU nulls indicating decreased NADH levels. NADH is consumed by lactate dehydrogenase to convert pyruvate to lactate for ATP synthesis. The lower concentrations of pyruvate in the hippocampus of MCU nulls compared to WT mice after HI further supports the increased glycolytic capacity of global MCU deficient mice (figure 4.10). The increased glycolytic consumption of NADH may thus suppress Complex I activity in G-MCU null neurons by depleting reducing equivalents needed to drive oxidative phosphorylation.²⁴⁹ To rule out the differences in NADH consumption due to different Complex I levels, complex I expression was measured by qRT-PCR (figure 4.11).

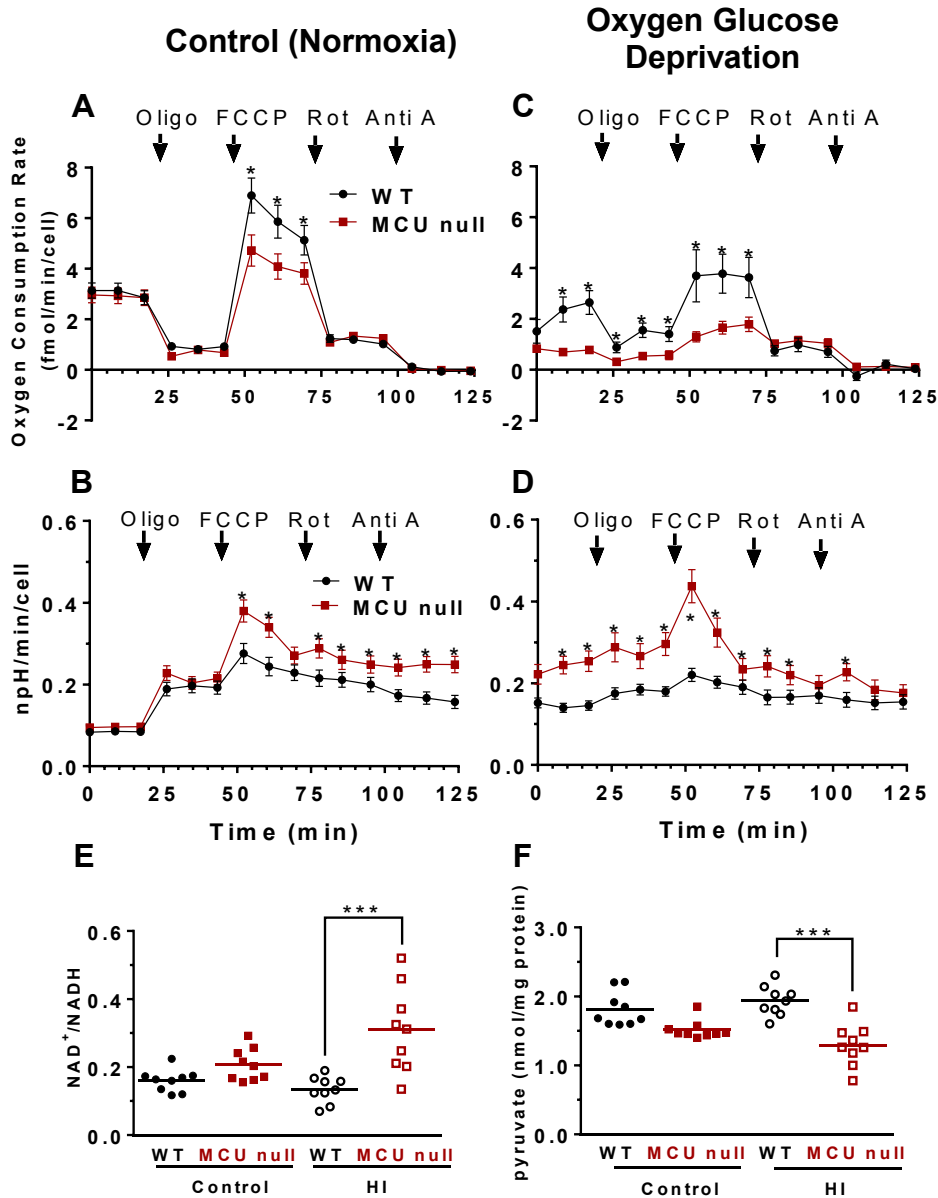


Figure 4.10 Analysis of mitochondrial function under basal conditions and after OGD

OCRs (A, C) and ECARs (B, D) for WT and G-MCU null neurons under control conditions (A and B) or 1 hr after OGD (C and D). * $p < 0.05$, Two-way ANOVA followed by Bonferroni's post-hoc test ($n = 4/\text{group}$). Striatal NAD⁺/NADH ratios (E) and hippocampal pyruvate (F) concentrations isolated from the ipsilateral hemisphere of wild-type (WT) and G-MCU null mice 30 min following exposure to sham conditions or HI. * $p < 0.05$, Two-way ANOVA followed by Bonferroni's post-hoc test.

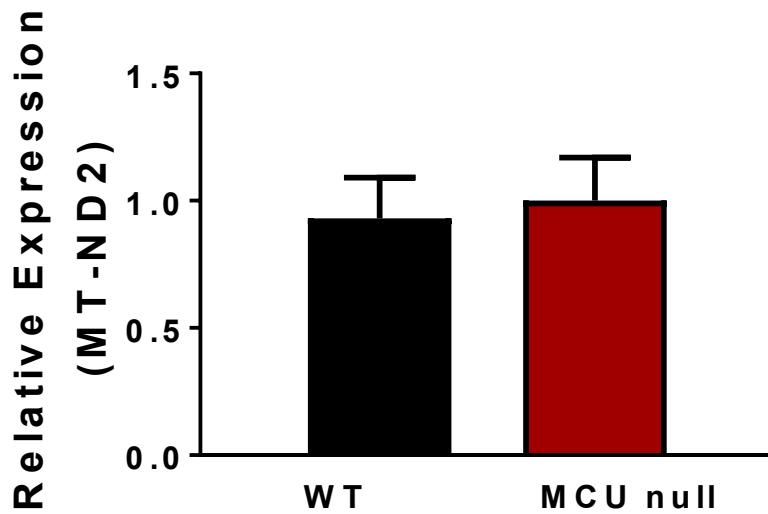


Figure 4.11 Relative mRNA levels of complex I member MT-ND2 in WT and global MCU cortical neurons

Relative mRNA levels for the Complex I member (MT-ND2) detected by qRT-PCR in MCU null and WT cortical neurons. There was no difference between these conditions as indicated by an unpaired t-test, $p > 0.05$, N.S.

4.2.7 Global MCU ablation and HPC increased the expression of apoptosis-related and Ca²⁺ handling genes in the hippocampus

I compared mRNA levels for BCL-2 family members (BCL-XL and BAX), Na⁺/Ca²⁺ exchangers from the plasma membrane (NCX-1, NCX-2, NCX-3) and PMCA-2 in the hippocampus of WT and global MCU null mice subjected to sham conditions or HPC. Relative to WT mice, levels of mRNAs for BCL-XL, BAX, NCX-1, NCX-2, NCX-3 and PMCA-2 were elevated by 2-3 fold in global MCU nulls (figure 4.12). HPC increased levels for all mRNAs in the hippocampi of WT mice. Except for a modest elevation of PMCA-2 mRNA levels (50%; figure 4.12), HPC did not produce a further induction of these genes in global MCU nulls (figure 4.12).

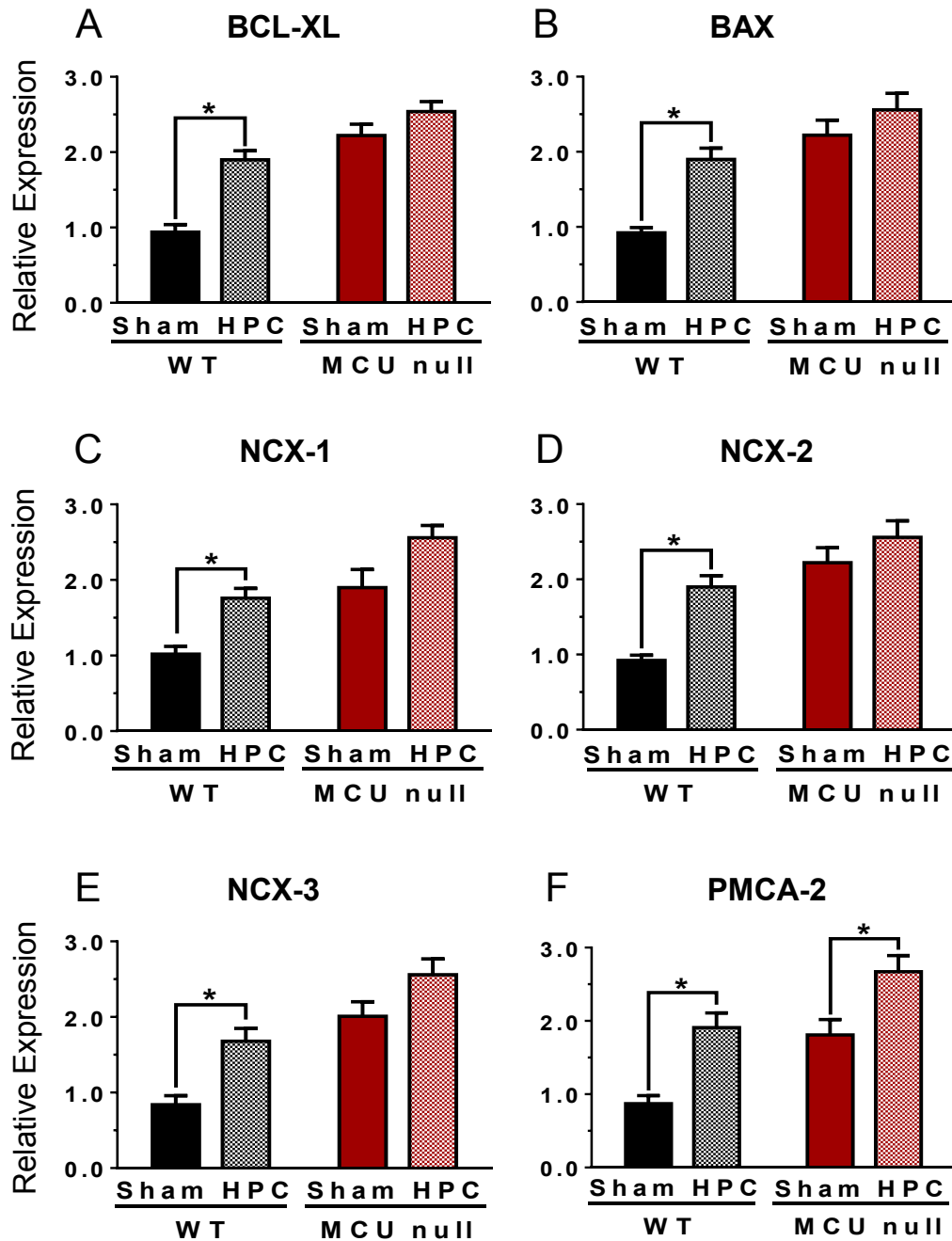


Figure 4.12 Relative levels of mitochondrial apoptotic mediators and plasma membrane Ca^{2+} handling genes

Relative levels of BCL-XL (7A), BAX (7B), NCX-1 (7C), NCX-2 (7D), NCX-3 (7E) and PMCA-2 (F) mRNAs detected in the dorsal hippocampi of WT or G-MCU null mice 4 hr after exposure to sham conditions or HPC (50 min of global hypoxia). * $p < 0.05$, Two-way ANOVA followed by Bonferroni's post-hoc test. Each bar represents the mean \pm SEM ($n = 7$ /group).

4.3 Discussion

4.3.1 Unaltered HI brain injury in global MCU nulls despite the inhibition of mitochondrial Ca^{2+} uptake and Ca^{2+} -induced mPTP opening

I have observed that global MCU deletion suppressed the uptake of Ca^{2+} by forebrain mitochondria (figure 4.1A). Ca^{2+} -induced mPTP opening, that executes both apoptotic²³¹ and necrotic^{234, 250} neuronal cell death, was also blocked in forebrain mitochondria isolated from global MCU nulls (figure 4.1B). Despite this inhibition of mPTP opening, global MCU nulls were not protected from HI-induced sensorimotor deficits (figure 4.2) and brain injury (figures 4.3-4.5) nor were cortical neurons isolated from these animals rendered more resistant to cell viability loss after a lethal period of OGD (figure 4.8). Electron microscopic analyses showed that mitochondria in the CA1 region of global MCU nulls also displayed similar morphological features of damage as WT mice after HI brain injury (figures 4.6 and 4.7). These findings are consistent with evidence that complete MCU ablation during development activates alternative mitochondrial Ca^{2+} handling mechanisms that compensate for global MCU ablation.²⁴²⁻²⁴⁴

4.3.2 Metabolic regulation by mitochondrial Ca²⁺ uptake was impaired in global MCU nulls

Since developmental inhibition of the MCU has been reported to increase the phosphorylation of PDH in cardiac myocytes,^{238, 242} I measured the phosphorylation levels for S232, S293 and P300 of PDH in WT and MCU null cortical neurons (figure 4.9). Relative to WT neurons, all of these PDH sites were hyper-phosphorylated in MCU cortical neurons resulting in about a 300% increase of total PDH phosphorylation (figure 4.9). Phosphorylation of these 3 sites by at least 4 PDH kinases (PDKs) produces additive reductions in PDH activity.²⁴⁷ The hyper-phosphorylation of PDH in MCU null neurons is likely explained by decreased mitochondrial Ca²⁺ uptake required to stimulate dephosphorylation by PDH phosphatases.²⁴⁷ However, elevations of cytosolic Ca²⁺ by glutamate or ionomycin still triggered the dephosphorylation of PDH in MCU null cortical neurons (figure 4.9). Since dephosphorylation of each of these 3 sites is mediated by Ca²⁺-induced phosphatases, these results suggest that MCU null cortical neurons use alternative mitochondrial Ca²⁺ transport mechanisms to regulate metabolic activity. This line of reasoning is further supported by my measurements of forebrain NADH and pyruvate levels in WT and MCU nulls. Under control conditions NADH and pyruvate were similar in WT and MCU nulls (figure 4.10). As a result, increased PDK activities driven by differences between the concentrations of these metabolic substrates cannot account for the hyper-phosphorylation of PDH in G-MCU null neurons.²⁴⁷

4.3.3 The induction of glycolysis by metabolic stress depleted NADH levels and suppressed Complex I activity in G-MCU null cortical neurons

To establish the effects of compensations for global MCU ablation on the metabolic function of cortical neurons, I compared the glycolytic rates and several aspects of mitochondrial performance in respiring cortical neurons derived from WT and global MCU nulls. These studies showed that basal respiration by G-MCU null neurons were unaltered despite a considerable reduction in mitochondrial Ca^{2+} uptake (figures 4.1 and 4.10). However, relative to WT neurons, maximal respiratory capacity stimulated with FCCP (2 μM) was reduced in G-MCU null neurons. This was accompanied by higher ECARs for G-MCU null than WT neurons (figure 4.10). Since increased lactate production is principally responsible for elevated neuronal ECARs,²⁵¹ these results reflect an increased reliance of G-MCU null neurons on glycolysis to produce ATP during increased energetic demand. This finding is consistent with recent evidence that active synaptic sites are fueled by the dynamic formation of glycolytic compartments.²⁴⁸ I also found that striatal NADH levels are reduced following HI in G-MCU nulls relative to WT mice (figure 4.10). This suggests that enhanced glycolysis depletes G-MCU null cortical neurons of NADH required to fuel oxidative phosphorylation causing a decrease in FCCP-induced maximal respiration (figure 4.10). This is supported by the pronounced inhibitory effects of OGD on mitochondrial respiration in G-MCU null neurons. Relative to WT neurons, G-MCU null neurons displayed greater reductions in basal respiration,

ATP production and maximal respiration after OGD (figure 4.10) that were closely associated with increased ECARs for each of these conditions (figure 4.10). Interestingly, FCCP produced a further burst of ECAR in G-MCU null neurons that rapidly declined to levels below those seen at baseline. I also interpret these findings as being reflective of an increased dependence on glycolysis for metabolic support that rapidly consumed NADH resulting in energy depletion. Rotenone normalized OCR in WT neurons to levels observed in G-MCU null neurons (figure 4.10) demonstrating that Complex I activity in G-MCU null neurons was suppressed after OGD. However, because my experiments were performed just 1 hr post OGD, I cannot rule out the possibility that the metabolic shift towards glycolysis is transient in surviving G-MCU null neurons.

The OCR experiments were performed in the presence of 2 mM pyruvate. Standard neurobasal media contains only 0.22 mM pyruvate that corresponds closely with the concentration of pyruvate (0.175 mM) detected in brain (figure 4.10). Pyruvate concentrations should therefore not have been a limiting factor for the respiration and Complex I activity of G-MCU null neurons. I also measured mRNA levels for the complex I member (MT-ND2) by qRT-PCR in G-MCU null and WT cortical neurons. There was no significant difference between WT and G-MCU deficient cortical neurons (figure 4.11). This indicated that reduced Complex I expression was not responsible for the lower OCRs of global MCU null relative to WT neurons following FCCP treatment or OGD.

4.3.4 Global MCU deficiency produced similar effects as HPC on apoptosis-related and Ca²⁺ handling gene expression in the hippocampus

Global MCU deficiency engaged mechanisms shared by HPC known to oppose impairments in mitochondrial function and cytosolic Ca²⁺ handling genes that promote ischemic brain damage.^{229, 230, 236} There was a remarkable concordance between hippocampal patterns of elevated gene expression for mitochondrial apoptosis-regulators (BCL-XL, BAX), Na⁺/Ca²⁺ exchangers from the plasma membrane (NCX-1, NCX-2, NCX-3) and the ATP-driven Ca²⁺ plasma membrane transporter (PMCA-2) in sham G-MCU nulls and WT mice subjected to HPC (figure 4.12F). These increases are consistent with adaptations in G-MCU nulls that compensate for chronic impairments in Ca²⁺ homeostasis.²⁴²

4.3.5 Global MCU nulls failed to benefit from HPC

Although HPC reduced HI-induced neurological deficits and brain injury in WT mice, G-MCU nulls failed to benefit from HPC. Apart from a modest 50% elevation of mRNA levels for PMCA-2 (figure 4.11F), HPC failed to produce a further increase in the hippocampal expression of BAX, BCL-XL, NCX-1, NCX-2, NCX-3 in global MCU null mice (figure 4.12A-E). These findings indicate that developmental compensations for constitutively impaired Ca²⁺ handling in global MCU nulls may have disrupted signaling mechanisms necessary for HPC. In keeping with these findings, constitutive MCU inhibition in the heart increases the expression of mitochondrial apoptosis-regulators (BCL-2 and BAX), stimulates NCX activity and sensitizes mitochondrial-mediated cell death pathways.²⁴² This

coupled with an increased reliance on glycolysis that suppresses Complex I activity may have contributed to the inability G-MCU nulls to benefit from HPC. Such adverse effects of these long-term compensations may also account for the failure of global MCU deletion to reduce mitochondrial damage, central neuron loss and neurological deficits following HI brain injury.

Chapter 5: Conditional Cre-mediated Ablation of the Mitochondrial Calcium Uniporter in Forebrain Neurons Protects Mice from Hypoxic/Ischemic Brain Injury

5.1 Introduction and rationale

Neurons depend heavily on mitochondria to buffer cytosolic Ca^{2+} concentrations and meet the dynamic metabolic demands imposed by neurotransmission.^{35, 171, 252} However, mitochondria can also trigger neuronal cell death. Excessive mitochondrial Ca^{2+} uptake triggers the formation of mPTP that executes both apoptotic^{231, 232} and necrotic^{233-235, 250} ischemic neuronal damage. Identification of the transport mechanisms for increased mitochondrial Ca^{2+} uptake that promote neuronal cell death and survival may thus open new therapeutic avenues for the prevention of ischemic brain injury.^{223, 236, 237}

The mitochondrial Ca^{2+} uniporter (MCU) is responsible for rapid and high capacity mitochondrial Ca^{2+} uptake in the heart.²³⁸ Genetic identification of the MCU in 2011^{239, 240} has enabled the generation of various genetic mouse lines in which MCU activity is blocked by either global MCU deletion,²³⁸ cardiac-specific expression of a dominant-negative MCU (DN-MCU)^{241, 242} or inducible cardiac MCU ablation at maturity.^{243, 244} Experimentation with these genetic lines has shown that conditional, but not constitutive (global MCU nulls or DN-MCU mice), MCU inhibition protects the heart from destructive increases of mitochondrial Ca^{2+} uptake.^{238, 241-244}

Given the considerable implications of these findings for ischemic neuronal cell death, I have recently examined the effects of global MCU (G-MCU) deletion on HI brain injury.²⁵³ Consistent with previous studies that examined the effects of constitutive MCU inhibition on ischemic heart damage, G-MCU nulls were not protected from sensorimotor deficits or neuronal damage following HI brain injury.²⁵³ Energetic stress enhanced glycolysis and depressed Complex I activity in G-MCU null, relative to wild-type (WT), cortical neurons. HI reduced forebrain NADH levels more in global MCU nulls than WT mice suggesting that increased glycolytic consumption of NADH suppressed Complex I activity. These findings suggest that metabolic compensations for global MCU loss compromised resistance to ischemic injury.²⁵³ To avoid these compensations, I have generated a novel transgenic line enabling the MCU to be selectively deleted at maturity in forebrain neurons. I show that these mice are resistant to HI brain injury and do not display metabolic compensations observed in global MCU nulls.

5.2 Results

Western blotting showed that MCU levels were reduced by over 80% in the hippocampus of CNS-MCU deficient mice (figure 5.1A). Relative to control (Thy1-cre/ERT2-eYFP) mice, CNS-MCU deficient mice displayed less severe sensorimotor deficits 24 h following HI (figure 5.1B). This was accompanied by decreased neuronal damage detected by Fluoro-Jade C staining in the dorsal hippocampus (CA1), dorsolateral striatum and motor cortex of CNS-MCU deficient mice compared to controls (figure 5.1C-K). EM images in the CA1

region of the hippocampus revealed mitochondrial damage 2 h following HI for control mice that was reduced in CNS-MCU deficient mice (figure 5.1 L-N). These results demonstrate that CNS-MCU deficiency protected mice from HI-induced sensorimotor deficits and neuronal damage. The accompanying reductions in mitochondrial damage suggest that MCU deficiency protected neurons by decreasing mitochondrial Ca^{2+} overloading and permeability transition pore opening implicated in ischemic neuronal death.^{234, 250}

I next examined the effects of siRNA mediated MCU knockdown on the loss of cell viability in primary cortical neuron cultures following OGD. This experimental approach was used for two reasons: (A) Thy1 is weakly expressed during embryonic development and (B) primary cortical neurons cultures do not tolerate treatment with 4-hydroxytamoxifen.^{254, 255} I found that siRNA-mediated MCU knockdown reduced MCU mRNA and protein levels by 80% and 50%, respectively (figure 5.2A and B). This degree of siRNA-mediated MCU knockdown has previously been shown to decrease N-methyl-D-aspartate-induced mitochondrial Ca^{2+} uptake in neurons.¹⁶ MCU knockdown increased cell viability 24 hr following OGD from 48% (control siRNA) to 71% (MCU siRNA; figure 5.2C). These findings further support the protective effects of decreased neuronal MCU levels against ischemic injury.

Phosphorylation of the pyruvate dehydrogenase (PDH) complex is rapidly reduced by the elevation of Ca^{2+} levels in the mitochondrial matrix.^{129, 253, 256} |

therefore measured the phosphorylation status of the complex to determine if siRNA-mediated MCU knockdown altered Ca^{2+} mediated changes in mitochondrial metabolism. Knockdown of the MCU did not alter phosphorylation of the PDH complex (figure 5.2D). Elevation of cytosolic Ca^{2+} concentrations with glutamate (25 μM , 30 minutes) also produced comparable reductions in the phosphorylation of PDH for control and MCU-knockdown cultures (figure 2D). The residual MCU-mediated Ca^{2+} uptake in MCU-knockdown neurons was therefore sufficient to regulate mitochondrial metabolism. By contrast, PDH phosphorylation in cortical neuron cultures derived from global MCU nulls was increased under basal and glutamate-stimulated conditions.²⁵³ Unlike CNS-MCU deficient mice, global MCU nulls were not resistant to HI brain injury.²⁵³ These findings suggest that there is an optimal level of MCU inhibition for neuroprotection.

To determine if mitochondria function was preserved by MCU-knockdown, I measured oxygen consumption rates (OCR) and extracellular acidification rates (ECAR), before and 1 h after OGD, using a Seahorse xF24 analyzer.

Mitochondrial function was probed by the sequential addition of oligomycin (2 μM), FCCP (2 μM), rotenone (300 nM) and antimycin A (5 μM). OCR or ECAR levels following these treatments were comparable in control and MCU-knockdown neurons before OGD (figure 5. 2E and G). After OGD, both basal and FCCP-induced maximal respiration were reduced to greater extents in control than MCU-knockdown neurons (figure 5.2F). These results indicate the presence

of a larger pool of functional mitochondria in MCU-knockdown neurons. ECARs following OGD were similar for the control and MCU-knockdown cortical neuron cultures (figure 5.2H). By contrast, I have previously shown that ECARs are markedly elevated for cortical neuron cultures derived from global MCU nulls following energetic stress induced by FCCP or OGD.²⁵³ Acute MCU-knockdown therefore did not produce metabolic compensations associated with reduced resistance to ischemic injury.

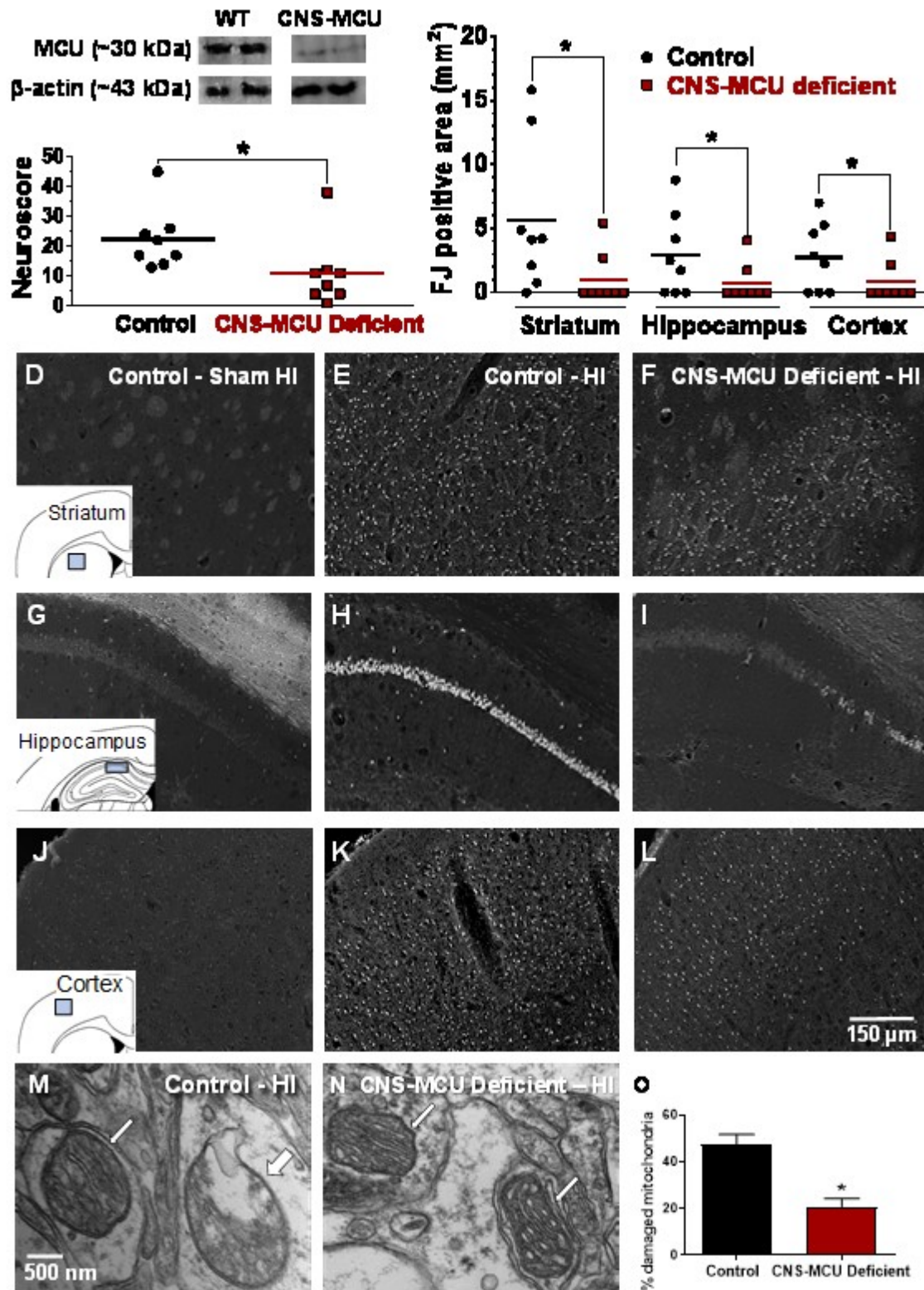


Figure 5.1 CNS-MCU deficient mice are protected from HI-induced motor deficits, neuronal and mitochondrial damage

A) MCU protein levels for control and CNS-MCU deficient mice. B) Neuroscores for control and CNS-MCU deficient mice after HI brain injury. Mice were graded on a 56-point scale that rated increased levels of neurobehavioural impairment. C) Quantification of Fluoro-Jade (FJ)-positive neurons damaged by HI brain injury in the dorsolateral striatum, CA1 region of the dorsal hippocampus and motor cortex of control and CNS-MCU deficient mice. D-L) Representation images of FJ-positive neurons in control mice 24 hours after sham HI surgery (Control-Sham HI; D, G and J) or HI (Control-HI; E, H and K) or CNS-MCU deficient mice (24 after HI (CNS-MCU Deficient-HI; F, I and L) the dorsolateral striatum, CA1 region of the dorsal hippocampus and motor cortex. HI damage was quantified by determining the area occupied by FJ-positive neurons within the indicated sectors of dorsolateral striatum, dorsal hippocampus and motor cortex (blue box for each of the inserts for D, G and J). M and N, Representative EM images showing intact (thin arrows) or damaged (thick arrow) mitochondria within neurons of the CA1 region of the dorsal hippocampus of 24 hours after HI in a control and CNS-MCU deficient mouse. O) Quantification of mitochondrial damage in the CA1 region of the dorsal hippocampus of 24 hours after HI in control and CNS-MCU deficient mice, n=4. *p<0.05 relative to control mice.

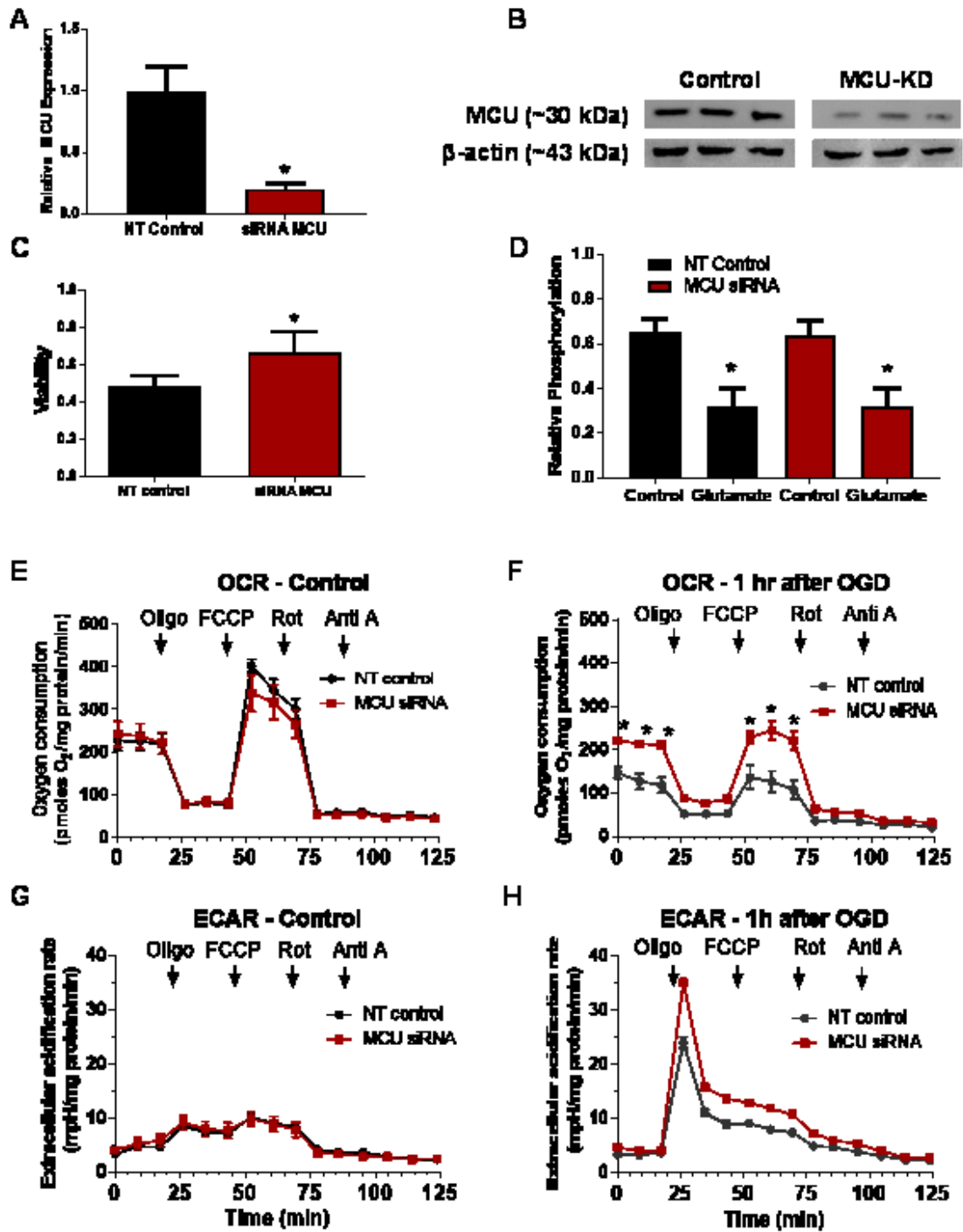


Figure 5.2 MCU knockdown protects primary cortical neuron cultures from the loss of cellular viability and mitochondrial function by OGD

A) Relative mRNA levels for primary cortical neuron cultures 72 hours after treatment with a non-targeting (NT) siRNA or siRNA against the MCU (siRNA MCU). B) MCU protein levels for NT and siRNA MCU cortical neuron cultures. C) Cell viability 24 hours after OGD for NT siRNA and siRNA MCU cortical neuron cultures. D) Phosphorylation levels for pyruvate dehydrogenase (PDH) under basal and glutamate-stimulated conditions for NT siRNA and siRNA MCU cortical neuron cultures. E-H) Oxygen consumption rates (OCR) and extracellular acidification rates (ECAR) under control conditions (E and G) or 1 hour after OGD (F and H) before and after the addition of oligomycin (2 μ M), FCCP (2 μ M), rotenone (300 nM) and antimycin A (5 μ M) in NT and siRNA MCU cortical neuron cultures. * $p < 0.05$ relative to NT controls (A, C and F) or treatment with glutamate (50 μ M) for 30 minutes (D).

5.3 Conclusions

I have shown that CNS-MCU deficiency protected mice from HI-induced motor deficits and forebrain neuron damage. Mitochondrial ultrastructure in the hippocampus of CNS-MCU deficient mice was also preserved following HI. Acute siRNA-mediated MCU knockdown also protected cortical neuron cultures from viability loss and mitochondrial deficits following OGD. Lastly, MCU-knockdown did not cause metabolic impairments previously observed in global MCU nulls.²⁵³ My results suggest that MCU inhibitors have therapeutic potential for the acute management of ischemic/reperfusion brain injury.

Chapter 6: Discussion

Stroke remains a leading cause of death and disability worldwide.⁴ Mitochondrial dysfunction has been strongly implicated in the pathophysiology of stroke and numerous other neurodegenerative disease.²⁵⁷ Mitochondria profoundly shape stroke-induced damage by the regulating Ca^{2+} buffering, cellular bioenergetics, free radical production and the threshold for both apoptotic and necrotic neuronal cell death. This thesis has investigated the impact of both pharmacologic and genetic manipulations that alleviate mitochondrial stress on the resistance of neurons to ischemic damage.

6.1 Ischemia/reperfusion-induced mitochondrial dysfunction and neuronal damage

Neurons heavily depend on oxidative phosphorylation for continual ATP production to support neurotransmission. Due to their dependence on oxidative phosphorylation, neurons are very sensitive to damage by compromised oxygen delivery.²⁵⁸ A major detrimental consequence of energy failure is the suppression of ATP-dependent ion pumps that causes a lethal disruption of ionic homeostasis. The immediate threat from a loss of ionic homeostasis is cellular swelling. The subsequent rise in intracellular Ca^{2+} concentrations initiates mitochondrial-mediated apoptotic neuronal cell death.²⁵⁷ With prolonged periods of ischemia, total bio-energetic collapse occurs resulting in cellular necrosis.²⁵⁹ Currently, the only effective therapeutic interventions for stroke are the administration of t-Pa or the endovascular restoration of blood flow.⁴ Although

limited to the acute treatment of stroke, these therapies improve clinical outcomes by restoring blood flow in brain regions at risk of irreversible damage. If oxygen supply is restored to neurons, they face a second insult termed reperfusion injury.²⁵⁹ The return of oxygen to mitochondria in neurons with elevated intracellular Ca^{2+} concentrations, created by the suppressed activity of ATP-dependent Ca^{2+} pumps, can result in mitochondrial Ca^{2+} overload.¹²³ The restoration of oxygen allows mitochondria to begin restoring mitochondrial membrane potential (Ψ_m). However, restoration of the Ψ_m in the presence of elevated cytosolic Ca^{2+} levels promotes the electrogenically-driven uptake of lethal amounts of Ca^{2+} into mitochondria. The MCU mediates this excessive mitochondrial Ca^{2+} uptake that triggers neuronal cell death.²⁴⁴

Ca^{2+} overloading initiates formation of the mitochondrial permeability transition pore that executes cell death. Excessive mitochondrial Ca^{2+} uptake following reperfusion also triggers the over-production of reactive oxygen species (ROS) that promote oxidative injury. The resultant mitochondrial damage impairs the efficiency of oxidative phosphorylation resulting in a further leak of ROS from the electron transport chain resulting a vicious cycle of ROS-induced ROS production.²³⁷

Flavonoids have been shown to reduce neuronal injury in cell-based and animal models of stroke by increasing anti-oxidant defense, inhibiting pro-inflammatory enzymes and enhancing cellular bioenergetics.⁹⁰ These findings coupled with

epidemiological links between reduced stroke incidence and increased dietary consumption of these polyphenolic compounds have resulted in considerable interest in their therapeutic applications for stroke. Since mitochondrial dysfunction is a central feature of ischemic neuronal cell death, a major goal of this thesis was to examine the effects of two common dietary flavonoids, quercetin and epicatechin, on neuronal mitochondrial function in models of ischemic stroke.

Quercetin and epicatechin were selected to investigate the effects of dietary flavonoids on neuronal mitochondrial function based on evidence that the apple peel-derived phenolic fraction termed AF4 was highly-protective in a mouse model of hypoxic/ischemic brain injury.⁸⁸ AF4 is comprised mainly of quercetin and epicatechin that account for about 85% of the total phenolic content of this apple peel extract.⁸⁸ Oral administration of AF4 also protected mice subjected to the experimental autoimmune encephalomyelitis (EAE) model of multiple sclerosis from spinal cord damage.⁸⁹ Neuroprotection by AF4 was associated with reduced spinal cord neuroinflammation and the elevated expression of genes that mediate mitochondrial biogenesis and remyelination.⁸⁹ These findings suggested that AF4 promoted recovery from EAE by stimulating mitochondrial function.

I have shown that epicatechin and quercetin synergistically protected cortical neurons from ischemic/reperfusion injury by dramatically improving various

aspects of mitochondrial performance. These actions were found to be mediated by the activation of distinct neuroprotective signaling pathways that converge on the mitochondrion. This resulted in elevated spare respiratory capacity known to increase the resistance of neurons to cytosolic Ca^{2+} overloading by improving mitochondrial Ca^{2+} handling and energetics. Epicatechin activated protein kinase B (Akt) while quercetin increased Ca^{2+} -mediated activity that caused synergistic elevations of CREB phosphorylation when these flavonoids were combined. A second major point of convergence was nitric oxide synthase (NOS) known to be activated at distinct sites by Akt and CamKII/V. Inhibition of NOS activity blocked neuroprotection by both epicatechin and quercetin. Based on these findings, I have proposed that the convergent benefits of increased CREB and NOS activity on mitochondrial biogenesis and energetics mediated synergistic neuroprotection by epicatechin and quercetin. These findings therefore provide mechanistic support for the benefits of a flavonoid-enriched diet in reducing the risk of stroke injury.²⁶⁰

Quercetin was shown to increase Ca^{2+} which recapitulated the increased cytosolic Ca^{2+} loads that mediate hypoxic preconditioning (HPC). The resultant elevation of mitochondrial Ca^{2+} uptake by HPC is known to stimulate mitochondrial biogenesis, improve antioxidant defence and enhance Ca^{2+} handling by increasing the expression of ionic plasma and mitochondrial membrane Ca^{2+} transporters. More recently, activity-induced neuroprotection in primary cultures of mouse hippocampal neurons has been linked to down-

regulation of MCU levels. The reduction of MCU levels protects neurons from glutamate-induced excitotoxicity by preventing mitochondrial Ca^{2+} overloading.¹⁶ Quercetin has also been shown to stimulate MCU activity in cultured neurons and brain.¹²⁵ Taken together, these findings suggest that MCU activity is modulated as part of a physiological adaptation to increased neuronal activity that mediates HPC and can also be activated with small molecules (flavonoids) to increase the resistance of neurons to excitotoxic/ischemic damage. Flavonoids may therefore serve as chemical pharmacophores that can be optimized to generate therapeutics with superior oral bioavailability, brain penetration and potency to increase resistance to stroke by modulating MCU activity.

The MCU functions to match metabolic demand with metabolic output but also may promote injurious mitochondrial Ca^{2+} overloading.^{243, 244} Modulation of MCU expression levels that maximize the response to metabolic demand, while minimizing mitochondrial Ca^{2+} overload could potentially render cells more resistant to ischemic insults. This proposal is further substantiated by a genetic neurodegenerative disorder resulting from loss of function of the negative MCU regulator known as MICU1.^{48, 49} Ablation of MICU1 function increases mitochondrial Ca^{2+} uptake resulting in a disorder characterized by myopathy, learning disability and neurodegeneration. Based on these findings, my next goals were therefore to establish the effects of global and conditional MCU loss on mitochondrial Ca^{2+} uptake, gene expression, cellular biogenetics and resistance to ischemic neuronal cell death.

6.2 Metabolic compensations for global MCU ablation compromise resistance to ischemic brain injury

I first used global MCU (G-MCU) knockout mice to investigate the effects of constitutive loss of this mitochondrial Ca^{2+} transporter on the resistance of forebrain neurons to ischemic damage. As expected, forebrain mitochondria isolated from G-MCU nulls displayed markedly reduced Ca^{2+} uptake and Ca^{2+} -induced mPTP opening. Despite evidence that these effects should have been neuroprotective, G-MCU nulls and wild-type (WT) mice had similar HI brain damage. However, the protective effects of HPC against HI brain injury in WT mice failed to occur in G-MCU nulls. In resolution of these seemingly discrepant findings, I showed that metabolic adaptations for G-MCU loss rendered cortical neurons more susceptible to Complex I suppression after OGD that models ischemia/reperfusion damage. Relative to WT cortical neurons, G-MCU null neurons depended more heavily on glycolysis to produce ATP following energetic stress. HI was found to deplete the G-MCU null forebrain of reducing equivalents (NADH) that are required to drive Complex I activity. The resultant energetic collapse may thus have promoted ischemic/reperfusion neuronal injury despite reduced mitochondrial Ca^{2+} uptake. To withstand the detrimental effects of chronically impaired mitochondrial Ca^{2+} uptake, G-MCU nulls appear to employ genetic adaptations common to HPC. These adaptations included the induction of mitochondrial apoptosis regulators and Ca^{2+} transporters that improve Ca^{2+} handling. However, such adaptations were insufficient to reduce HI brain damage and may also have interfered with the signaling pathways

necessary for neuroprotection by HPC in G-MCU nulls. These results suggest that long-term compensations for constitutive MCU inhibition negate the protective effects of MCU ablation.²⁵³

6.3 Conditional MCU ablation in forebrain neurons at adulthood protects mice from HI brain injury

To avoid developmental compensations resulting from global MCU deficiency, I generated a transgenic line enabling the MCU to be deleted selectively in forebrain neurons at adulthood. This was done by crossing Thy-1 CreER^{T2}-YFP mice with animals in which the MCU had been floxed. Administration of tamoxifen to the offspring activated Cre-mediated deletion of the MCU in Thy-1 expression forebrain neurons. The MCU was also silenced in primary neuronal cultures by siRNA-mediated MCU knockdown. Western blotting revealed that MCU levels in the hippocampus of conditional neuron-specific (CNS)-MCU nulls were reduced by about 80%. MCU knockdown by siRNA exposure for 3 days reduced MCU levels in cortical neuron cultures by approximately 50%. Both CNS-MCU deficient mice and MCU knockdown in primary cortical neuron cultures were protected from injury by experimental conditions that mimicked the effects of a stroke. Unlike G-MCU null neurons, MCU knockdown did not reduce spare respiratory capacity or increase glycolysis in primary cortical neuron cultures. Moreover, MCU knockdown preserved spare respiratory capacity following OGD. Electron microscopic analysis in the hippocampus of CNS-MCU deficient mice exposed to HI brain injury confirmed that MCU deficiency reduced

neuronal mitochondria damage. MCU deficiency therefore appeared to increase the resistance of neurons to ischemic damage by preserving mitochondrial function. The absence of metabolic changes following MCU knockdown suggested that reductions in MCU activity of 50% were well-tolerated and did not impair mitochondrial Ca^{2+} signaling. The ability of residual MCU activity to maintain an adequate response to increased energetic demand was further supported by similar basal and Ca^{2+} -stimulated levels of PDH phosphorylation in control and MCU deficient neurons. These findings support the safety and efficacy of acute MCU inhibition for the treatment of ischemic stroke.

6.4 Transcriptional repression of the MCU is neuroprotective without disrupting mitochondrial activity

MCU mRNA levels are suppressed by activity-dependent increases in Ca^{2+} signaling mediated by the activation CamKII that stimulates the transcriptional regulating factor NPAS4¹⁵. NPAS4 partially reduces MCU activity (~50%) by transcriptional repression of the MCU. Activity-dependent activation of this Ca^{2+} signaling pathway thus protects neurons from excitotoxic damage by reducing, but not completely inhibiting, MCU-mediated Ca^{2+} uptake. The presence of a physiological mechanism that protects mitochondria from excessive Ca^{2+} uptake without compromising Ca^{2+} -induced oxidative phosphorylation further supports the therapeutic viability of MCU inhibitors. This is an attractive therapeutic approach because MCU inhibitors need only achieve brain concentrations sufficient to reduce MCU activity by about 50%. The failure of G-MCU nulls to be

protected from HI brain injury suggests that the complete inhibition of MCU activity should be avoided.²⁵³ Mitochondria play a central role in buffering cytosolic Ca^{2+} . Hence, the complete absence of MCU activity could threaten neuronal viability by disrupting Ca^{2+} homeostasis. A total suppression of mitochondrial Ca^{2+} uptake may also impair neuronal function by inhibiting Ca^{2+} -induced increases in mitochondrial respiration. This hypothesis is supported by the compensatory increases of mRNA levels for plasma and mitochondrial membrane Ca^{2+} transporters observed in the hippocampus of G-MCU nulls. These adaptations, known to improve Ca^{2+} handling, likely enable G-MCU null neurons to harness alternative mitochondrial Ca^{2+} transport to regulate Ca^{2+} homeostasis and energy production. This was suggested by the ability of ionomycin- and glutamate-induced increases in cytosolic Ca^{2+} to promote the dephosphorylation of mitochondrial enzyme PDH in G-MCU null neurons. These findings further suggest that partial rather than complete inhibition of the MCU would be a better therapeutic strategy to protect the brain from damage by a stroke.

6.5 Future studies to validate the MCU as a drug target

Current therapies for stroke require the identification of whether the insult is ischemic or hemorrhagic. Administration of t-PA to hemorrhagic strokes may cause fatal bleeding. Brain imaging must be performed first to rule out if hemorrhagic stroke is responsible for the interruption of cerebral blood flow.⁴ The delay required to make a diagnosis of ischemic stroke delays t-PA administration

resulting in increased injury by extending the hypoxic insult.²⁶¹ The ideal neuroprotectant should be of immediate therapeutic benefit regardless of whether the stroke is hemorrhagic or ischemic. In the case of ischemic stroke, this treatment should also extend the efficacy and therapeutic window for t-PA. Future studies showing that CNS-MCU deficient mice are also protected from hemorrhagic stroke would further support the therapeutic development of brain penetrant MCU inhibitors. In this regard, the MCU inhibitor ruthenium red has been found to reduce brain damage in rodent model of subarachnoid hemorrhage model.²⁶² However, ruthenium red and chemically-related MCU inhibitors do not readily cross the blood-brain-barrier and block other Ca^{2+} transport mechanisms.²⁶³ Nevertheless, these studies support the therapeutic potential of MCU inhibitors for the acute treatment of hemorrhagic stroke.

As previously mentioned, MCU expression is suppressed as a part of a neuroprotective signal transduction pathway activated by Ca^{2+} -sensitive kinases. Kaempferol and quercetin have been shown to stimulate the MCU, either by increasing cytosolic Ca^{2+} levels and/or possibly by direct activation of this mitochondrial Ca^{2+} transporter.^{127, 128} This suggests that it may be possible to use these flavonoids to activate Ca^{2+} signaling pathways that suppress MCU activity. These compounds may thus precondition neurons against injury by a stroke. Numerous epidemiological studies have found a link between increased dietary consumption of these flavonoids and a reduced risk of stroke. My findings provide mechanistic support for the therapeutic use of quercetin and epicatechin

to reduce the risk of stroke, particularly in high-risk populations (diabetics, hypertensives, obese individuals and smokers).^{81, 81, 83, 264}

In addition to the therapeutic potential of prophylactically reducing MCU levels, those who have suffered a stroke may also benefit from the neuroprotective benefits of acute MCU inhibition. Interestingly, minocycline has been suggested to exert neuroprotective properties in animals and humans by blocking MCU activity.²⁶⁵⁻²⁶⁷ These studies provide compelling rationale to develop a more selective and potent MCU inhibitor.

6.6 Limitations

Stroke is a highly heterogenous condition that affects people in diverse ways making it difficult to accurately model in animals. As such, no *in vivo* model is able to fully recapitulate all aspects of stroke. This thesis utilized the Levine/Vannucci model of HI brain injury. Two hours following permanent occlusion of the common carotid artery by electrocauterization or two tied sutures, animals were placed in a sealed chamber, immersed in a 37°C water bath, flushed with hypoxic gas (8% oxygen content) to induce the infarct. Mice used in this thesis were males of 8-12 weeks of age.

This model has several limitations. The first major limitation is the high mortality rate, which increases with recovery time. Animals were thus allowed to recover for 24 hours to limit animal loss. My findings are thus relevant to only the relatively early events responsible for HI brain injury. I have therefore not

investigated long-term pathophysiology processes such as neuroinflammation that may also contribute to stroke damage. Additionally, healthy and young male mice aged 8-12 weeks were used to limit mortality. The young age of these mice is therefore not reflective of aged humans at higher risk of a stroke. Multiple co-morbidities are also frequently observed in older humans that are not observed in healthy and younger male mice. Typical mortality rates observed in the mouse model I have employed for 40-50 minutes of HI are 30-40% within the first 24h and increased with prolonged recovery times.²⁶⁸ By contrast, the mortality rate for ischemic stroke is higher at 57%.²⁶⁹ However, it would not have been ethically justifiable to increase the HI duration to match the human mortality rate.

As the mice were placed in a closed container to induce HI, this limited the ability to obtain hemodynamic and cerebral blood flow measurements. This problem has been addressed by other groups using a modified procedure in which the low oxygen gas was delivered during anesthesia by a face mask instead of in a closed chamber, but was not used in this thesis in order to increase animal throughput.²⁶⁸ This modified model reduced cerebral blood flow to approximately 20% of baseline while in the hypoxic chamber, cerebral blood flow returned to approximately 40% of baseline upon return to normoxic conditions. The poor reperfusion achieved following return to normoxic conditions represents another limitation since full reperfusion does not occur. Reductions in cerebral blood flow to less than 25% of baseline have been shown to achieve infarction with a high probability (>90%).²⁶⁸ These findings may account for the failure to produce HI

brain injury in more than 60% of the experimental subjects. Placing animals in the hypoxic chamber also results in systemic hypoxia that impacts tissue beyond the desired brain region. Although the combination of both hypoxia and the occlusion of a common carotid artery are required to induce a unilateral infarct, global hypoxia will alter normal physiological responses and energy production.²⁷⁰

Primary cortical neuron cultures were used as the experimental system to investigate the neuron specific effects of flavonoid treatments and MCU inhibition on mitochondrial function, energy metabolism, gene expression, kinase activation and cell viability following OGD. The neuronal cultures were derived from the cortices of embryos at days 14-16 *in utero* and used at days 7-10 *in vitro*. These neurons by nature are embryonic and developmentally immature. The properties of these embryonic neurons therefore differ from adult neurons. Additionally, the primary cultures which are composed primarily of neurons (95% pure) and thus do not represent the diverse cellular population, such as endothelial cells, microglia, astrocytes, oligodendrocytes and neurons found in brain. Although permitting neuron-specific investigations, the physiological impact of these other cell types on neurons and of neurons on these other cell types were not modeled.

Reference List

1. Mozaffarian D, Benjamin EJ, Go AS, Arnett DK, Blaha MJ, Cushman M, Das SR, de FS, Despres JP, Fullerton HJ, Howard VJ, Huffman MD, Isasi CR, Jimenez MC, Judd SE, Kissela BM, Lichtman JH, Lisabeth LD, Liu S, Mackey RH, Magid DJ, McGuire DK, Mohler ER, III, Moy CS, Muntner P, Mussolino ME, Nasir K, Neumar RW, Nichol G, Palaniappan L, Pandey DK, Reeves MJ, Rodriguez CJ, Rosamond W, Sorlie PD, Stein J, Towfighi A, Turan TN, Virani SS, Woo D, Yeh RW, Turner MB (2016) Executive Summary: Heart Disease and Stroke Statistics--2016 Update: A Report From the American Heart Association. *Circulation* 133: 447-454, PM:26811276.
2. Krishnamurthi RV, Moran AE, Forouzanfar MH, Bennett DA, Mensah GA, Lawes CM, Barker-Collo S, Connor M, Roth GA, Sacco R, Ezzati M, Naghavi M, Murray CJ, Feigin VL (2014) The global burden of hemorrhagic stroke: a summary of findings from the GBD 2010 study. *Glob.Heart* 9: 101-106, PM:25432119.
3. Feigin VL, Norrving B, Mensah GA (2017) Global Burden of Stroke *Circ.Res.* 120: 439-448, PM:28154096.
4. Casaubon LK, Boulanger JM, Blacquiere D, Boucher S, Brown K, Goddard T, Gordon J, Horton M, Lalonde J, LaRiviere C, Lavoie P, Leslie P, McNeill J, Menon BK, Moses B, Penn M, Perry J, Snieder E, Tymianski D, Foley N, Smith EE, Gubitz G, Hill MD, Glasser E, Lindsay P (2015) Canadian Stroke Best Practice Recommendations: Hyperacute Stroke Care Guidelines, Update 2015. *Int.J.Stroke* 10: 924-940, PM:26148019.
5. Parker S, Ali Y (2015) Changing contraindications for t-PA in acute stroke: review of 20 years since NINDS. *Curr.Cardiol.Rep.* 17: 81, PM:26277361.
6. Schurr A, Reid KH, Tseng MT, West C, Rigor BM (1986) Adaptation of adult brain tissue to anoxia and hypoxia in vitro. *Brain Res.* 374: 244-248, PM:3719335.
7. Murry CE, Jennings RB, Reimer KA (1986) Preconditioning with ischemia: a delay of lethal cell injury in ischemic myocardium. *Circulation* 74: 1124-1136, PM:3769170.
8. Li S, Hafeez A, Noorulla F, Geng X, Shao G, Ren C, Lu G, Zhao H, Ding Y, Ji X (2017) Preconditioning in neuroprotection: From hypoxia to ischemia. *Prog.Neurobiol.* PM:28110083.

9. Sharp FR, Ran R, Lu A, Tang Y, Strauss KI, Glass T, Ardizzone T, Binau M (2004) Hypoxic preconditioning protects against ischemic brain injury. *NeuroRx*. 1: 26-35, PM:15717005.
10. Almeida A, Moncada S, Bolanos JP (2004) Nitric oxide switches on glycolysis through the AMP protein kinase and 6-phosphofructo-2-kinase pathway. *Nat. Cell Biol.* 6: 45-51, PM:14688792.
11. Samoilov M, Churilova A, Gluschenko T, Rybnikova E (2014) Neocortical pCREB and BDNF expression under different modes of hypobaric hypoxia: role in brain hypoxic tolerance in rats. *Acta Histochem.* 116: 949-957, PM:24746628.
12. Shu L, Wang C, Wang J, Zhang Y, Zhang X, Yang Y, Zhuo J, Liu J (2016) The neuroprotection of hypoxic preconditioning on rat brain against traumatic brain injury by up-regulated transcription factor Nrf2 and HO-1 expression. *Neurosci.Lett.* 611: 74-80, PM:26590328.
13. Kopach O, Maistrenko A, Lushnikova I, Belan P, Skibo G, Voitenko N (2016) HIF-1alpha-mediated upregulation of SERCA2b: The endogenous mechanism for alleviating the ischemia-induced intracellular Ca(2+) store dysfunction in CA1 and CA3 hippocampal neurons. *Cell Calcium* 59: 251-261, PM:26969192.
14. Sisalli MJ, Secondo A, Esposito A, Valsecchi V, Savoia C, Di Renzo GF, Annunziato L, Scorziello A (2014) Endoplasmic reticulum refilling and mitochondrial calcium extrusion promoted in neurons by NCX1 and NCX3 in ischemic preconditioning are determinant for neuroprotection. *Cell Death.Differ.* 21: 1142-1149, PM:24632945.
15. Qiu J, Tan YW, Hagenston AM, Martel MA, Kneisel N, Skehel PA, Wyllie DJ, Bading H, Hardingham GE (2013) Mitochondrial calcium uniporter Mcu controls excitotoxicity and is transcriptionally repressed by neuroprotective nuclear calcium signals. *Nat. Commun.* 4: 2034, PM:23774321.
16. Qiu J, Tan YW, Hagenston AM, Martel MA, Kneisel N, Skehel PA, Wyllie DJ, Bading H, Hardingham GE (2013) Mitochondrial calcium uniporter Mcu controls excitotoxicity and is transcriptionally repressed by neuroprotective nuclear calcium signals. *Nat. Commun.* 4: 2034, PM:23774321.
17. Mink JW, Blumenshine RJ, Adams DB (1981) Ratio of central nervous system to body metabolism in vertebrates: its constancy and functional basis. *Am.J.Physiol* 241: R203-R212, PM:7282965.

18. Harris JJ, Jolivet R, Attwell D (2012) Synaptic energy use and supply. *Neuron* 75: 762-777, PM:22958818.
19. Sobieski C, Fitzpatrick MJ, Mennerick SJ (2017) Differential Presynaptic ATP Supply for Basal and High-Demand Transmission. *J.Neurosci.* 37: 1888-1899, PM:28093477.
20. Jang S, Nelson JC, Bend EG, Rodriguez-Laureano L, Tueros FG, Cartagena L, Underwood K, Jorgensen EM, Colon-Ramos DA (2016) Glycolytic Enzymes Localize to Synapses under Energy Stress to Support Synaptic Function. *Neuron* 90: 278-291, PM:27068791.
21. Chang DT, Honick AS, Reynolds IJ (2006) Mitochondrial trafficking to synapses in cultured primary cortical neurons. *J.Neurosci.* 26: 7035-7045, PM:16807333.
22. Herrero-Mendez A, Almeida A, Fernandez E, Maestre C, Moncada S, Bolanos JP (2009) The bioenergetic and antioxidant status of neurons is controlled by continuous degradation of a key glycolytic enzyme by APC/C-Cdh1. *Nat.Cell Biol.* 11: 747-752, PM:19448625.
23. Saotome M, Safiulina D, Szabadkai G, Das S, Fransson A, Aspenstrom P, Rizzuto R, Hajnoczky G (2008) Bidirectional Ca²⁺-dependent control of mitochondrial dynamics by the Miro GTPase. *Proc.Natl.Acad.Sci.U.S.A* 105: 20728-20733, PM:19098100.
24. Saxton WM, Hollenbeck PJ (2012) The axonal transport of mitochondria. *J.Cell Sci.* 125: 2095-2104, PM:22619228.
25. Sheng ZH (2017) The Interplay of Axonal Energy Homeostasis and Mitochondrial Trafficking and Anchoring. *Trends Cell Biol.* 27: 403-416, PM:28228333.
26. Llorente-Folch I, Rueda CB, Pardo B, Szabadkai G, Duchen MR, Satrustegui J (2015) The regulation of neuronal mitochondrial metabolism by calcium. *J.Physiol* 593: 3447-3462, PM:25809592.
27. Rabus R (2014) Fifteen years of physiological proteo(gen)omics with (marine) environmental bacteria. *Arch.Physiol Biochem.* 120: 173-187, PM:25233489.
28. Saez I, Duran J, Sinadinos C, Beltran A, Yanes O, Tevy MF, Martinez-Pons C, Milan M, Guinovart JJ (2014) Neurons have an active glycogen metabolism that contributes to tolerance to hypoxia. *J.Cereb.Blood Flow Metab* 34: 945-955, PM:24569689.
29. Pellerin L, Magistretti PJ (1994) Glutamate uptake into astrocytes stimulates aerobic glycolysis: a mechanism coupling neuronal activity to

glucose utilization. *Proc.Natl.Acad.Sci.U.S.A* 91: 10625-10629, PM:7938003.

30. Lee Y, Morrison BM, Li Y, Lengacher S, Farah MH, Hoffman PN, Liu Y, Tsingalia A, Jin L, Zhang PW, Pellerin L, Magistretti PJ, Rothstein JD (2012) Oligodendroglia metabolically support axons and contribute to neurodegeneration. *Nature* 487: 443-448, PM:22801498.
31. Hasel P, Dando O, Jiwaji Z, Baxter P, Todd AC, Heron S, Markus NM, McQueen J, Hampton DW, Torvell M, Tiwari SS, McKay S, Eraso-Pichot A, Zorzano A, Masgrau R, Galea E, Chandran S, Wyllie DJA, Simpson TI, Hardingham GE (2017) Neurons and neuronal activity control gene expression in astrocytes to regulate their development and metabolism. *Nat. Commun.* 8: 15132, PM:28462931.
32. Traba J, Satrustegui J, del AA (2009) Characterization of SCaMC-3-like/slc25a41, a novel calcium-independent mitochondrial ATP-Mg/Pi carrier. *Biochem.J.* 418: 125-133, PM:18928449.
33. Del AA, Contreras L, Pardo B, Satrustegui J (2016) Calcium regulation of mitochondrial carriers. *Biochim.Biophys.Acta* 1863: 2413-2421, PM:27033520.
34. Llorente-Folch I, Rueda CB, Amigo I, del AA, Saheki T, Pardo B, Satrustegui J (2013) Calcium-regulation of mitochondrial respiration maintains ATP homeostasis and requires ARALAR/AGC1-malate aspartate shuttle in intact cortical neurons. *J.Neurosci.* 33: 13957-71, 13971a, PM:23986233.
35. Llorente-Folch I, Rueda CB, Pardo B, Szabadkai G, Duchen MR, Satrustegui J (2015) The regulation of neuronal mitochondrial metabolism by calcium. *J.Physiol* 593: 3447-3462, PM:25809592.
36. Kirichok Y, Krapivinsky G, Clapham DE (2004) The mitochondrial calcium uniporter is a highly selective ion channel. *Nature* 427: 360-364, PM:14737170.
37. Nichols BJ, Rigoulet M, Denton RM (1994) Comparison of the effects of Ca²⁺, adenine nucleotides and pH on the kinetic properties of mitochondrial NAD(+)-isocitrate dehydrogenase and oxoglutarate dehydrogenase from the yeast *Saccharomyces cerevisiae* and rat heart. *Biochem.J.* 303 (Pt 2): 461-465, PM:7980405.
38. Denton RM (2009) Regulation of mitochondrial dehydrogenases by calcium ions. *Biochim.Biophys.Acta* 1787: 1309-1316, PM:19413950.

39. Territo PR, Mootha VK, French SA, Balaban RS (2000) Ca²⁺ activation of heart mitochondrial oxidative phosphorylation: role of the F₀/F₁-ATPase. *Am.J.Physiol Cell Physiol* 278: C423-C435, PM:10666039.
40. Sancak Y, Markhard AL, Kitami T, Kovacs-Bogdan E, Kamer KJ, Udeshi ND, Carr SA, Chaudhuri D, Clapham DE, Li AA, Calvo SE, Goldberger O, Mootha VK (2013) EMRE is an essential component of the mitochondrial calcium uniporter complex. *Science* 342: 1379-1382, PM:24231807.
41. Kovacs-Bogdan E, Sancak Y, Kamer KJ, Plovanich M, Jambhekar A, Huber RJ, Myre MA, Blower MD, Mootha VK (2014) Reconstitution of the mitochondrial calcium uniporter in yeast. *Proc.Natl.Acad.Sci.U.S.A* 111: 8985-8990, PM:24889638.
42. Oxenoid K, Dong Y, Cao C, Cui T, Sancak Y, Markhard AL, Grabarek Z, Kong L, Liu Z, Ouyang B, Cong Y, Mootha VK, Chou JJ (2016) Architecture of the mitochondrial calcium uniporter. *Nature* 533: 269-273, PM:27135929.
43. De SD, Raffaello A, Teardo E, Szabo I, Rizzuto R (2011) A forty-kilodalton protein of the inner membrane is the mitochondrial calcium uniporter. *Nature* 476: 336-340, PM:21685888.
44. Baughman JM, Perocchi F, Girgis HS, Plovanich M, Belcher-Timme CA, Sancak Y, Bao XR, Strittmatter L, Goldberger O, Bogorad RL, Kotliansky V, Mootha VK (2011) Integrative genomics identifies MCU as an essential component of the mitochondrial calcium uniporter. *Nature* 476: 341-345, PM:21685886.
45. Raffaello A, De SD, Sabbadin D, Teardo E, Merli G, Picard A, Checchetto V, Moro S, Szabo I, Rizzuto R (2013) The mitochondrial calcium uniporter is a multimer that can include a dominant-negative pore-forming subunit. *EMBO J.* 32: 2362-2376, PM:23900286.
46. Jhun BS, Mishra J, Monaco S, Fu D, Jiang W, Sheu SS, Uchi J (2016) The mitochondrial Ca²⁺ uniporter: regulation by auxiliary subunits and signal transduction pathways. *Am.J.Physiol Cell Physiol* 311: C67-C80, PM:27122161.
47. Csordas G, Golenar T, Seifert EL, Kamer KJ, Sancak Y, Perocchi F, Moffat C, Weaver D, de la Fuente PS, Bogorad R, Kotliansky V, Adjianto J, Mootha VK, Hajnoczky G (2013) MICU1 controls both the threshold and cooperative activation of the mitochondrial Ca²⁺ uniporter. *Cell Metab* 17: 976-987, PM:23747253.
48. Matesanz-Isabel J, Arias-del-Val J, Alvarez-Illera P, Fonteriz RI, Montero M, Alvarez J (2016) Functional roles of MICU1 and MICU2 in

mitochondrial Ca(2+) uptake. *Biochim.Biophys.Acta* 1858: 1110-1117, PM:26903221.

49. Bhosale G, Sharpe JA, Koh A, Kouli A, Szabadkai G, Duchen MR (2017) Pathological consequences of MICU1 mutations on mitochondrial calcium signalling and bioenergetics. *Biochim.Biophys.Acta* 1864: 1009-1017, PM:28132899.
50. Plovanich M, Bogorad RL, Sancak Y, Kamer KJ, Strittmatter L, Li AA, Girgis HS, Kuchimanchi S, De GJ, Speciner L, Taneja N, Oshea J, Koteliansky V, Mootha VK (2013) MICU2, a paralog of MICU1, resides within the mitochondrial uniporter complex to regulate calcium handling. *PLoS.One.* 8: e55785, PM:23409044.
51. Mammucari C, Raffaello A, Vecellio RD, Rizzuto R (2016) Molecular structure and pathophysiological roles of the Mitochondrial Calcium Uniporter. *Biochim.Biophys.Acta* 1863: 2457-2464, PM:26968367.
52. Rizzuto R, De SD, Raffaello A, Mammucari C (2012) Mitochondria as sensors and regulators of calcium signalling. *Nat.Rev.Mol.Cell Biol.* 13: 566-578, PM:22850819.
53. De SD, Rizzuto R, Pozzan T (2016) Enjoy the Trip: Calcium in Mitochondria Back and Forth. *Annu.Rev.Biochem.* 85: 161-192, PM:27145841.
54. Brookes PS, Parker N, Buckingham JA, Vidal-Puig A, Halestrap AP, Gunter TE, Nicholls DG, Bernardi P, Lemasters JJ, Brand MD (2008) UCPs--unlikely calcium porters. *Nat.Cell Biol.* 10: 1235-1237, PM:18978830.
55. Tsai MF, Jiang D, Zhao L, Clapham D, Miller C (2014) Functional reconstitution of the mitochondrial Ca²⁺/H⁺ antiporter Letm1. *J.Gen.Physiol* 143: 67-73, PM:24344246.
56. Jiang D, Zhao L, Clish CB, Clapham DE (2013) Letm1, the mitochondrial Ca²⁺/H⁺ antiporter, is essential for normal glucose metabolism and alters brain function in Wolf-Hirschhorn syndrome. *Proc.Natl.Acad.Sci.U.S.A* 110: E2249-E2254, PM:23716663.
57. Sparagna GC, Gunter KK, Sheu SS, Gunter TE (1995) Mitochondrial calcium uptake from physiological-type pulses of calcium. A description of the rapid uptake mode. *J.Biol.Chem.* 270: 27510-27515, PM:7499209.

58. Buntinas L, Gunter KK, Sparagna GC, Gunter TE (2001) The rapid mode of calcium uptake into heart mitochondria (RaM): comparison to RaM in liver mitochondria. *Biochim.Biophys.Acta* 1504: 248-261, PM:11245789.
59. Wei AC, Liu T, Winslow RL, O'Rourke B (2012) Dynamics of matrix-free Ca²⁺ in cardiac mitochondria: two components of Ca²⁺ uptake and role of phosphate buffering. *J.Gen.Physiol* 139: 465-478, PM:22641641.
60. Bondarenko AI, Jean-Quartier C, Malli R, Graier WF (2013) Characterization of distinct single-channel properties of Ca²⁺(+) inward currents in mitochondria. *Pflugers Arch.* 465: 997-1010, PM:23397170.
61. Palty R, Silverman WF, Hershfinkel M, Caporale T, Sensi SL, Parnis J, Nolte C, Fishman D, Shoshan-Barmatz V, Herrmann S, Khananshvil D, Sekler I (2010) NCLX is an essential component of mitochondrial Na⁺/Ca²⁺ exchange. *Proc.Natl.Acad.Sci.U.S.A* 107: 436-441, PM:20018762.
62. Palty R, Sekler I (2012) The mitochondrial Na⁽⁺⁾/Ca⁽²⁺⁾ exchanger. *Cell Calcium* 52: 9-15, PM:22430014.
63. Luongo TS, Lambert JP, Gross P, Nwokedi M, Lombardi AA, Shanmughapriya S, Carpenter AC, Kolmetzky D, Gao E, van Berlo JH, Tsai EJ, Molkentin JD, Chen X, Madesh M, Houser SR, Elrod JW (2017) The mitochondrial Na⁺/Ca²⁺ exchanger is essential for Ca²⁺ homeostasis and viability. *Nature* 545: 93-97, PM:28445457.
64. Kroemer G, Petit P, Zamzami N, Vayssiere JL, Mignotte B (1995) The biochemistry of programmed cell death. *FASEB J.* 9: 1277-1287, PM:7557017.
65. Tait SW, Green DR (2013) Mitochondrial regulation of cell death. *Cold Spring Harb.Perspect.Biol.* 5: PM:24003207.
66. Tait SW, Ichim G, Green DR (2014) Die another way--non-apoptotic mechanisms of cell death. *J.Cell Sci.* 127: 2135-2144, PM:24833670.
67. Galluzzi L, Blomgren K, Kroemer G (2009) Mitochondrial membrane permeabilization in neuronal injury. *Nat.Rev.Neurosci.* 10: 481-494, PM:19543220.
68. Giorgio V, Guo L, Bassot C, Petronilli V, Bernardi P (2017) Calcium and regulation of the mitochondrial permeability transition. *Cell Calcium* PM:28522037.
69. Czabotar PE, Lessene G, Strasser A, Adams JM (2014) Control of apoptosis by the BCL-2 protein family: implications for physiology and therapy. *Nat.Rev.Mol.Cell Biol.* 15: 49-63, PM:24355989.

70. Jonas EA, Porter GA, Alavian KN (2014) Bcl-xL in neuroprotection and plasticity. *Front Physiol* 5: 355, PM:25278904.
71. Nicholson DW (1999) Caspase structure, proteolytic substrates, and function during apoptotic cell death. *Cell Death.Differ.* 6: 1028-1042, PM:10578171.
72. Polster BM, Basanez G, Etxebarria A, Hardwick JM, Nicholls DG (2005) Calpain I induces cleavage and release of apoptosis-inducing factor from isolated mitochondria. *J.Biol.Chem.* 280: 6447-6454, PM:15590628.
73. Zhou B, Yu P, Lin MY, Sun T, Chen Y, Sheng ZH (2016) Facilitation of axon regeneration by enhancing mitochondrial transport and rescuing energy deficits. *J.Cell Biol.* 214: 103-119, PM:27268498.
74. Burte F, Carelli V, Chinnery PF, Yu-Wai-Man P (2015) Disturbed mitochondrial dynamics and neurodegenerative disorders. *Nat.Rev.Neurol.* 11: 11-24, PM:25486875.
75. Lightowers RN, Taylor RW, Turnbull DM (2015) Mutations causing mitochondrial disease: What is new and what challenges remain? *Science* 349: 1494-1499, PM:26404827.
76. Morissette M, Di PT (2017) Non-human primate models of PD to test novel therapies. *J.Neural Transm.(Vienna.)* PM:28391443.
77. Borlongan CV, Koutouzis TK, Sanberg PR (1997) 3-Nitropropionic acid animal model and Huntington's disease. *Neurosci.Biobehav.Rev.* 21: 289-293, PM:9168265.
78. Johnson ME, Bobrovskaya L (2015) An update on the rotenone models of Parkinson's disease: their ability to reproduce the features of clinical disease and model gene-environment interactions. *Neurotoxicology* 46: 101-116, PM:25514659.
79. Ten VS, Starkov A (2012) Hypoxic-ischemic injury in the developing brain: the role of reactive oxygen species originating in mitochondria. *Neurol.Res.Int.* 2012: 542976, PM:22548167.
80. Wilkins HM, Weidling IW, Ji Y, Swerdlow RH (2017) Mitochondria-Derived Damage-Associated Molecular Patterns in Neurodegeneration. *Front Immunol.* 8: 508, PM:28491064.
81. Cassidy A, Rimm EB, O'Reilly EJ, Logroscino G, Kay C, Chiuve SE, Rexrode KM (2012) Dietary flavonoids and risk of stroke in women. *Stroke* 43: 946-951, PM:22363060.

82. Chen L, Bi XY, Zhu LX, Qiu YQ, Ding SJ, Deng BQ (2011) [Flavonoids of puerarin versus tanshinone II A for ischemic stroke: a randomized controlled trial]. *Zhong.Xi.Yi.Jie.He.Xue.Bao.* 9: 1215-1220, PM:22088587.
83. Hirvonen T, Virtamo J, Korhonen P, Albanes D, Pietinen P (2000) Intake of flavonoids, carotenoids, vitamins C and E, and risk of stroke in male smokers. *Stroke* 31: 2301-2306, PM:11022054.
84. Tang Z, Li M, Zhang X, Hou W (2016) Dietary flavonoid intake and the risk of stroke: a dose-response meta-analysis of prospective cohort studies. *BMJ Open.* 6: e008680, PM:27279473.
85. Cherubini A, Ruggiero C, Morand C, Lattanzio F, Dell'aquila G, Zuliani G, Di IA, Andres-Lacueva C (2008) Dietary antioxidants as potential pharmacological agents for ischemic stroke. *Current Medicinal Chemistry* 15: 1236-1248, PM:18473816.
86. Williams CA, Grayer RJ (2004) Anthocyanins and other flavonoids. *Nat.Prod.Rep.* 21: 539-573, PM:15282635.
87. Jones QR, Warford J, Rupasinghe HP, Robertson GS (2012) Target-based selection of flavonoids for neurodegenerative disorders. *Trends in Pharmacological Sciences* 33: 602-610, PM:22980637.
88. Keddy PG, Dunlop K, Warford J, Samson ML, Jones QR, Rupasinghe HP, Robertson GS (2012) Neuroprotective and anti-inflammatory effects of the flavonoid-enriched fraction AF4 in a mouse model of hypoxic-ischemic brain injury. *PLoS.One.* 7: e51324, PM:23251498.
89. Warford J, Jones QR, Nichols M, Sullivan V, Rupasinghe HP, Robertson GS (2014) The flavonoid-enriched fraction AF4 suppresses neuroinflammation and promotes restorative gene expression in a mouse model of experimental autoimmune encephalomyelitis. *Journal of Neuroimmunology* 268: 71-83, PM:24485149.
90. Rendeiro C, Rhodes JS, Spencer JP (2015) The mechanisms of action of flavonoids in the brain: Direct versus indirect effects. *Neurochem.Int.* 89: 126-139, PM:26260546.
91. Jones QR, Warford J, Rupasinghe HP, Robertson GS (2012) Target-based selection of flavonoids for neurodegenerative disorders. *Trends Pharmacol.Sci.* 33: 602-610, PM:22980637.
92. Bustin SA, Benes V, Garson JA, Hellemans J, Huggett J, Kubista M, Mueller R, Nolan T, Pfaffl MW, Shipley GL, Vandesompele J, Wittwer CT (2009) The MIQE guidelines: minimum information for publication of

- quantitative real-time PCR experiments. *Clin.Chem* 55: 611-622, PM:19246619.
93. LEVINE S (1960) Anoxic-ischemic encephalopathy in rats. *Am.J.Pathol.* 36: 1-17, PM:14416289.
 94. Prasain JK, Carlson SH, Wyss JM (2010) Flavonoids and age-related disease: risk, benefits and critical windows. *Maturitas* 66: 163-171, PM:20181448.
 95. Ross JA, Kasum CM (2002) Dietary flavonoids: bioavailability, metabolic effects, and safety. *Annual Review of Nutrition* 22: 19-34, PM:12055336.
 96. Harwood M, Danielewska-Nikiel B, Borzelleca JF, Flamm GW, Williams GM, Lines TC (2007) A critical review of the data related to the safety of quercetin and lack of evidence of in vivo toxicity, including lack of genotoxic/carcinogenic properties. *Food and Chemical Toxicology* 45: 2179-2205, PM:17698276.
 97. Gutierrez-Merino C, Lopez-Sanchez C, Lagoa R, Samhan-Arias AK, Bueno C, Garcia-Martinez V (2011) Neuroprotective actions of flavonoids. *Current Medicinal Chemistry* 18: 1195-1212, PM:21291366.
 98. Simonyi A, Wang Q, Miller RL, Yusof M, Shelat PB, Sun AY, Sun GY (2005) Polyphenols in cerebral ischemia: novel targets for neuroprotection. *Molecular Neurobiology* 31: 135-147, PM:15953817.
 99. Joshipura KJ, Ascherio A, Manson JE, Stampfer MJ, Rimm EB, Speizer FE, Hennekens CH, Spiegelman D, Willett WC (1999) Fruit and vegetable intake in relation to risk of ischemic stroke. *JAMA* 282: 1233-1239, PM:10517425.
 100. He FJ, Nowson CA, MacGregor GA (2006) Fruit and vegetable consumption and stroke: meta-analysis of cohort studies. *Lancet* 367: 320-326, PM:16443039.
 101. Mursu J, Voutilainen S, Nurmi T, Tuomainen TP, Kurl S, Salonen JT (2008) Flavonoid intake and the risk of ischaemic stroke and CVD mortality in middle-aged Finnish men: the Kuopio Ischaemic Heart Disease Risk Factor Study. *Br.J.Nutr.* 100: 890-895, PM:18377681.
 102. Mizrahi A, Knekt P, Montonen J, Laaksonen MA, Heliovaara M, Jarvinen R (2009) Plant foods and the risk of cerebrovascular diseases: a potential protection of fruit consumption. *Br.J.Nutr.* 102: 1075-1083, PM:19646291.
 103. Hollman PC, Geelen A, Kromhout D (2010) Dietary flavonol intake may lower stroke risk in men and women. *Journal of Nutrition* 140: 600-604, PM:20089788.

104. Wang XQ, Yao RQ, Liu X, Huang JJ, Qi DS, Yang LH (2011) Quercetin protects oligodendrocyte precursor cells from oxygen/glucose deprivation injury in vitro via the activation of the PI3K/Akt signaling pathway. *Brain Research Bulletin* 86: 277-284, PM:21803128.
105. Kim J, Lee S, Shim J, Kim HW, Kim J, Jang YJ, Yang H, Park J, Choi SH, Yoon JH, Lee KW, Lee HJ (2012) Caffeinated coffee, decaffeinated coffee, and the phenolic phytochemical chlorogenic acid up-regulate NQO1 expression and prevent H₂O₂-induced apoptosis in primary cortical neurons. *Neurochemistry International* 60: 466-474, PM:22353630.
106. Lin MT, Beal MF (2006) Mitochondrial dysfunction and oxidative stress in neurodegenerative diseases. *Nature* 443: 787-795, PM:17051205.
107. Sanderson TH, Reynolds CA, Kumar R, Przyklenk K, Huttemann M (2013) Molecular mechanisms of ischemia-reperfusion injury in brain: pivotal role of the mitochondrial membrane potential in reactive oxygen species generation. *Molecular Neurobiology* 47: 9-23, PM:23011809.
108. Zeiger SL, Stankowski JN, McLaughlin B (2011) Assessing neuronal bioenergetic status. *Methods Mol. Biol.* 758: 215-235, PM:21815069.
109. Zhao L, Wientjes MG, Au JL (2004) Evaluation of combination chemotherapy: integration of nonlinear regression, curve shift, isobologram, and combination index analyses. *Clin. Cancer Res.* 10: 7994-8004, PM:15585635.
110. Finck BN, Kelly DP (2006) PGC-1 coactivators: inducible regulators of energy metabolism in health and disease. *J. Clin. Invest* 116: 615-622, PM:16511594.
111. Handschin C (2009) The biology of PGC-1alpha and its therapeutic potential. *Trends in Pharmacological Sciences* 30: 322-329, PM:19446346.
112. Cheng A, Wan R, Yang JL, Kamimura N, Son TG, Ouyang X, Luo Y, Okun E, Mattson MP (2012) Involvement of PGC-1alpha in the formation and maintenance of neuronal dendritic spines. *Nat. Commun.* 3: 1250, PM:23212379.
113. Chen LW, Horng LY, Wu CL, Sung HC, Wu RT (2012) Activating mitochondrial regulator PGC-1alpha expression by astrocytic NGF is a

- therapeutic strategy for Huntington's disease. *Neuropharmacology* 63: 719-732, PM:22633948.
114. Mayr B, Montminy M (2001) Transcriptional regulation by the phosphorylation-dependent factor CREB. *Nature Reviews: Molecular Cell Biology* 2: 599-609, PM:11483993.
 115. Downward J (2004) PI 3-kinase, Akt and cell survival. *Seminars in Cell & Developmental Biology* 15: 177-182, PM:15209377.
 116. Schroeter H, Bahia P, Spencer JP, Sheppard O, Rattray M, Cadenas E, Rice-Evans C, Williams RJ (2007) (-)Epicatechin stimulates ERK-dependent cyclic AMP response element activity and up-regulates GluR2 in cortical neurons. *Journal of Neurochemistry* 101: 1596-1606, PM:17298385.
 117. Wang J, Ferruzzi MG, Ho L, Blount J, Janle EM, Gong B, Pan Y, Gowda GA, Raftery D, Arrieta-Cruz I, Sharma V, Cooper B, Lobo J, Simon JE, Zhang C, Cheng A, Qian X, Ono K, Teplow DB, Pavlides C, Dixon RA, Pasinetti GM (2012) Brain-targeted proanthocyanidin metabolites for Alzheimer's disease treatment. *Journal of Neuroscience* 32: 5144-5150, PM:22496560.
 118. Schaffer S, Halliwell B (2012) Do polyphenols enter the brain and does it matter? Some theoretical and practical considerations. *Genes Nutr.* 7: 99-109, PM:22012276.
 119. Abd El Mohsen MM, Kuhnle G, Rechner AR, Schroeter H, Rose S, Jenner P, Rice-Evans CA (2002) Uptake and metabolism of epicatechin and its access to the brain after oral ingestion. *Free Radic.Biol.Med.* 33: 1693-1702, PM:12488137.
 120. Lin WY, Chang YC, Lee HT, Huang CC (2009) CREB activation in the rapid, intermediate, and delayed ischemic preconditioning against hypoxic-ischemia in neonatal rat. *Journal of Neurochemistry* 108: 847-859, PM:19183266.
 121. Kitagawa K (2007) CREB and cAMP response element-mediated gene expression in the ischemic brain. *FEBS Journal* 274: 3210-3217, PM:17565598.
 122. Mabuchi T, Kitagawa K, Kuwabara K, Takasawa K, Ohtsuki T, Xia Z, Storm D, Yanagihara T, Hori M, Matsumoto M (2001) Phosphorylation of cAMP response element-binding protein in hippocampal neurons as a protective response after exposure to glutamate in vitro and ischemia in vivo. *Journal of Neuroscience* 21: 9204-9213, PM:11717354.

123. Hajnoczky G, Robb-Gaspers LD, Seitz MB, Thomas AP (1995) Decoding of cytosolic calcium oscillations in the mitochondria. *Cell* 82: 415-424, PM:7634331.
124. Fiorani M, Guidarelli A, Blasa M, Azzolini C, Candiracci M, Piatti E, Cantoni O (2010) Mitochondria accumulate large amounts of quercetin: prevention of mitochondrial damage and release upon oxidation of the extramitochondrial fraction of the flavonoid. *J.Nutr.Biochem.* 21: 397-404, PM:19278846.
125. Montero M, Lobaton CD, Hernandez-Sanmiguel E, Santodomingo J, Vay L, Moreno A, Alvarez J (2004) Direct activation of the mitochondrial calcium uniporter by natural plant flavonoids. *Biochemical Journal* 384: 19-24, PM:15324303.
126. Vay L, Hernandez-Sanmiguel E, Santo-Domingo J, Lobaton CD, Moreno A, Montero M, Alvarez J (2007) Modulation of Ca(2+) release and Ca(2+) oscillations in HeLa cells and fibroblasts by mitochondrial Ca(2+) uniporter stimulation. *J.Physiol* 580: 39-49, PM:17234694.
127. Sanganahalli BG, Herman P, Hyder F, Kannurpatti SS (2013) Mitochondrial functional state impacts spontaneous neocortical activity and resting state fMRI. *PLoS One* 8: e63317, PM:23650561.
128. Sanganahalli BG, Herman P, Hyder F, Kannurpatti SS (2013) Mitochondrial calcium uptake capacity modulates neocortical excitability. *J.Cereb.Blood Flow Metab* 33: 1115-1126, PM:23591650.
129. Denton RM (2009) Regulation of mitochondrial dehydrogenases by calcium ions. *Biochimica et Biophysica Acta: Protein Structure and Molecular Enzymology* 1787: 1309-1316, PM:19413950.
130. Balaban RS (2002) Cardiac energy metabolism homeostasis: role of cytosolic calcium. *J.Mol.Cell Cardiol.* 34: 1259-1271, PM:12392982.
131. Satrustegui J, Pardo B, del AA (2007) Mitochondrial transporters as novel targets for intracellular calcium signaling. *Physiol Rev.* 87: 29-67, PM:17237342.
132. Territo PR, Mootha VK, French SA, Balaban RS (2000) Ca(2+) activation of heart mitochondrial oxidative phosphorylation: role of the F(0)/F(1)-ATPase. *Am.J.Physiol Cell Physiol* 278: C423-C435, PM:10666039.
133. Saponara S, Sgaragli G, Fusi F (2002) Quercetin as a novel activator of L-type Ca(2+) channels in rat tail artery smooth muscle cells. *British Journal of Pharmacology* 135: 1819-1827, PM:11934824.

134. Lee BH, Choi SH, Shin TJ, Pyo MK, Hwang SH, Kim BR, Lee SM, Lee JH, Kim HC, Park HY, Rhim H, Nah SY (2010) Quercetin enhances human $\alpha 7$ nicotinic acetylcholine receptor-mediated ion current through interactions with $\text{Ca}(2+)$ binding sites. *Mol.Cells* 30: 245-253, PM:20803082.
135. Baran I, Ganea C (2013) RyR3 in situ regulation by $\text{Ca}(2+)$ and quercetin and the RyR3-mediated $\text{Ca}(2+)$ release flux in intact Jurkat cells. *Arch.Biochem.Biophys.* 540: 145-159, PM:24211435.
136. Gonzalez-Zulueta M, Feldman AB, Klesse LJ, Kalb RG, Dillman JF, Parada LF, Dawson TM, Dawson VL (2000) Requirement for nitric oxide activation of p21(ras)/extracellular regulated kinase in neuronal ischemic preconditioning. *Proc.Natl.Acad.Sci.U.S.A* 97: 436-441, PM:10618436.
137. Ramirez-Sanchez I, Aguilar H, Ceballos G, Villarreal F (2012) (-)-Epicatechin-induced calcium independent eNOS activation: roles of HSP90 and AKT. *Mol.Cell Biochem.* 370: 141-150, PM:22865466.
138. Kuhlmann CR, Schaefer CA, Kosok C, Abdallah Y, Walther S, Ludders DW, Neumann T, Tillmanns H, Schafer C, Piper HM, Erdogan A (2005) Quercetin-induced induction of the NO/cGMP pathway depends on $\text{Ca}2+$ -activated $\text{K}+$ channel-induced hyperpolarization-mediated $\text{Ca}2+$ -entry into cultured human endothelial cells. *Planta Med.* 71: 520-524, PM:15971122.
139. Khoo NK, White CR, Pozzo-Miller L, Zhou F, Constance C, Inoue T, Patel RP, Parks DA (2010) Dietary flavonoid quercetin stimulates vasorelaxation in aortic vessels. *Free Radic.Biol.Med.* 49: 339-347, PM:20423726.
140. Ha HJ, Kwon YS, Park SM, Shin T, Park JH, Kim HC, Kwon MS, Wie MB (2003) Quercetin attenuates oxygen-glucose deprivation- and excitotoxin-induced neurotoxicity in primary cortical cell cultures. *Biological & Pharmaceutical Bulletin* 26: 544-546, PM:12673040.
141. Yang EJ, Kim GS, Kim JA, Song KS (2013) Protective effects of onion-derived quercetin on glutamate-mediated hippocampal neuronal cell death. *Pharmacogn.Mag.* 9: 302-308, PM:24124281.
142. Silva B, Oliveira PJ, Dias A, Malva JO (2008) Quercetin, kaempferol and biapigenin from *Hypericum perforatum* are neuroprotective against excitotoxic insults. *Neurotox.Res.* 13: 265-279, PM:18522906.
143. Ishige K, Schubert D, Sagara Y (2001) Flavonoids protect neuronal cells from oxidative stress by three distinct mechanisms. *Free Radic.Biol.Med.* 30: 433-446, PM:11182299.

144. Soundararajan R, Wishart AD, Rupasinghe HP, Arcellana-Panlilio M, Nelson CM, Mayne M, Robertson GS (2008) Quercetin 3-glucoside protects neuroblastoma (SH-SY5Y) cells in vitro against oxidative damage by inducing sterol regulatory element-binding protein-2-mediated cholesterol biosynthesis. *Journal of Biological Chemistry* 283: 2231-2245, PM:18032389.
145. Wagner C, Vargas AP, Roos DH, Morel AF, Farina M, Nogueira CW, Aschner M, Rocha JB (2010) Comparative study of quercetin and its two glycoside derivatives quercitrin and rutin against methylmercury (MeHg)-induced ROS production in rat brain slices. *Archives of Toxicology* 84: 89-97, PM:19902180.
146. Roshanzamir F, Yazdanparast R (2014) Quercetin attenuates cell apoptosis of oxidant-stressed SK-N-MC cells while suppressing up-regulation of the defensive element, HIF-1alpha. *Neuroscience* 277: 780-793, PM:25108166.
147. Wagner C, Fachinetto R, Dalla Corte CL, Brito VB, Severo D, de Oliveira Costa DG, Morel AF, Nogueira CW, Rocha JB (2006) Quercitrin, a glycoside form of quercetin, prevents lipid peroxidation in vitro. *Brain Research* 1107: 192-198, PM:16828712.
148. Karuppagounder SS, Madathil SK, Pandey M, Haobam R, Rajamma U, Mohanakumar KP (2013) Quercetin up-regulates mitochondrial complex-I activity to protect against programmed cell death in rotenone model of Parkinson's disease in rats. *Neuroscience* 236: 136-148, PM:23357119.
149. Filomeni G, Graziani I, De ZD, Dini L, Centonze D, Rotilio G, Ciriolo MR (2012) Neuroprotection of kaempferol by autophagy in models of rotenone-mediated acute toxicity: possible implications for Parkinson's disease. *Neurobiology of Aging* 33: 767-785, PM:20594614.
150. Mercer LD, Kelly BL, Horne MK, Beart PM (2005) Dietary polyphenols protect dopamine neurons from oxidative insults and apoptosis: investigations in primary rat mesencephalic cultures. *Biochemical Pharmacology* 69: 339-345, PM:15627486.
151. Liu RL, Xiong QJ, Shu Q, Wu WN, Cheng J, Fu H, Wang F, Chen JG, Hu ZL (2012) Hyperoside protects cortical neurons from oxygen-glucose deprivation-reperfusion induced injury via nitric oxide signal pathway. *Brain Research* 1469: 164-173, PM:22771858.
152. Wang CP, Li JL, Zhang LZ, Zhang XC, Yu S, Liang XM, Ding F, Wang ZW (2013) Isoquercetin protects cortical neurons from oxygen-glucose deprivation-reperfusion induced injury via suppression of TLR4-NF-small

- ka, CyrillicB signal pathway. *Neurochemistry International* 63: 741-749, PM:24099731.
153. Shah ZA, Li RC, Ahmad AS, Kensler TW, Yamamoto M, Biswal S, Dore S (2010) The flavanol (-)-epicatechin prevents stroke damage through the Nrf2/HO1 pathway. *J.Cereb.Blood Flow Metab* 30: 1951-1961, PM:20442725.
 154. Orban-Gyapai O, Raghavan A, Vasas A, Forgo P, Hohmann J, Shah ZA (2014) Flavonoids Isolated from *Rumex aquaticus* Exhibit Neuroprotective and Neurorestorative Properties by Enhancing Neurite Outgrowth and Synaptophysin. *CNS.Neurol.Disord Drug Targets*. 13: 1458-1464, PM:25345505.
 155. Leonardo CC, Agrawal M, Singh N, Moore JR, Biswal S, Dore S (2013) Oral administration of the flavanol (-)-epicatechin bolsters endogenous protection against focal ischemia through the Nrf2 cytoprotective pathway. *European Journal of Neuroscience* 38: 3659-3668, PM:24112193.
 156. Gundimeda U, McNeill TH, Elhiani AA, Schiffman JE, Hinton DR, Gopalakrishna R (2012) Green tea polyphenols precondition against cell death induced by oxygen-glucose deprivation via stimulation of laminin receptor, generation of reactive oxygen species, and activation of protein kinase Cepsilon. *Journal of Biological Chemistry* 287: 34694-34708, PM:22879598.
 157. Manach C, Williamson G, Morand C, Scalbert A, Remesy C (2005) Bioavailability and bioefficacy of polyphenols in humans. I. Review of 97 bioavailability studies. *American Journal of Clinical Nutrition* 81: 230S-242S, PM:15640486.
 158. Williamson G, Manach C (2005) Bioavailability and bioefficacy of polyphenols in humans. II. Review of 93 intervention studies. *American Journal of Clinical Nutrition* 81: 243S-255S, PM:15640487.
 159. Ho L, Ferruzzi MG, Janle EM, Wang J, Gong B, Chen TY, Lobo J, Cooper B, Wu QL, Talcott ST, Percival SS, Simon JE, Pasinetti GM (2013) Identification of brain-targeted bioactive dietary quercetin-3-O-glucuronide as a novel intervention for Alzheimer's disease. *FASEB Journal* 27: 769-781, PM:23097297.
 160. Rangel-Ordóñez L, Noldner M, Schubert-Zsilavecz M, Wurglics M (2010) Plasma levels and distribution of flavonoids in rat brain after single and repeated doses of standardized Ginkgo biloba extract EGb 761(R). *Planta Med*. 76: 1683-1690, PM:20486074.

161. Ossola B, Kaariainen TM, Mannisto PT (2009) The multiple faces of quercetin in neuroprotection. *Expert.Opin.Drug Saf* 8: 397-409, PM:19538101.
162. Scalbert A, Manach C, Morand C, Remesy C, Jimenez L (2005) Dietary polyphenols and the prevention of diseases. *Crit Rev.Food Sci.Nutr.* 45: 287-306, PM:16047496.
163. Spencer JP (2007) The interactions of flavonoids within neuronal signalling pathways. *Genes Nutr.* 2: 257-273, PM:18850181.
164. Hostetler G, Riedl K, Cardenas H, Dios-Toro M, Arango D, Schwartz S, Doseff AI (2012) Flavone deglycosylation increases their anti-inflammatory activity and absorption. *Molecular Nutrition & Food Research* 56: 558-569, PM:22351119.
165. Perez-Vizcaino F, Duarte J, Santos-Buelga C (2012) The flavonoid paradox: conjugation and deconjugation as key steps for the biological activity of flavonoids. *Journal of the Science of Food and Agriculture* PM:22555950.
166. Li HY, Hu J, Zhao S, Yuan ZY, Wan HJ, Lei F, Ding Y, Xing DM, DU LJ (2012) Comparative study of the effect of baicalin and its natural analogs on neurons with oxygen and glucose deprivation involving innate immune reaction of TLR2/TNFalpha. *Journal of Biomedicine and Biotechnology* 2012: 267890, PM:22536016.
167. Dranka BP, Hill BG, Darley-Usmar VM (2010) Mitochondrial reserve capacity in endothelial cells: The impact of nitric oxide and reactive oxygen species. *Free Radic.Biol.Med.* 48: 905-914, PM:20093177.
168. Xun Z, Lee DY, Lim J, Canaria CA, Barnebey A, Yanonne SM, McMurray CT (2012) Retinoic acid-induced differentiation increases the rate of oxygen consumption and enhances the spare respiratory capacity of mitochondria in SH-SY5Y cells. *Mech.Ageing Dev.* 133: 176-185, PM:22336883.
169. Schneider L, Giordano S, Zelickson BR, Johnson S, Benavides A, Ouyang X, Fineberg N, Darley-Usmar VM, Zhang J (2011) Differentiation of SH-SY5Y cells to a neuronal phenotype changes cellular bioenergetics and the response to oxidative stress. *Free Radic.Biol.Med.* 51: 2007-2017, PM:21945098.
170. Divakaruni AS, Brand MD (2011) The regulation and physiology of mitochondrial proton leak. *Physiology.(Bethesda.)* 26: 192-205, PM:21670165.

171. Brand MD, Nicholls DG (2011) Assessing mitochondrial dysfunction in cells. *Biochemical Journal* 435: 297-312, PM:21726199.
172. Cooper O, Seo H, Andrabi S, Guardia-Laguarta C, Graziotto J, Sundberg M, McLean JR, Carrillo-Reid L, Xie Z, Osborn T, Hargus G, Deleidi M, Lawson T, Bogetofte H, Perez-Torres E, Clark L, Moskowitz C, Mazzulli J, Chen L, Volpicelli-Daley L, Romero N, Jiang H, Uitti RJ, Huang Z, Opala G, Scarffe LA, Dawson VL, Klein C, Feng J, Ross OA, Trojanowski JQ, Lee VM, Marder K, Surmeier DJ, Wszolek ZK, Przedborski S, Krainc D, Dawson TM, Isacson O (2012) Pharmacological rescue of mitochondrial deficits in iPSC-derived neural cells from patients with familial Parkinson's disease. *Sci. Transl. Med.* 4: 141ra90, PM:22764206.
173. Nandagopal K, Dawson TM, Dawson VL (2001) Critical role for nitric oxide signaling in cardiac and neuronal ischemic preconditioning and tolerance. *Journal of Pharmacology and Experimental Therapeutics* 297: 474-478, PM:11303032.
174. Keynes RG, Garthwaite J (2004) Nitric oxide and its role in ischaemic brain injury. *Current Molecular Medicine* 4: 179-191, PM:15032712.
175. Murillo D, Kamga C, Mo L, Shiva S (2011) Nitrite as a mediator of ischemic preconditioning and cytoprotection. *Nitric Oxide*. 25: 70-80, PM:21277988.
176. Atochin DN, Clark J, Demchenko IT, Moskowitz MA, Huang PL (2003) Rapid cerebral ischemic preconditioning in mice deficient in endothelial and neuronal nitric oxide synthases. *Stroke* 34: 1299-1303, PM:12677017.
177. Gutsaeva DR, Carraway MS, Suliman HB, Demchenko IT, Shitara H, Yonekawa H, Piantadosi CA (2008) Transient hypoxia stimulates mitochondrial biogenesis in brain subcortex by a neuronal nitric oxide synthase-dependent mechanism. *Journal of Neuroscience* 28: 2015-2024, PM:18305236.
178. Nisoli E, Clementi E, Paolucci C, Cozzi V, Tonello C, Sciorati C, Bracale R, Valerio A, Francolini M, Moncada S, Carruba MO (2003) Mitochondrial biogenesis in mammals: the role of endogenous nitric oxide. *Science* 299: 896-899, PM:12574632.
179. Huang Z, Huang PL, Ma J, Meng W, Ayata C, Fishman MC, Moskowitz MA (1996) Enlarged infarcts in endothelial nitric oxide synthase knockout mice are attenuated by nitro-L-arginine. *J. Cereb. Blood Flow Metab* 16: 981-987, PM:8784243.
180. Li ST, Pan J, Hua XM, Liu H, Shen S, Liu JF, Li B, Tao BB, Ge XL, Wang XH, Shi JH, Wang XQ (2014) Endothelial nitric oxide synthase protects

neurons against ischemic injury through regulation of brain-derived neurotrophic factor expression. *CNS.Neurosci.Ther.* 20: 154-164, PM:24397751.

181. Scorziello A, Santillo M, Adornetto A, Dell'aversano C, Sirabella R, Damiano S, Canzoniero LM, Renzo GF, Annunziato L (2007) NO-induced neuroprotection in ischemic preconditioning stimulates mitochondrial Mn-SOD activity and expression via Ras/ERK1/2 pathway. *Journal of Neurochemistry* 103: 1472-1480, PM:17680990.
182. Dinerman JL, Dawson TM, Schell MJ, Snowman A, Snyder SH (1994) Endothelial nitric oxide synthase localized to hippocampal pyramidal cells: implications for synaptic plasticity. *Proc.Natl.Acad.Sci.U.S.A* 91: 4214-4218, PM:7514300.
183. Dawson VL, Kizushi VM, Huang PL, Snyder SH, Dawson TM (1996) Resistance to neurotoxicity in cortical cultures from neuronal nitric oxide synthase-deficient mice. *Journal of Neuroscience* 16: 2479-2487, PM:8786424.
184. Yousef T, Neubacher U, Eysel UT, Volgushev M (2004) Nitric oxide synthase in rat visual cortex: an immunohistochemical study. *Brain Res.Brain Res.Protoc.* 13: 57-67, PM:15063842.
185. Bredt DS (1999) Endogenous nitric oxide synthesis: biological functions and pathophysiology. *Free Radic.Res.* 31: 577-596, PM:10630682.
186. Garthwaite J (2008) Concepts of neural nitric oxide-mediated transmission. *European Journal of Neuroscience* 27: 2783-2802, PM:18588525.
187. Moncada S, Bolanos JP (2006) Nitric oxide, cell bioenergetics and neurodegeneration. *Journal of Neurochemistry* 97: 1676-1689, PM:16805776.
188. Sasaki M, Gonzalez-Zulueta M, Huang H, Herring WJ, Ahn S, Ginty DD, Dawson VL, Dawson TM (2000) Dynamic regulation of neuronal NO synthase transcription by calcium influx through a CREB family transcription factor-dependent mechanism. *Proc.Natl.Acad.Sci.U.S.A* 97: 8617-8622, PM:10900019.
189. Bickler PE, Fahlman CS (2004) Moderate increases in intracellular calcium activate neuroprotective signals in hippocampal neurons. *Neuroscience* 127: 673-683, PM:15283966.
190. Bickler PE, Fahlman CS, Gray J, McKleroy W (2009) Inositol 1,4,5-triphosphate receptors and NAD(P)H mediate Ca²⁺ signaling required for

- hypoxic preconditioning of hippocampal neurons. *Neuroscience* 160: 51-60, PM:19217932.
191. Brenman JE, Chao DS, Gee SH, McGee AW, Craven SE, Santillano DR, Wu Z, Huang F, Xia H, Peters MF, Froehner SC, Brecht DS (1996) Interaction of nitric oxide synthase with the postsynaptic density protein PSD-95 and alpha1-syntrophin mediated by PDZ domains. *Cell* 84: 757-767, PM:8625413.
 192. Fleming I, Bauersachs J, Busse R (1997) Calcium-dependent and calcium-independent activation of the endothelial NO synthase. *J.Vasc.Res.* 34: 165-174, PM:9226298.
 193. Lee JK, Kwak HJ, Piao MS, Jang JW, Kim SH, Kim HS (2011) Quercetin reduces the elevated matrix metalloproteinases-9 level and improves functional outcome after cerebral focal ischemia in rats. *Acta Neurochir.(Wien.)* 153: 1321-1329, PM:21120545.
 194. Ahmad A, Khan MM, Hoda MN, Raza SS, Khan MB, Javed H, Ishrat T, Ashafaq M, Ahmad ME, Safhi MM, Islam F (2011) Quercetin protects against oxidative stress associated damages in a rat model of transient focal cerebral ischemia and reperfusion. *Neurochemical Research* 36: 1360-1371, PM:21472457.
 195. Kovalenko TM, Osadchenko IO, Tsupykov OM, Pivneva TA, Shalamai AS, Moibenko OO, Skybo HH (2006) [Neuroprotective effect of quercetin during experimental brain ischemia]. *Fiziol.Zh.* 52: 21-27, PM:17176835.
 196. Pu F, Mishima K, Irie K, Motohashi K, Tanaka Y, Orito K, Egawa T, Kitamura Y, Egashira N, Iwasaki K, Fujiwara M (2007) Neuroprotective effects of quercetin and rutin on spatial memory impairment in an 8-arm radial maze task and neuronal death induced by repeated cerebral ischemia in rats. *J.Pharmacol.Sci.* 104: 329-334, PM:17666865.
 197. Cunningham P, Afzal-Ahmed I, Naftalin RJ (2006) Docking studies show that D-glucose and quercetin slide through the transporter GLUT1. *Journal of Biological Chemistry* 281: 5797-5803, PM:16407180.
 198. Passamonti S, Terdoslavich M, Franca R, Vanzo A, Tramer F, Braidot E, Petrusa E, Vianello A (2009) Bioavailability of flavonoids: a review of their membrane transport and the function of bilitranslocase in animal and plant organisms. *Curr.Drug Metab* 10: 369-394, PM:19519345.
 199. Morris ME, Zhang S (2006) Flavonoid-drug interactions: effects of flavonoids on ABC transporters. *Life Sciences* 78: 2116-2130, PM:16455109.

200. Lee JH, Lee JE, Kim Y, Lee H, Jun HJ, Lee SJ (2014) Multidrug and toxic compound extrusion protein-1 (MATE1/SLC47A1) is a novel flavonoid transporter. *Journal of Agricultural and Food Chemistry* 62: 9690-9698, PM:25241911.
201. Day AJ, Gee JM, DuPont MS, Johnson IT, Williamson G (2003) Absorption of quercetin-3-glucoside and quercetin-4'-glucoside in the rat small intestine: the role of lactase phlorizin hydrolase and the sodium-dependent glucose transporter. *Biochemical Pharmacology* 65: 1199-1206, PM:12663055.
202. Youdim KA, Qaiser MZ, Begley DJ, Rice-Evans CA, Abbott NJ (2004) Flavonoid permeability across an in situ model of the blood-brain barrier. *Free Radic.Biol.Med.* 36: 592-604, PM:14980703.
203. Arredondo F, Echeverry C, Abin-Carriquiry JA, Blasina F, Antunez K, Jones DP, Go YM, Liang YL, Dajas F (2010) After cellular internalization, quercetin causes Nrf2 nuclear translocation, increases glutathione levels, and prevents neuronal death against an oxidative insult. *Free Radic.Biol.Med.* 49: 738-747, PM:20554019.
204. Amphoux A, Vialou V, Drescher E, Bruss M, Mannoury la CC, Rochat C, Millan MJ, Giros B, Bonisch H, Gautron S (2006) Differential pharmacological in vitro properties of organic cation transporters and regional distribution in rat brain. *Neuropharmacology* 50: 941-952, PM:16581093.
205. Ortega R, Garcia N (2009) The flavonoid quercetin induces changes in mitochondrial permeability by inhibiting adenine nucleotide translocase. *Journal of Bioenergetics and Biomembranes* 41: 41-47, PM:19296209.
206. Sisalli MJ, Secondo A, Esposito A, Valsecchi V, Savoia C, Di Renzo GF, Annunziato L, Scorziello A (2014) Endoplasmic reticulum refilling and mitochondrial calcium extrusion promoted in neurons by NCX1 and NCX3 in ischemic preconditioning are determinant for neuroprotection. *Cell Death.Differ.* 21: 1142-1149, PM:24632945.
207. Stout AK, Raphael HM, Kanterewicz BI, Klann E, Reynolds IJ (1998) Glutamate-induced neuron death requires mitochondrial calcium uptake. *Nature Neuroscience* 1: 366-373, PM:10196525.
208. Pietsch K, Saul N, Menzel R, Sturzenbaum SR, Steinberg CE (2009) Quercetin mediated lifespan extension in *Caenorhabditis elegans* is modulated by age-1, daf-2, sek-1 and unc-43. *Biogerontology*. 10: 565-578, PM:19043800.

209. Liu CM, Zheng GH, Cheng C, Sun JM (2013) Quercetin protects mouse brain against lead-induced neurotoxicity. *Journal of Agricultural and Food Chemistry* 61: 7630-7635, PM:23855546.
210. Ma H, Groth RD, Cohen SM, Emery JF, Li B, Hoedt E, Zhang G, Neubert TA, Tsien RW (2014) gammaCaMKII shuttles Ca(2+)(+)/CaM to the nucleus to trigger CREB phosphorylation and gene expression. *Cell* 159: 281-294, PM:25303525.
211. Lee J, Kim CH, Simon DK, Aminova LR, Andreyev AY, Kushnareva YE, Murphy AN, Lonze BE, Kim KS, Ginty DD, Ferrante RJ, Ryu H, Ratan RR (2005) Mitochondrial cyclic AMP response element-binding protein (CREB) mediates mitochondrial gene expression and neuronal survival. *Journal of Biological Chemistry* 280: 40398-40401, PM:16207717.
212. St-Pierre J, Drori S, Uldry M, Silvaggi JM, Rhee J, Jager S, Handschin C, Zheng K, Lin J, Yang W, Simon DK, Bachoo R, Spiegelman BM (2006) Suppression of reactive oxygen species and neurodegeneration by the PGC-1 transcriptional coactivators. *Cell* 127: 397-408, PM:17055439.
213. Moreno-Ulloa A, Romero-Perez D, Villarreal F, Ceballos G, Ramirez-Sanchez I (2014) Cell membrane mediated (-)-epicatechin effects on upstream endothelial cell signaling: evidence for a surface receptor. *Bioorganic and Medicinal Chemistry Letters* 24: 2749-2752, PM:24794111.
214. Ramirez-Sanchez I, Maya L, Ceballos G, Villarreal F (2011) (-)-Epicatechin induces calcium and translocation independent eNOS activation in arterial endothelial cells. *Am.J.Physiol Cell Physiol* 300: C880-C887, PM:21209365.
215. Dimmeler S, Fleming I, Fisslthaler B, Hermann C, Busse R, Zeiher AM (1999) Activation of nitric oxide synthase in endothelial cells by Akt-dependent phosphorylation. *Nature* 399: 601-605, PM:10376603.
216. Aquilano K, Baldelli S, Ciriolo MR (2014) Nuclear recruitment of neuronal nitric-oxide synthase by alpha-syntrophin is crucial for the induction of mitochondrial biogenesis. *Journal of Biological Chemistry* 289: 365-378, PM:24235139.
217. Lira VA, Brown DL, Lira AK, Kavazis AN, Soltow QA, Zeanah EH, Criswell DS (2010) Nitric oxide and AMPK cooperatively regulate PGC-1 in skeletal muscle cells. *J.Physiol* 588: 3551-3566, PM:20643772.

218. Di CA (2009) Human and economic burden of stroke. *Age and Ageing* 38: 4-5, PM:19141505.
219. Anderson CS, Carter KN, Brownlee WJ, Hackett ML, Broad JB, Bonita R (2004) Very long-term outcome after stroke in Auckland, New Zealand. *Stroke* 35: 1920-1924, PM:15178818.
220. Dirnagl U, Becker K, Meisel A (2009) Preconditioning and tolerance against cerebral ischaemia: from experimental strategies to clinical use. *Lancet Neurol.* 8: 398-412, PM:19296922.
221. Iadecola C, Anrather J (2011) Stroke research at a crossroad: asking the brain for directions. *Nature Neuroscience* 14: 1363-1368, PM:22030546.
222. Gidday JM (2006) Cerebral preconditioning and ischaemic tolerance. *Nature Reviews: Neuroscience* 7: 437-448, PM:16715053.
223. Lo EH, Dalkara T, Moskowitz MA (2003) Mechanisms, challenges and opportunities in stroke. *Nature Reviews: Neuroscience* 4: 399-415, PM:12728267.
224. Bading H (2013) Nuclear calcium signalling in the regulation of brain function. *Nature Reviews: Neuroscience* 14: 593-608, PM:23942469.
225. Dezfulian C, Garrett M, Gonzalez NR (2013) Clinical application of preconditioning and postconditioning to achieve neuroprotection. *Transl. Stroke Res.* 4: 19-24, PM:24323188.
226. Sheng ZH, Cai Q (2012) Mitochondrial transport in neurons: impact on synaptic homeostasis and neurodegeneration. *Nature Reviews: Neuroscience* 13: 77-93, PM:22218207.
227. Saxton WM, Hollenbeck PJ (2012) The axonal transport of mitochondria. *Journal of Cell Science* 125: 2095-2104, PM:22619228.
228. Saotome M, Safiulina D, Szabadkai G, Das S, Fransson A, Aspenstrom P, Rizzuto R, Hajnoczky G (2008) Bidirectional Ca²⁺-dependent control of mitochondrial dynamics by the Miro GTPase. *Proc.Natl.Acad.Sci.U.S.A* 105: 20728-20733, PM:19098100.
229. Sisalli MJ, Annunziato L, Scorziello A (2015) Novel Cellular Mechanisms for Neuroprotection in Ischemic Preconditioning: A View from Inside Organelles. *Front Neurol.* 6: 115, PM:26074868.
230. Cuomo O, Vinciguerra A, Cerullo P, Anzilotti S, Brancaccio P, Bilo L, Scorziello A, Molinaro P, Di RG, Pignataro G (2015) Ionic homeostasis in brain conditioning. *Front Neurosci.* 9: 277, PM:26321902.

231. Robertson GS, Crocker SJ, Nicholson DW, Schulz JB (2000) Neuroprotection by the inhibition of apoptosis. *Brain Pathol.* 10: 283-292, PM:10764048.
232. Green DR, Galluzzi L, Kroemer G (2014) Cell biology. Metabolic control of cell death. *Science* 345: 1250256, PM:25237106.
233. Nakagawa T, Shimizu S, Watanabe T, Yamaguchi O, Otsu K, Yamagata H, Inohara H, Kubo T, Tsujimoto Y (2005) Cyclophilin D-dependent mitochondrial permeability transition regulates some necrotic but not apoptotic cell death. *Nature* 434: 652-658, PM:15800626.
234. Schinzel AC, Takeuchi O, Huang Z, Fisher JK, Zhou Z, Rubens J, Hetz C, Danial NN, Moskowitz MA, Korsmeyer SJ (2005) Cyclophilin D is a component of mitochondrial permeability transition and mediates neuronal cell death after focal cerebral ischemia. *Proc.Natl.Acad.Sci.U.S.A* 102: 12005-12010, PM:16103352.
235. Baines CP, Kaiser RA, Purcell NH, Blair NS, Osinska H, Hambleton MA, Brunskill EW, Sayen MR, Gottlieb RA, Dorn GW, Robbins J, Molkentin JD (2005) Loss of cyclophilin D reveals a critical role for mitochondrial permeability transition in cell death. *Nature* 434: 658-662, PM:15800627.
236. Pignataro G, Cuomo O, Vinciguerra A, Sirabella R, Esposito E, Boscia F, Di RG, Annunziato L (2013) NCX as a key player in the neuroprotection exerted by ischemic preconditioning and postconditioning. *Advances in Experimental Medicine and Biology* 961: 223-240, PM:23224883.
237. Halestrap AP (2006) Calcium, mitochondria and reperfusion injury: a pore way to die. *Biochemical Society Transactions* 34: 232-237, PM:16545083.
238. Pan X, Liu J, Nguyen T, Liu C, Sun J, Teng Y, Fergusson MM, Rovira II, Allen M, Springer DA, Aponte AM, Gucek M, Balaban RS, Murphy E, Finkel T (2013) The physiological role of mitochondrial calcium revealed by mice lacking the mitochondrial calcium uniporter. *Nature Cell Biology* 15: 1464-1472, PM:24212091.
239. De SD, Raffaello A, Teardo E, Szabo I, Rizzuto R (2011) A forty-kilodalton protein of the inner membrane is the mitochondrial calcium uniporter. *Nature* 476: 336-340, PM:21685888.
240. Baughman JM, Perocchi F, Girgis HS, Plovanich M, Belcher-Timme CA, Sancak Y, Bao XR, Strittmatter L, Goldberger O, Bogorad RL, Kotliansky V, Mootha VK (2011) Integrative genomics identifies MCU as an essential component of the mitochondrial calcium uniporter. *Nature* 476: 341-345, PM:21685886.

241. Wu Y, Rasmussen TP, Koval OM, Joiner ML, Hall DD, Chen B, Luczak ED, Wang Q, Rokita AG, Wehrens XH, Song LS, Anderson ME (2015) The mitochondrial uniporter controls fight or flight heart rate increases. *Nat. Commun.* 6: 6081, PM:25603276.
242. Rasmussen TP, Wu Y, Joiner ML, Koval OM, Wilson NR, Luczak ED, Wang Q, Chen B, Gao Z, Zhu Z, Wagner BA, Soto J, McCormick ML, Kutschke W, Weiss RM, Yu L, Boudreau RL, Abel ED, Zhan F, Spitz DR, Buettner GR, Song LS, Zingman LV, Anderson ME (2015) Inhibition of MCU forces extramitochondrial adaptations governing physiological and pathological stress responses in heart. *Proc.Natl.Acad.Sci.U.S.A* 112: 9129-9134, PM:26153425.
243. Kwong JQ, Lu X, Correll RN, Schwanekamp JA, Vagnozzi RJ, Sargent MA, York AJ, Zhang J, Bers DM, Molckentin JD (2015) The Mitochondrial Calcium Uniporter Selectively Matches Metabolic Output to Acute Contractile Stress in the Heart. *Cell Rep.* 12: 15-22, PM:26119742.
244. Luongo TS, Lambert JP, Yuan A, Zhang X, Gross P, Song J, Shanmughapriya S, Gao E, Jain M, Houser SR, Koch WJ, Cheung JY, Madesh M, Elrod JW (2015) The Mitochondrial Calcium Uniporter Matches Energetic Supply with Cardiac Workload during Stress and Modulates Permeability Transition. *Cell Rep.* 12: 23-34, PM:26119731.
245. Nicholls DG (2004) Mitochondrial dysfunction and glutamate excitotoxicity studied in primary neuronal cultures. *Current Molecular Medicine* 4: 149-177, PM:15032711.
246. Llorente-Folch I, Rueda CB, Amigo I, del AA, Saheki T, Pardo B, Satrustegui J (2013) Calcium-regulation of mitochondrial respiration maintains ATP homeostasis and requires ARALAR/AGC1-malate aspartate shuttle in intact cortical neurons. *Journal of Neuroscience* 33: 13957-71, 13971a, PM:23986233.
247. Patel MS, Nemeria NS, Furey W, Jordan F (2014) The pyruvate dehydrogenase complexes: structure-based function and regulation. *Journal of Biological Chemistry* 289: 16615-16623, PM:24798336.
248. Jang S, Nelson JC, Bend EG, Rodriguez-Laureano L, Tueros FG, Cartagena L, Underwood K, Jorgensen EM, Colon-Ramos DA (2016) Glycolytic Enzymes Localize to Synapses under Energy Stress to Support Synaptic Function. *Neuron* 90: 278-291, PM:27068791.
249. Wirth C, Brandt U, Hunte C, Zickermann V (2016) Structure and function of mitochondrial complex I. *Biochimica et Biophysica Acta: Protein Structure and Molecular Enzymology* 1857: 902-914, PM:26921811.

250. Vaseva AV, Marchenko ND, Ji K, Tsirka SE, Holzmann S, Moll UM (2012) p53 opens the mitochondrial permeability transition pore to trigger necrosis. *Cell* 149: 1536-1548, PM:22726440.
251. Mookerjee SA, Goncalves RL, Gerencser AA, Nicholls DG, Brand MD (2015) The contributions of respiration and glycolysis to extracellular acid production. *Biochimica et Biophysica Acta: Protein Structure and Molecular Enzymology* 1847: 171-181, PM:25449966.
252. Duchen MR (2000) Mitochondria and calcium: from cell signalling to cell death. *J.Physiol* 529 Pt 1: 57-68, PM:11080251.
253. Nichols M, Elustondo PA, Warford J, Thirumaran A, Pavlov EV, Robertson GS (2016) Global ablation of the mitochondrial calcium uniporter increases glycolysis in cortical neurons subjected to energetic stressors. *J.Cereb.Blood Flow Metab* PM:27909264.
254. Barlow JZ, Huntley GW (2000) Developmentally regulated expression of Thy-1 in structures of the mouse sensory-motor system. *J.Comp Neurol.* 421: 215-233, PM:10813783.
255. Heimer-McGinn V, Young P (2011) Efficient inducible Pan-neuronal cre-mediated recombination in SLICK-H transgenic mice. *Genesis.* 49: 942-949, PM:21671347.
256. Denton RM, Randle PJ, Martin BR (1972) Stimulation by calcium ions of pyruvate dehydrogenase phosphate phosphatase. *Biochemical Journal* 128: 161-163, PM:4343661.
257. Nicholls DG (2009) Mitochondrial calcium function and dysfunction in the central nervous system. *Biochimica et Biophysica Acta: Protein Structure and Molecular Enzymology* 1787: 1416-1424, PM:19298790.
258. Harris JJ, Jolivet R, Attwell D (2012) Synaptic energy use and supply. *Neuron* 75: 762-777, PM:22958818.
259. Eltzschig HK, Eckle T (2011) Ischemia and reperfusion--from mechanism to translation. *Nature Medicine* 17: 1391-1401, PM:22064429.
260. Nichols M, Zhang J, Polster BM, Elustondo PA, Thirumaran A, Pavlov EV, Robertson GS (2015) Synergistic neuroprotection by epicatechin and quercetin: Activation of convergent mitochondrial signaling pathways. *Neuroscience* 308: 75-94, PM:26363153.
261. Alberts MJ (2017) Stroke Treatment With Intravenous Tissue-Type Plasminogen Activator: More Proof That Time Is Brain. *Circulation* 135: 140-142, PM:28069710.

262. Yan H, Zhang D, Hao S, Li K, Hang CH (2015) Role of Mitochondrial Calcium Uniporter in Early Brain Injury After Experimental Subarachnoid Hemorrhage. *Mol.Neurobiol.* 52: 1637-1647, PM:25370932.
263. Charuk JH, Pirraglia CA, Reithmeier RA (1990) Interaction of ruthenium red with Ca²⁺(+)-binding proteins. *Anal.Biochem.* 188: 123-131, PM:1699445.
264. Liu RH (2003) Health benefits of fruit and vegetables are from additive and synergistic combinations of phytochemicals. *American Journal of Clinical Nutrition* 78: 517S-520S, PM:12936943.
265. Schwartz J, Holmuhamedov E, Zhang X, Lovelace GL, Smith CD, Lemasters JJ (2013) Minocycline and doxycycline, but not other tetracycline-derived compounds, protect liver cells from chemical hypoxia and ischemia/reperfusion injury by inhibition of the mitochondrial calcium uniporter. *Toxicol.Appl.Pharmacol.* 273: 172-179, PM:24012766.
266. Amiri-Nikpour MR, Nazarbaghi S, Hamdi-Holasou M, Rezaei Y (2015) An open-label evaluator-blinded clinical study of minocycline neuroprotection in ischemic stroke: gender-dependent effect. *Acta Neurol.Scand.* 131: 45-50, PM:25155474.
267. Padma Srivastava MV, Bhasin A, Bhatia R, Garg A, Gaikwad S, Prasad K, Singh MB, Tripathi M (2012) Efficacy of minocycline in acute ischemic stroke: a single-blinded, placebo-controlled trial. *Neurol.India* 60: 23-28, PM:22406775.
268. Adhami F, Liao G, Morozov YM, Schloemer A, Schmithorst VJ, Lorenz JN, Dunn RS, Vorhees CV, Wills-Karp M, Degen JL, Davis RJ, Mizushima N, Rakic P, Dardzinski BJ, Holland SK, Sharp FR, Kuan CY (2006) Cerebral ischemia-hypoxia induces intravascular coagulation and autophagy. *Am.J.Pathol.* 169: 566-583, PM:16877357.
269. Koton S, Schneider AL, Rosamond WD, Shahar E, Sang Y, Gottesman RF, Coresh J (2014) Stroke incidence and mortality trends in US communities, 1987 to 2011. *JAMA* 312: 259-268, PM:25027141.
270. Prabhakar NR (2006) O₂ sensing at the mammalian carotid body: why multiple O₂ sensors and multiple transmitters? *Exp.Physiol* 91: 17-23, PM:16239252.

Appendix



RightsLink®

Home



Title: The regulation of neuronal mitochondrial metabolism by calcium
Author: I. Llorente-Folch, C. B. Rueda, B. Pardo, G. Szabadkai, M. R. Duchén, J. Satrustegui
Publication: Journal of Physiology
Publisher: John Wiley and Sons
Date: Aug 14, 2015

Logged in as:
Matthew Nichols
Account #: 3000992491

© 2015 The Authors. The Journal of Physiology © 2015 The Physiological Society

Order Completed

Thank you for your order.

This Agreement between Matthew J Nichols ("You") and John Wiley and Sons ("John Wiley and Sons") consists of your license details and the terms and conditions provided by John Wiley and Sons and Copyright Clearance Center.

Your confirmation email will contain your order number for future reference.

[Printable details.](#)

License Number	4123730328984
License date	Jun 07, 2017
Licensed Content Publisher	John Wiley and Sons
Licensed Content Publication	Journal of Physiology
Licensed Content Title	The regulation of neuronal mitochondrial metabolism by calcium
Licensed Content Author	I. Llorente-Folch, C. B. Rueda, B. Pardo, G. Szabadkai, M. R. Duchén, J. Satrustegui
Licensed Content Date	Aug 14, 2015
Licensed Content Pages	16
Type of use	Dissertation/Thesis
Requestor type	University/Academic
Format	Print and electronic
Portion	Figure/table
Number of figures/tables	1

Original Wiley figure/table number(s)	figure 1
Will you be translating?	No
Title of your thesis / dissertation	Mitochondrial control of neuronal bioenergetics, cell death and survival
Expected completion date	Aug 2017
Expected size (number of pages)	175
Requestor Location	Matthew J Nichols 1348 summer st halifax, NS b3h 4r2 Canada Attn: Matthew J Nichols
Publisher Tax ID	EU826007151
Billing Type	Invoice
Billing address	Matthew J Nichols 1348 summer st halifax, NS b3h 4r2 Canada Attn: Matthew J Nichols
Total	0.00 CAD

Would you like to purchase the full text of this article? If so, please continue on to the content ordering system located here: [Purchase PDF](#)

If you click on the buttons below or close this window, you will not be able to return to the content ordering system.

ORDER MORE | CLOSE WINDOW

Copyright © 2017 [Copyright Clearance Center, Inc.](#) All Rights Reserved. [Privacy statement](#). [Terms and Conditions](#).
Comments? We would like to hear from you. E-mail us at customercare@copyright.com



Home

Account Info

Help





Title: Molecular structure and pathophysiological roles of the Mitochondrial Calcium Uniporter

Author: Cristina Mammucari, Anna Raffaello, Denis Vecellio Reane, Rosario Rizzuto

Publication: Biochimica et Biophysica Acta (BBA) - Molecular Cell Research

Publisher: Elsevier

Date: October 2016

© 2016 The Authors. Published by Elsevier B.V.

Logged in as:
Matthew Nichols

Account #:
3000992491

[LOGOUT](#)

Creative Commons Attribution-NonCommercial-No Derivatives License (CC BY NC ND)

This article is published under the terms of the [Creative Commons Attribution-NonCommercial-No Derivatives License \(CC BY NC ND\)](#).

For non-commercial purposes you may copy and distribute the article, use portions or extracts from the article in other works, and text or data mine the article, provided you do not alter or modify the article without permission from Elsevier. You may also create adaptations of the article for your own personal use only, but not distribute these to others. You must give appropriate credit to the original work, together with a link to the formal publication through the relevant DOI, and a link to the Creative Commons user license above. If changes are permitted, you must indicate if any changes are made but not in any way that suggests the licensor endorses you or your use of the work.

Permission is not required for this non-commercial use. For commercial use please continue to request permission via Rightslink.

[BACK](#)

[CLOSE WINDOW](#)

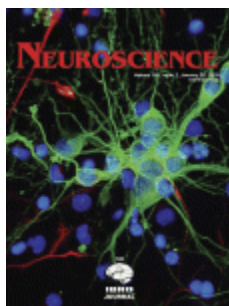
Copyright © 2017 [Copyright Clearance Center, Inc.](#) All Rights Reserved. [Privacy statement](#). [Terms and Conditions](#). Comments? We would like to hear from you. E-mail us at customer care@copyright.com



[Home](#)

[Account Info](#)

[Help](#)



Title: Synergistic neuroprotection by epicatechin and quercetin: Activation of convergent mitochondrial signaling pathways

Author: M. Nichols, J. Zhang, B.M. Polster, P.A. Elustondo, A. Thirumaran, E.V. Pavlov, G.S. Robertson

Publication: Neuroscience

Logged in as:
Matthew Nichols

Account #:
3000992491

[LOGOUT](#)


Publisher: Elsevier

Date: 12 November 2015

Copyright © 2015 IBRO. Published by Elsevier Ltd. All rights reserved.

About Your Thesis / Dissertation

Please select from the thesis / dissertation you are currently working on and click 'Continue'. If you need to add a new thesis / dissertation please click the 'New Work' button below.

Thesis / Dissertation Title	
	Mitochondrial control of neuronal bioenergetics, cell death and survival

[BACK](#) [NEW WORK](#) [CONTINUE](#)

Copyright © 2017 [Copyright Clearance Center, Inc.](#) All Rights Reserved. [Privacy statement](#). [Terms and Conditions](#).
Comments? We would like to hear from you. E-mail us at customercare@copyright.com



RightsLink®

[Home](#)

[Account Info](#)

[Help](#)



Title: Global ablation of the mitochondrial calcium uniporter increases glycolysis in cortical neurons subjected to energetic stressors
Author: Matthew Nichols, Pia A Elustondo, Jordan Warford, et al
Publication: Journal of Cerebral Blood Flow & Metabolism
Publisher: SAGE Publications
Date: 01/01/2016
Copyright © 2016, © SAGE Publications

Logged in as:
Matthew Nichols
Account #:
3000992491

[LOGOUT](#)

If you are a SAGE journal author requesting permission to reuse material from your journal article, please note you may be able to reuse your content without requiring permission from SAGE. Please review SAGE's author re-use and archiving policies at <https://us.sagepub.com/en-us/nam/journal-author-archiving-policies-and-re-use> for more information.

If your request does not fall within SAGE's reuse guidelines, please proceed with submitting your request by selecting one of the other reuse categories that describes your use. Please note, a fee may

be charged for reuse of content requiring permission. Please contact permissions@sagepub.co.uk if you have questions.

BACK

CLOSE WINDOW

Copyright © 2017 [Copyright Clearance Center, Inc.](#) All Rights Reserved. [Privacy statement](#). [Terms and Conditions](#).
Comments? We would like to hear from you. E-mail us at customercare@copyright.com